Climate and biodiversity : application of recent methodological developments in the study and the modelling of transepidermal evaporative water loss in an amphibian

Thomas Wardziak

N° d'ordre 135 - 2013 Année 2013

THESE DE L'UNIVERSITE DE LYON

Délivrée par

L'UNIVERSITE CLAUDE BERNARD LYON 1

ET L'ECOLE DOCTORALE Evolution Ecosystèmes Microbiologie Modélisation

DIPLOME DE DOCTORAT
(arrêté du 7 août 2006)

Soutenue publiquement le 26 septembre 2013

par

Thomas WARDZIAK

CLIMAT ET BIODIVERSITE : APPLICATION DE RECENTS DEVELOPPEMENTS METHODOLOGIQUES A L'ETUDE ET LA MODELISATION DES PERTES EN EAU PAR EVAPORATION CHEZ UN AMPHIBIEN

Directeur de thèse : Pierre JOLY ; Co-directeur : Laurent OXARANGO

JURY :

M. Mathieu DENOËL	Chercheur qualifié du F.R.S. – FNRS, Liège
M. Emmanuel DESOUHANT	Professeur, UMR 5558, LBBE, Lyon1
M. Anthony HERREL	Chargé de Recherche, UMR 7179, MNHN, Paris
M. Marc PRAT	Directeur de Recherche, UMR 5502, IMFT, Toulouse
M. Pierre JOLY	Directeur de Recherche UMR 5023, LEHNA, Lyon1
M. Laurent OXARANGO	Maître de conférences, UMR 5564, LTHE, Grenoble

Dans un contexte de changement climatique, il est essentiel de prévoir comment les organismes peuvent être affectés dans leurs relations physiques avec l'environnement. Les amphibiens représentent le groupe des vertébrés le plus sensible aux changements environnementaux, en raison d'une perte en eau par évaporation transépidermique (PEET) permanente. Ma thèse vise à mettre en place des approches pour mesurer et modéliser avec précision les surfaces de la peau contribuant à la PEET; établir les lois de transfert d'eau amphibien-environnement; et fournir une meilleure compréhension des réponses physiologiques face au pathogène *Batrachochytrium dendrobatidis*. Ces expériences ont été réalisées sur des tritons palmés (*Lissotriton helveticus*) mâles adultes en phase terrestre. Nos résultats suggèrent que *L. helveticus* ne présente aucune adaptation physiologique pour limiter la PEET, les moyens étant limités à l'expression d'une posture en forme de "S". Une méthode de reconstruction 3D basée sur l'Imagerie par Résonance Magnétique a été utilisée pour générer des géométries 3D des tritons utilisables pour mesurer leur surface, et à des fins de simulation. Nous avons ainsi réalisé une analyse numérique en 3D des PEET, et avons proposé une relation pour estimer cette perte dans une large gamme de conditions climatiques. Enfin, nos résultats supportent l'hypothèse de dysfonctionnement épidermique, suggérant que *B. dendrobatidis* compromet la capacité des amphibiens à se réhydrater. Ma thèse devrait contribuer à développer de nouvelles approches en sciences des relations eau-amphibiens, et à améliorer nos connaissances sur les effets des changements environnementaux sur les organismes.

Climate and biodiversity: application of recent methodological developments in the study and the modelling of transepidermal evaporative water loss in an amphibian

In a context of climate change, it is critical to predict how organisms might be affected in their physical relations with environment. Amphibians are among the vertebrate groups the most affected by ecological changes, because of permanent transepidermal evaporative water loss (TEWL) through their skin. My thesis aims at setting up approaches to measure and model accurately the functional skin surface areas that contribute to TEWL, establishing laws of water transfer between an amphibian and its physical environment, and providing understanding on physiological responses to the skin pathogen *Batrachochytrium dendrobatidis*. We conducted experiments on adult males of the palmate newt (*Lissotriton helveticus*) during their terrestrial phase. Our results suggest that *L. helveticus* did not show any physiological adaptations to restrain TEWL. The ways to reduce TEWL result essentially in the expression of a stereotyped "S"-shaped water-conserving posture. We used a Magnetic Resonance Imaging-based 3D reconstruction method to generate 3D geometries of newt that is suitable for measuring skin surface areas, and for simulation purposes. We successfully performed 3D numerical analysis of TEWL, and proposed an original relationship to estimate TEWL rates in a large range of temperature and humidity. Finally, our results support the epidermal dysfunction hypothesis, which suggests that *B. dendrobatidis* compromises the ability of amphibians to rehydrate. My thesis would contribute to open new approaches to the science of amphibian water relations, and improve our knowledge of the effects of ecological changes on organisms.

Ecophysiologie – Ecologie biophysique

Mots-clés: Amphibien ; Changement climatique ; Evapotranspiration ; Comportement ; Modélisation ; Imagerie ; Pathogène

Key-words: Amphibian ; Climate change ; Water loss ; Water-conserving behaviour ; Modelling ; Imaging ; Pathogen

UMR CNRS 5023 Laboratoire d'Ecologie des Hydrosystèmes Naturels et Anthropisés (LEHNA)
Université Lyon1, 43 Bd. Du 11 novembre 1918, 69622 Villeurbanne cedex.

REMERCIEMENTS

Tout d'abord, un grand merci aux membres du jury qui ont accepté de prendre de leur temps pour évaluer l'ensemble de ce travail, en particulier à Mathieu Denoël et Marc Prat, rapporteurs de ce manuscrit.

Me voilà donc arrivé au terme d'une grande aventure qui aura duré près de 4 années. Cette thèse est le fruit d'un long travail que je dois à l'implication et au soutien d'un certain nombre de personnes :

En premier lieu, je tiens à remercier Pierre Joly, mon directeur de thèse pour m'avoir donné l'opportunité de faire, et de mener à bien jusqu'au bout, cette thèse multidisciplinaire extrêmement enrichissante en tout point de vue, et Laurent Oxarango, mon co-directeur pour m'avoir accompagné et soutenu dans toute la partie biophysique de ce travail. Je garde un excellent souvenir de notre collaboration qui, j'espère, se poursuivra dans l'avenir.

Je tiens également à remercier chaleureusement Emilien Luquet (« Milou ») et Sandrine Plenet, pour leur immense investissement dans notre projet commun sur Bd, qui représente le premier gros travail de ma thèse. Merci aussi à Jean-Paul Léna pour sa précieuse aide sur les stats (en espérant que tu ne gardes pas trop de mauvais souvenirs de ces modèles mixtes !).

Un immense merci à Sébastien Valette et Laurent Mahieu-Williame (du CREATIS-LRMN, Lyon) pour m'avoir permis de réaliser des IRM sur mes tritons et de m'avoir fourni tout le nécessaire pour obtenir des « tritons numériques » en 3D.

Merci à tous ceux qui ont volontairement donné de leur personne pour m'aider sur mes manips en labo sur le « séchage » de tritons ou sur le terrain. En particulier, je tiens à remercier Estefanía Perez-Broto ma toute première stagiaire, venue d'Espagne, pour sa précieuse aide, mais surtout pour tous les bons moments que l'on a passé ensemble (et merci pour m'avoir fait découvrir une Espagne que je ne connaissais pas !). Merci aussi à Marion Javal et Théotime Colin pour m'avoir accompagné et aidé dans mes manips d'été alors que

rien ne vous y obligeait. Et merci aussi à Odile Grolet pour son aide sur le terrain pour la capture des tritons.

Je remercie aussi tous les collègues du LEHNA, de l'équipe E2C et de l'équipe enseignante pour leurs conseils, l'ambiance générale et les discussions que j'ai eues avec la plupart d'entre vous : Bernard Kaufmann, Thierry Lengagne, Nathalie Mondy, Caroline Romestaing, Nadjette Houriez, Cédric Soulier, Michel Creuzé des Châtelliers, Frédéric Hervant, Pierre Marmonier, Laurent Simon, Pierre Sagnes, Gudrun Bornette.

Merci aux anciens thésards du labo, ou encore thésards aujourd'hui que j'ai pu côtoyer et avec qui j'ai eu la chance de partager de très bons moments, et pour la super ambiance au labo : Karine Salin, Milou, Cécile Capderrey, David Eme, Clémentine François, Natacha Foucreau, Tania Zakowski, Mélissa De Wilde. Dédicace spéciale à Gaëlle Robin et Sabine Lotteau (du labo de physio à côté du notre), ainsi qu'à Alice Merle. Je termine bien entendu par remercier mes compagnons d'aventure Sieur Brepson et Dame chombi, Sieurs Prunier, Troïanowski, et Gippet. Cette thèse je la dois aussi et surtout à vous pour votre immense soutien, pour avoir répondu présent pendant les moments difficiles, mais également pour tous les excellents moments que j'ai partagés avec vous au cours de ces 4 dernières années (ballades, musiques, bonnes bouffes, soirées, barbeuc, et j'en passe…). Vous êtes bien entendu, et vous l'aurez compris, mes amis les plus proches.

Enfin, je tiens à remercier ma famille pour leur soutien sans faille, au cours de ces années de thèses (mais aussi pendant toute la durée de mes études), mais également pour m'avoir toujours encouragé dans les choix que je prenais.

TABLE OF CONTENT

GENERAL INTRODUCTION

Global changes of environmental conditions on earth imply major modifications of the selective pressures that shape the evolution of living forms, as well as their extinction probabilities (Thomas et al. 2004, Parmesan 2006, Maclean and Wilson 2011, Bellard et al. 2012). Organisms and their environment are closely coupled up through exchanges of energy (i.e. heat) and mass (e.g. water, electrolytes and respiratory gasses). To cope with local heterogeneous environmental conditions, organisms have evolved physiological, morphological and behavioural adaptations to maintain **homeostasis** (e.g. water and electrolyte equilibrium) (Kearney and Porter 2009, Biozinovic et al. 2011). However, environmental conditions are changing rapidly over time and space (IPCC 2007) and may lead to detrimental thermal and/or hydric conditions for organisms (e.g. shelter loss, intense drought periods with reduced water availability) that prevent them to maintain homeostasis with direct physiological and functional consequences (Spotila & Berman 1976, Spotila et al. 1992, Shoemaker et al. 1992). As a possible consequence, this may diminish the capacity of an organism to deal with potential stress such as pathogen attacks (Rachowicz et al. 2005, Blaustein et al. 2012) and exacerbate detrimental effects of environmental changes on organism survival (Rachowicz et al. 2005, Blaustein et al. 2012, Fisher et al. 2012). Consequently, both physical environmental changes and diseases may ultimately lead, through complex ways, to local and/or global population declines and extinctions.

In such context, predicting how ecological changes might affect organisms and their physical relations (in terms of energy and mass transfers) with the environment is a critical and urgent interdisciplinary challenge for developing effective conservation strategies. For this purpose, the interdisciplinary field of biophysical ecology combines fundamental

physical laws that govern general fluid motion (i.e. heat, mass and momentum transfer principles) with ecophysiology, behavioural ecology, and properties of the animal (size, shape, skin characteristics, etc.) to derive mechanistic models of energy and mass balance at different scales. However, providing efficient biophysical models requires an overview of major mechanisms and phenomena at the organism scale implicated in the physical individual-environment relations. Furthermore, heat and mass transfers occur between the skin surface area and the environment. Thus, setting up biophysical models also needs a precise estimation of this functional surface area which is dependent on the animal's posture and the nature of the environment.

Amphibians are ideal for such overview. These wet-skinned **ectotherms** are characterized by permanent exchanges of gasses, heat and water through their permeable and well vascularized skin (Shoemaker and Nagy 1977, Feder and Burggren 1984, Spotila et al. 1992, Shoemaker et al. 1992, Lillywhite 2006, Hillman et al. 2009, and see Box 1). Such characteristics make them particularly sensitive to their physical environment. As a consequence, they are the vertebrate taxon the most threatened by environmental changes (Stuart et al. 2004). Understanding the physical amphibian-environment relations in an environmental changes context represents a challenge in biological conservation. Whereas models of dynamic exchanges of energy and mass have been established for the amphibians (Tracy 1976, Shoemaker et al. 1992, Spotila et al. 1992, Hillman et al. 2009) and generalized to other wet-skinned taxa, they have to be revisited under the light of i) recent progresses on water exchange understandings and ii) by the use of modern modelling tools (e.g. multiphysics engineering modelling and simulation software), to model and simulate any physics-based system. Such an approach should benefit recent technological and algorithmic advances in image acquisition and processing (Audette et al. 2011, Jacinto et al. 2012,

Kechichian et al. 2012, Laforsh et al. 2012) to model the complex outer morphology of an amphibian and obtain the functional skin surface areas involved in mass transfers (Box 4).

In our review, we first provide mechanistic insights on water transfers with atmospheric environment, focusing on water evaporation driving phenomena (WEDP). We then review mechanistic insights on mass transfers between animals and their substrate environment. Water intake from the soil is the major and critical way for amphibians to balance water loss (Tracy 1976, Shoemaker and Nagy 1977, Spotila et al. 1992, Shoemaker et al. 1992, Hillman et al. 2009). Finally, we discuss how an external biotic factor the emergent fungal pathogen *Batrachochytrium dendrobatidis* (Bd), implicated in numerous amphibian population declines and extinction throughout the world (Skerrat et al. 2007, Fisher et al. 2009, Kilpatrick et al. 2010, Blaustein et al. 2012) may influence the amphibian relations with its environment.

Box 1. The amphibian skin: a critical pathway of water exchanges in terrestrial environment. The amphibian skin is a thin multilayered epithelium (Fig. 1) where the outermost layer or cornified layer of epidermis, the *stratum corneum*, is composed of no more than a few keratinized dead cell layers (unlike squamates, birds or mammals) and consequently do not constitute a barrier for mass transfers (Shoemaker et al. 1992, Lillywhite 2006, Hillman et al. 2009). The *stratum corneum* is followed by the *stratum granulosum*, the *stratum spinosum* and the *stratum germinativum* to form the epidermis, and by the *stratum spongiousum* (of the dermis) that contains the developed capillary networks (Farquhar and Palade 1964, Shoemaker et al. 1992, Hillman et al. 2009). The living layers of the s. granulosum to the s. germinativum are composed of two cell types: principal

cells which represent the vast majority, interspersed by the mitochondria-rich cells which are fewer (Shoemaker et al. 1992, Hillman et al. 2009). The outermost living cell layer (the *s. granulosum*) constitutes the limiting barrier for mass transfers across the skin because apical membranes of *s. granulosum* cells are attached each other by tight junctions. Furthermore, these apical membranes form the active pathway for water and electrolytes transport across the skin accomplished by active complex hormonal (i.e. **arginine vasotocin**, (AVT))-AMP-regulated pathways implying specific water channels (AVT-stimulated aquaporins) and electrolyte epithelial channels (Fig. 2; Guo et al. 2003, Suzuki et al. 2007, Hillman et al. 2009, Suzuki and Tanaka 2009, Hillyard and Willumsen 2011). In the terrestrial environment, these notable skin characteristics (highly permeable, heavily vascularized and physiologically active) allow an efficient pathway for gas exchanges, and water and electrolyte absorption (transepidermal water absorption, TWA) but represent a disadvantage for water retention and make amphibians highly sensitive to transepidermal evaporative water loss (TEWL) (Shoemaker and Nagy 1977, Feder and Burggren 1984, Spotila et al. 1992, Shoemaker et al. 1992, Lillywhite 2006, Hillman et al. 2009). Amphibians experiencing a bi-directional water flux across their skin generally characterized by a permanent and obligatory (passive) TEWL through the dorsum, and an active TWA that takes place specifically through specialized ventral skin regions in contact with moistened substrates. A TWA occurs when an osmotic and an electrochemical gradients across the skin is established. This is accomplished by the active hormonal-AMP-regulated pathways of water and electrolyte transport, and by a vascular perfusion of the *s. spongiousum* (McClanahan and Baldwin 1969, Shoemaker and Nagy 1977, Shoemaker et al. 1992, Hillman et al. 2009, Guo et al. 2003, Hillyard and Willumsen 2011). Consequently, the amphibian skin represents the key organ in maintaining homeostatic functions, and especially water and electrolytes equilibrium.

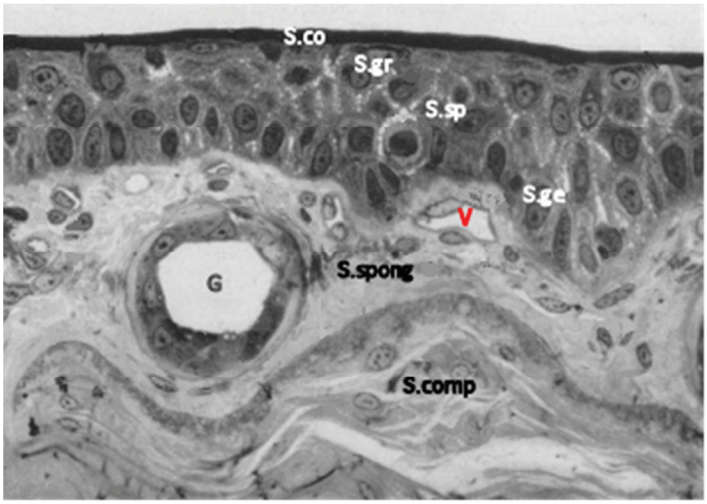

Fig. 1. Cross-section of abdominal skin from *Rana pipiens* showing the general organization of the epithelial cell layers. The epidermis is a stratified epithelium composed of the *stratum corneum* (S.co), the *stratum granulosum* (S.gr), the *stratum spinosum* (S.sp), and the basal *stratum germinativum* (S.ge). The underlying dermis includes the *stratum spongiousum* (S.spong) that contains blood vessels (V) and skin glands (G), and the *stratum compactum* (S.comp) that contains a network of collagen fibers (from Farquhar and Pallade 1964).

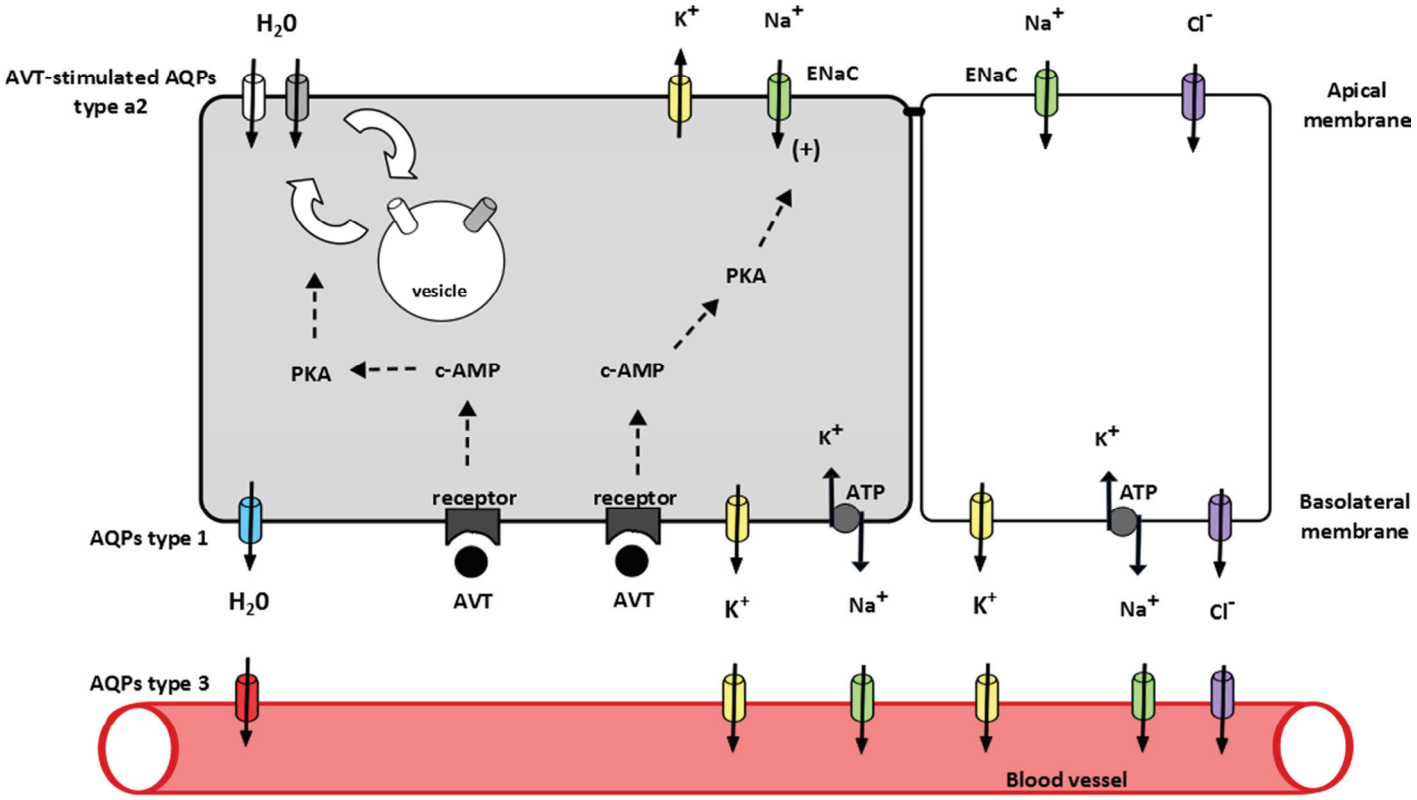

Fig. 2. Schematic drawing of the pathway for water and electrolytes absorption across the specialized ventral skin regions in anurans. Principal cells (grey) and mitochondria-rich cells (white) of the epidermis (from the *s. granulosum* to the *s. germinativum*) can be represented as a single compartment bounded by an apical and basolateral membrane. Na^+ is moved across the epidermis

via epithelial channels (ENaC) in the apical membrane and via Na^+/K^+ ATPase in the basolateral membrane. Note that, apical entry of Na^+ is regulated by arginine vasotocin (AVT) binding to specific receptors and stimulating a cyclic AMP (c-AMP) – protein kinase A (PKA) pathway that increases the ENaC activity. The excess of K^+ absorbed by cells is recycled to blood vessel via K^+ channels in the basolateral membrane. The transepithelial potential difference generated drives the absorption of Cl^- by mitochondria-rich cells. The NaCl absorption generates an osmotic gradient that drives the absorption of water via aquaporins (AQPs). Water apical entry is regulated via AVT-c-AMP-PKA pathway as well, that stimulates the insertion of subapical vesicles containing specific AQPs, termed AVT-stimulated AQPs (belonging to type a2, specific to anurans). Water flow across the basolateral membrane is mediated by type 3 AQPs and continues into capillary networks via type 1 AQPs (adapted from Hillman et al. 2009, Suzuki and Tanaka 2009, and Campbell et al. 2012).

Mechanistic insights of water exchanges with atmospheric environment and evaporation driving phenomena (WEDP)

The basic law governing mass transfer of water in air at the molecular diffusion level is the Fick's first law. It describes the relationship of a diffusive mass flux of a gas component through a unit area as a function of the concentration gradient often expressed as the component density gradient (Jaynes and Rogowski, 1983). For water vapour diffusion, this relation can be described by an empirical statement corresponding to:

$$\vec{j}_D = -D\,\vec{\nabla}\rho_v \qquad (1)$$

where D is the diffusion coefficient of the water vapor in air and ($\vec{\nabla}\rho_v$) is the local vapor density gradient used to describe the driving force for molecular diffusion. The negative sign indicates that the mass diffusion is taking place in the direction of decreasing density of water vapour. Fick's equation suggests that the diffusive mass flux is primarily dependents on the ambient temperature since it determines the diffusion coefficient of water vapour in air and the maximum vapor density ρ_{vs} (Tracy et al. 1980, Jaynes and Rogowski, 1983). For convenience, the relative humidity (RH) of air is often introduced as:

$$\varphi = \frac{\rho_v}{\rho_{vs}(T)} \qquad (2)$$

The air motion also contributes to the water vapour mass flux through an advective (or velocity driven) flux that reads as:

$$\vec{J}_A = \rho_v \vec{U} \qquad (3)$$

where $\vec{U}$ is the air velocity.

The atmospheric variables (temperature, RH, and air motion) are properties of the physical environment and cannot be modified by the organism itself unless through microhabitat selections. The skin area that interacts with atmospheric environment depends primarily on intrinsic characteristics of the organism (i.e. morphology, shape, body mass) and can be modified through particular stereotyped behavioural adaptations in amphibians, termed the water-conserving postures (e.g. Alvarado 1967, Gehlbach et al. 1969, Tracy 1976, Poughet al. 1983, Shoemaker et al. 1992, Hillman et al. 2009).

Procedures for calculating mass transfer of water vapour have been detailed for the leopard frog (*Rana pipiens*) (Tracy, 1976). The empirical mechanistic evaporative model (under steady-state) is constructed by analogy with the convective heat transfer near a surface using an empirical correlation. It corresponds to the integral of the flux on the skin surface taking into account the vapour transport (described by equation (1) and (2)) in the boundary layer surrounding the animal (Box 2). The expression of the total mass flux J_v reads as:

$$J_v = \frac{A_e}{(R_s + R_{bl})}(\varphi_{skin}\rho_{vs\,skin} - \varphi_{\infty}\rho_{vs\,\infty}) \qquad (4)$$

where A_e is the skin area that interacts with the atmosphere, φ_{skin} and φ_{∞} are the RH at the skin surface and outside the boundary layer respectively, $\rho_{vs\,skin}$ and $\rho_{vs\,\infty}$ are the saturated water vapor density at the skin surface and outside the boundary layer respectively (at the

corresponding temperatures). $(R_s + R_{bl})$ represents the overall resistance to mass transfer of water vapor dependent on the resistance provided by the skin characteristics and the boundary layer, respectively. In most amphibian species (see Lillywhite 2006 for a review) skin characteristics provide negligible resistance to water movement across the multilayered epithelium (see also Box 1). Even the secretion of mucus, that plays a role in keeping the skin hydrated and moist, apparently does not affect TEWL (Shoemaker and Nagy 1977, Young et al. 2005, Lillywhite 2006). We neglect here the waterproof skin lipids secreted by specialized mucous glands in arboreal anuran species or waterproof extra-cutaneous cocoon in some aestivating xeric anuran species that provide considerably higher skin resistance to TEWL equivalent to that of some reptiles, birds and mammals, whose skin epidermis has a thick *stratum corneum* (Lillywhite 2006). Consequently, TEWL rate in most species is of the same magnitude as evaporation from a free water surface which has no capacity to limit evaporation from its surface. Under this assumption, the skin resistance R_s nullifies and the RH at the skin surface is maximum (φ_{skin} = 1). The inverse of R_{bl} is the mass transfer coefficient (h) which expresses the ability of water vapor molecules to transfer through the boundary layer. h is functionally related to both organismal and air variables (Tracy 1976, Spotila et al. 1992, Shoemaker et al. 1992) and is defined as:

$$h = \frac{1}{R_{bl}} = 0.3\left(\frac{D}{L}\right)\left(\frac{U_\infty L}{v}\right)^{0.6} \qquad (5)$$

where L is the characteristic length of the animal; for amphibians this parameter is defined as the snout-vent length (dependent on the body mass; see Hillman et al. 2009 for an empirical relationship), U_∞ is the air flow velocity on top of the boundary layer which represents, as discuss below, a forced advection, v is the kinematic viscosity of the air.

As described by the mechanistic models of Tracy (1976), the difference in saturated water vapour density across the skin and the water vapour diffusion coefficient are not the only physical factors determining TEWL. Under natural conditions, transport of water vapour by air motion (e.g. under an external air flow, such as wind, eq. (3)) is the most important environmental variable because it can considerably enhance TEWL rate compared to pure molecular diffusion (Debbissi et al 2003, Jodat and Moghiman 2012). With regards to the mass transfer coefficient (eq. (5)), Tracy's model of TEWL describes specifically a water vapour transport by molecular diffusion coupled with a WEDP. The WEDP is the **forced advection** mechanism, i.e. an external and permanent air flow governed by the Reynolds number (Re). This dimensionless number is the ratio (UL/v) which approximates the relative weight of the forced advection force (air flow velocity) versus viscous forces (v/L). However, Tracy's TEWL model is only valid under an external and permanent air flow velocity. In eq. (5), TEWL is dependent on the air flow velocity in such a way that for a lack of forced advection the amphibians TEWL (and more precisely the mass transfer coefficient) nullify. That is not realistic in accordance to the Fick's law (eq. (1)). Furthermore, terrestrial amphibians express water-conserving behaviours that consist generally in avoiding unfavourable ambient conditions (temperature, RH, and wind speed) by seeking microhabitat shelters (e.g. Pough et al. 1983, Dobkins et al. 1987, Shoemaker et al. 1992, Schwarzkopf and Alford 1996, Seebacher and Alford 2002, Browne and Paszkowski 2010) that could present especially a lack of wind, or very low values of wind speed.

A forced advection WEDP may not represent the only process influencing TEWL at relative small scale (i.e. relevant compared to relative small organisms as amphibians) since recent engineering and physical papers have described a **free advection** (autonomous) phenomenon in water droplets (e.g. Debbissi et al 2003, Shahidzadeh-Bonn et al. 2006,

Weon et al. 2011, Jodat and Moghiman 2012). In an initially quiescent air environment, water vapour molecules can be transported away from the evaporative area (that interacts with atmospheric environment) by the air motion generated by buoyancy, because all things being equal, humid air is lighter than dry air. The intensity of this free advection WEDP could be estimated by the dimensionless mass transfer Rayleigh number (Ra), which approximates the ratio of the buoyant (gravitational) forces (causing free mass transport mechanisms) versus viscous forces (working against it):

$$\mathrm{Ra} = \frac{g L^3 \Delta\rho}{v\, D\, \rho} \qquad (6)$$

where g is the gravitational acceleration, ρ is the humid air density and $\Delta\rho/\rho$ is the reduced humid air density across the skin. Situations providing a high Rayleigh number are likely to promote the free advection mechanism. However, experimental evidences of natural WEDP in initially quiescent atmosphere are currently scarce (Shahidzadeh-Bonn et al. 2006, Weon et al. 2011). The studies of Shahidzadeh-Bonn et al. (2006) and Weon et al. (2011) have focused on the evaporating behavior of small water droplets. In these studies, the theoretical predictions based on pure diffusion have recurrently under-estimated evaporation rate, thus suggesting that water evaporation in quiescent air is not purely diffusive. These authors suggested that the gradient of humid air density above water droplets could create an air flow susceptible to enhance water evaporation. The characteristic speed for the natural mass transport is estimated within a range from 1 $cm.s^{-1}$ (Shahidzadeh-Bonn et al. 2006) to 10 $cm.s^{-1}$ (Weon et al. 2011), thus supporting the hypothesis of a strong contribution of a free advection WEDP to the evaporation process.

Considering the limitation of the existing model proposed by Tracy, the situation of quiescent air would benefit from further studies. In this scope, the relative weight of

molecular diffusion, forced advection at low air velocity and free advection should be analysed with care in order to provide a realistic mechanistic model of TEWL for amphibians.

Effect of the microhabitat properties on TEWL

Water vapour transfers in ambient air that drive TEWL are controlled by the vapour concentration gradients imposed between the animal and its environment. Thus, the shape and nature of the microhabitat most probably have a crucial influence on the intensity of TEWL rate. As far as shelters, and specially soil cavities, are considered, several factors should limit the TEWL rate: geometric factors such as the volume of the shelter and the shape of its connection with the atmosphere, thermal factors such as the temperature decrease with depth in soils, hygrometric factors such as the moisture transfer from the soil to the air inside a cavity or the effect of transpiring vegetation. Such effects put forward the gap existing between the environmental conditions which are really imposed to the animal and the available meteorological data, generally acquired in a free atmosphere. Currently, few studies focused on the amphibian microhabitat characterisations (Seebacher and Alford 2002, Browne and Paszkowski 2010) and their effect on TEWL (Schwarzkopf and Alford 1996, Seebacher and Alford 2002). It is often based on climatic factors affecting the microhabitat selection by the means of radio-telemetry or radio-tracking which offer practical methods in microhabitat use studies, but are currently limited to large animals (e.g. Schwarzkopf and Alford 1996, Jehle et al. 2000, Seebacher and Alford 2002, Schabetsberger et al. 2004). Concerning small amphibian species (or juveniles), no currently available tracking apparatus could be used. This field of research remains widely opened and should bring extremely precious data to study the interaction between such small species and their environment.

Box 2. Boundary layers concept in mass transfer. The boundary layer applied to wet-skinned organisms corresponds to the volume of air surrounding the animal where the gradients of velocity and water vapour concentration are located. To facilitate the representation of these boundary layers, the skin interacting with atmospheric environment may be represented by an infinite plane surface (Fig. 3).

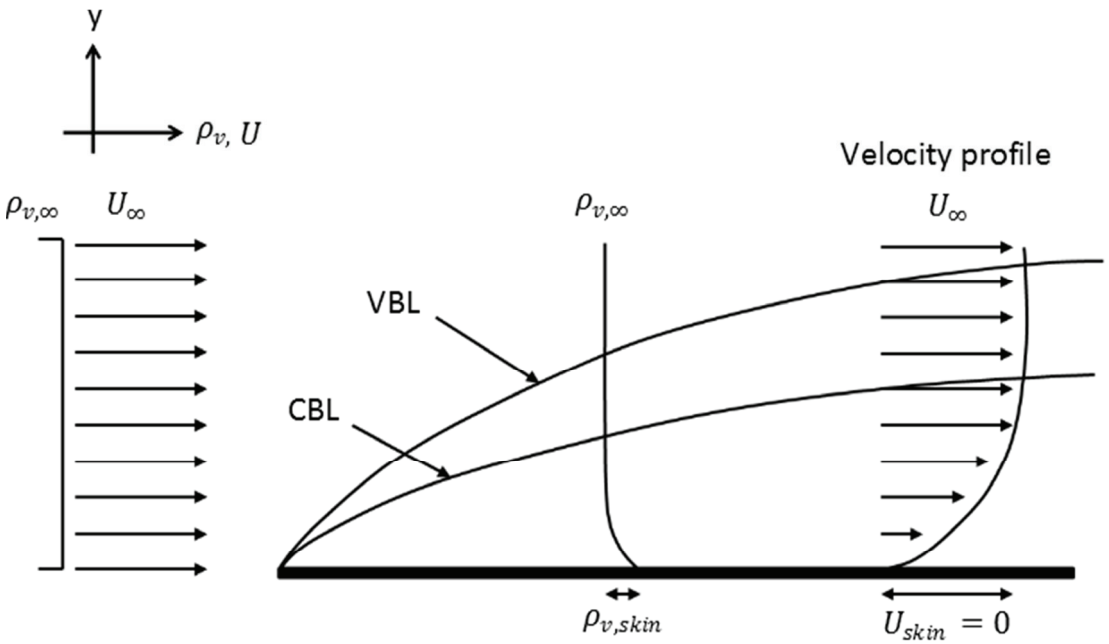

Fig. 3. Schematic showing one example of a concentration profile and mass transfer boundary layer (CBL) together with velocity boundary layer (VBL). (Redrawn from Datta 2002).

Consider a bi-dimensional permanent and laminar viscous air flow parallel to the skin, U is the local air flow velocity and U_∞ is the current air flow velocity. The classical no-slip condition imposes a null velocity on the animal skin ($U_{skin} = 0$). Depending on the shear stress (fluid viscosity), the velocity U increases from zero at the skin surface to U_∞. The volume presenting this velocity gradient is termed the velocity boundary layer (VBL). Its thickness is generally defined on the y-axis δ_v such as $(U_{(\delta_v)}/U_\infty) = 0.99$. Consequently the VBL is a region of low velocity adjacent to the skin surface that tends to become saturated with water vapour in which diffusion is the main mechanism of water transport. After having

crossed the VBL, water vapour molecules are transported away from the evaporative skin surface by the forced advection. In this way, the VBL imposes a resistance to the molecular diffusion of water vapour. Furthermore, the air velocity gradient generates a water vapour density distribution that varies from a density value $\rho_{v,skin}$ at the skin surface to a current value $\rho_{v,\infty}$ at the outer flow (with $\rho_{v,skin} > \rho_{v,\infty}$). This volume presenting a concentration gradient determines another boundary layer generally termed the concentration boundary layer (CBL) with a thickness defined as the y-axis δ_c such as $(\rho_{v,skin} - \rho_{(\delta_c)}) / (\rho_{v,skin} - \rho_{v,\infty}) = 0.99$. (See Sobey 2000, Schliting and Gersten 2004, Garde 2006 for complementary information). Numerous studies focused on the analysis of boundary layers since it allows a practical simplification of the general equations of fluid motion and mass transfer. It is thus possible to derive analytically friction and mass transfer coefficients.

Mechanistic insights of water exchange with substrate environment

The soil is the essential source of water for TWA in amphibians. By definition the soil is a heterogeneous porous medium composed of a solid matrix (the soil solid particles) and its geometric supplement, which is the porous space determined by particle heterogeneities. This porous space is occupied either by a liquid (commonly water) or a gas (commonly air) (Hillel 1998). The porous space can be thought as a random network of capillary tubes of varying size. Soil's physical properties, especially the pore-size distribution (larger pores *vs.* smaller pores) related to the soil structure and texture (e.g. sandy (coarse) *vs.* clayey (fine) soils) determine water flow process through the geometric characteristic of the porous spaces in which water is retained (by capillary forces, or **capillarity**) (Hillel 1998, Barari et al. 2009, Richards and Peth 2009, Genuchten and Pachepsky 2011, and see Box 3 Figs. 4a,b).

Given the complex hydraulic properties implicated in liquid water flow processes in **unsaturated** soils (soil potential hydric and hydraulic conductivity see Box 3), water exchanges between an amphibian and its substrate is difficult to describe. These exchanges are characterized by a diffusive mass transfer phenomenon of liquid water implying primarily the combination of capillary and effects involving active processes within the skin of the animal (Tracy 1976, Shoemaker et al. 1992, Spotila et al. 1992, Guo et al. 2003, Suzuki et al. 2007, Hillman et al. 2009, Suzuki and Tanaka 2009, Hillyard and Willumsen 2011). The general liquid water flow in unsaturated soils is described by the partial differential flow equation known as the Richards's equation ensuing from the Darcy's law for **saturated** soils (Hillel 1998, Barari et al. 2009, Genuchten and Pachepsky 2011). The general three-dimensional water potential (Ψ)-based formulation (see also Box 3 for parameter and function definitions) can be written:

$$\frac{\partial \theta}{\partial t} = -\nabla \cdot [K(\Psi)\nabla\Psi] + \frac{\partial K}{\partial z} \quad (7)$$

where the left hand side term is the accumulation of water expressed as the soil volumetric water content (θ) variation. Ψ is the soil hydric potential and $K(\Psi)$ is the hydraulic conductivity function strongly dependent on Ψ .The water flux driven by capillarity is defined as $q_c = -K(\Psi)\nabla\Psi$. The water flux driven by gravity is defined as $q_g = K(\Psi)$ along z direction. The Richards equation, due to both strongly nonlinear and **hysteretic** functions $\theta(\Psi)$, $\mathrm{K}(\Psi)$, cannot be solved analytically except in special cases (Hillel 1998). The generalized transient-state model describing water exchange between the frog *R. pipiens* and an unsaturated soil developed by Tracy (1976) offers an analytical solution of the Richards's equation assuming constant soil properties and the frog water potential. Given

the complex description of the Tracy's model, we opt for the simplified model described by Spotila et al. (1992) as:

$$\frac{dm}{dt} = A_v\, K'(\Psi - \Psi_a) \quad (8)$$

where (dm/dt) is the TWA rate through a given skin area in contact with the soil (A_{v}), K' is an overall mass transfer coefficient taking into account both the hydraulic conductivity of soil and frog, and $(\Psi - \Psi_a)$ is the driving force of water uptake described by the water potential gradient between the soil (Ψ) and the frog (Ψ_a). As for TEWL, the skin area in contact with the substrate depends on intrinsic characteristics of the organism and can be modified through particular postures (termed drinking postures) allowing the establishment of a close contact between the specialized ventral skin regions and thus promote TWA from moist surfaces (Shoemaker et al. 1992, Hillman et al. 2009). For amphibians, the water potential defines an osmotic potential, which is considered as a "suction" force functionally related to the osmotic concentration of the body fluids of the animal (*C*), and consequently to the hydration level, by the general equation $\Psi_a = CRT$, where *R* is the gas constant and *T* the amphibian body temperature (Shoemaker et al. 1992, Spotila et al. 1992, Hillman et al. 2009). As suggested by the empirical model, an amphibian is theoretically able to take up water from a soil when its water potential is more negative than that of the soil. However, given the effect of soil texture on soil water retention (Box 3 Fig. 4a) it would be more difficult for an amphibian to take up water from clayley soils than sandy soils. During amphibian dehydration, the concentration of its body fluids increases and its ability to take up water (its "suction force") increases. Consequently, all beings equal, a dehydrated amphibian presents a TWA rate more important than fully hydrated one, and it can absorb water from drier soils. The lowest water potential at which TWA occurs is termed the

absorptive threshold (Spight 1967). One should note that there is interspecific variation in TWA rates and in the absorptive threshold which seems to be related to habitat moisture availability, as well as phylogenetic difference (Spight 1967, Spotila 1972, Shoemaker et al. 1992, Hillman et al. 2009). While some xeric amphibians are able to generate water potentials beyond -200 kPa, species from the temperate zone generate water potentials generally between -80 and -200 kPa. Such thresholds reflect the dehydration tolerance of these organisms (see below).

Liquid water uptake mathematical models based on the Richards equation (Tracy 1976, Spotila et al. 1992) have been never improved yet, despite several empirical and theoretical relationships on soil hydraulic properties $\theta(\Psi), K(\Psi)$ available for a large number of soils (Genuchten 1980, Leij et al. 1997, Hillel 1998, Kosugi et al. 2002, Barari et al. 2009, Genuchten and Pachepsky 2011). Furthermore, the amphibian skin is a critical active pathway of TWA and the models should consider now the major active phenomena of the amphibian skin implying changes in biological variables such as the skin hydraulic conductivity and/or the osmotic potential of the animal. In fact TWA depends on the hormonal state of the animal. For example Arginine vasotocin (AVT) (see box 1) modifies the hydraulic conductivity of the specialized ventral skin regions (Hillyard and Willumsen 2011).

Currently, the study of Guo et al. (2003) is the only mechanistic paper considering an empirical model of water absorption across the amphibian skin coupled with the active electrolyte transport at the apical membranes of the *stratum granulosum* cells (specifically Na^+, Cl^-). The authors have developed a two-barrier functional compartment model that considers the amphibian skin as a well-stirred compartment in series contrarily to the models of Tracy (1976) and Spotila (1992). However, as discussed above, TWA requires also an active epithelial water transport through water channels (i.e. aquaporins) and a vascular

perfusion. The integration of these active biological process implicated in TWA in actual and future mathematical models is an important step for biophysical ecology studies.

Box 3. Hydraulic properties of unsaturated soil: basic understandings. The "suction" force with which a given soil retains water is termed the soil water potential (negative values) which is the result from the effect of capillary forces (capillarity). By convention, free water surface is taken as a reference for capillary forces and is assigned a value of zero. Capillary forces are the results of complex interactions between the solid matrix and the fluid phases. It depends on the surface tension of the liquid phase, the contact angle between the solid matrix and the liquid phase, and the geometric characteristic of the porous spaces. Liquid/gas interfaces apply a mechanical force on the water phase. The classical situation of a high wettability soil material tends to promote a preferential accumulation of liquid water in the smallest pores of the soil. As a result, the suction reaches higher values for low volumetric water content. The complex relationship between water content and soil water potential is commonly referred to as the soil water retention curve $\theta(\Psi)$ (Fig. 4a). The ability of a soil to transmit water is termed the soil hydraulic conductivity (K) which depends strongly on the distribution of water in the porous medium (Fig. 4b). The saturated hydraulic conductivity K_s is reached when the soil is saturated by water and is the maximum of the function K. It decreases strongly as the soil desaturates since only the smaller pores are available for water flow. These complex relationships $\theta(\Psi)$ and $K(\Psi)$ are commonly termed the soil hydraulic conductivity curves. The knowledge of soil water retention curves and soil hydraulic conductivity curves is essential for describing water flow in unsaturated porous media. They are strongly nonlinear functions and are subject to hysteresis phenomena.

These relationships have been experimentally measured for a large number of soils and empirical or theoretical based equation have been derived to predict them (see Genuchten 1980, Leij et al. 1997, Kosugi et al. 2002, Hillel 1998, Barari et al. 2009, Richards and Peth 2009, Genuchten and Pachepsky 2011 for complementary information).

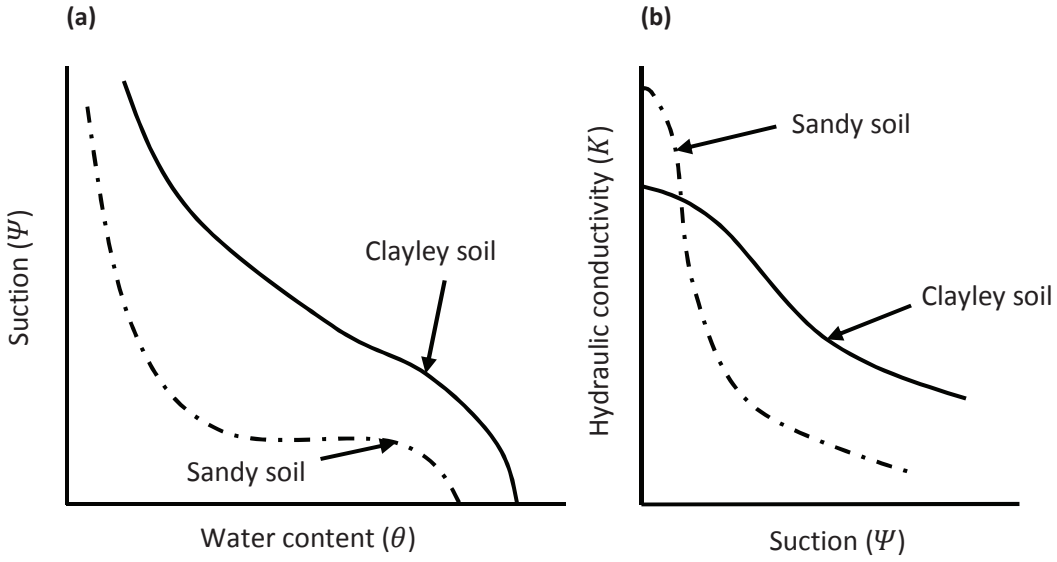

Fig. 4. (a) The effect of soil texture on soil water retention. The suction reaches higher values (more negative) for low volumetric water content; (b) Dependence of soil hydraulic conductivity on suction in different soils (log-log scale). (Redrawn from Hillel 1998).

Dehydration tolerance

As previously indicated there are very few physiological adaptations for coping with harsh environmental conditions and maintain body water equilibrium. They mainly rely on behaviour, such as microhabitat selection and/or the adoption of characteristics postures to limit TEWL and promote TWA. However, one of the unique capacities of amphibians is their ability to resist to high levels of body water loss. The limit of dehydration tolerance is usually referred to as the "critical activity point", and expresses the percentage of body water loss at which an amphibian is unable to right itself when flipped on its dorsum (Ray 1958). Dehydration requires some tolerance to the increasing concentration of body fluids (i.e. the

hyper-osmotic stress), which from a certain threshold is likely to generate serious problems in blood circulation and systemic physiology (as a reduced cardiovascular capacity, due to an increase in blood viscosity) leading to a reduction in oxygen availability and in the functioning of cells and organs, and ultimately to death (see Shoemaker et al. 1992, Withers & Hillman 2001, Hillman et al. 2009). Two mechanisms appear to be necessary for a greater tolerance to dehydration: i) a cardiovascular specialization (related to the ventricular mass, and to the organism's aerobic capacity or its tolerance to a reduced oxygen availability); and ii) a systemic circulation tolerance to hyper-osmolality. In general, anurans have a higher tolerance to dehydration than urodeles (30-50% *versus* 10-35%), and the tolerance is related to their extent of terrestriality (Ray 1958, Spight 1968, Alvarado 1972, Marangio and Anderson 1977, Pough et al. 1983, Shoemaker et al. 1992, Hillman et al. 2009).

A pathogen as a biotic factor influencing water transfers in amphibian skin?

Biotic factors, in the same way as the abiotic factors, might influence water transfers of wet-skinned organisms. For amphibians, their skin is a moist and also a nutritive substrate on which microorganisms can flourish. The critical importance of the skin in this taxon in maintaining homeostasis functions (water, electrolytes) (Box 1) makes amphibians extremely sensitive to potential skin pathogens. However, the amphibian skin synthesizes and secretes (via the skin glands) defensive antibiotic peptides that would prevent microbe proliferation (Rollins-Smith and Woodhams 2011).

The most notable example is the skin pathogenic fungus *Batrachochytrium dendrobatidis* (*Bd*) responsible to chytridiomycosis an emergent skin disease (Berger et al. 1998, Kilpatrick et al. 2010, Rosenblum et al. 2010, Voyles et al. 2011). Chytridiomycosis is a potentially lethal skin infection of amphibian implicated in numerous amphibian population declines

and extinction throughout the world (Rachowicz et al. 2005, Skerrat et al. 2007, Fisher et al. 2009, Kilpatrick et al. 2010, Blaustein et al. 2012). Not all amphibian species are susceptible to the pathogen. *Bd* pathogenicity studies have become a focal point of recent ecophysiology research since this keratinophilic pathogen colonizes the superficial dead and living cell layers of the epidermis, i.e. the *stratum corneum* and the *stratum granulosum* (Berger et al. 2005) which is the active pathway for water and electrolytes transport (Box 1). The reproductive lifecycle of *Bd* in amphibian epidermis is well documented (see Berger et al. 2005, Rosenblum et al. 2008, Killpatrick et al. 2010, Voyles et al. 2011, Van Rooij et al. 2012). *Bd* takes few days to colonise the epidermis, its whole life cycle taking 4-5 days (Berger et al. 2005). It produces toxins and other active compounds either before or after infection (Blaustein et al. 2005, Rosenblum et al. 2008). Colonization gives rise to pathological abnormalities including epidermal thickening (hyperplasia and hyperkeratosis), excessive shedding of the epidermis and other complex pathological changes at the cellular level (Berger et al. 1998, Berger et al. 2005, Voyles et al. 2009, Carver et al. 2010). Consequently, two major, non-mutually exclusive, mechanisms have been proposed (Berger et al. 1998, Berger et al. 2005, Pessier et al. 1999) to explain how a pathogen restricted to the superficial epidermis leads to global amphibian declines and numerous species extinction: i) the epidermal thickening can physically block transepidermal mass transfers, and/or ii) fungal toxins (or other active compounds) released by the pathogen, can interfere with critical active homeostasis functions of the outermost living cells of the epidermis (the epidermal dysfunction hypothesis), leading to water and electrolytes imbalance and ultimately to death. Recent laboratory studies suggest impairments of the normal epidermis homeostasis functions in *Bd* infected frogs, as electrolytes depletion (Na^+, K^+ and Cl^-), osmotic imbalance (Voyles et al. 2007, Voyles et al. 2009, Marcum et al. 2010, Voyles et al.

2012) and disruption in the ability of TWA with no effects on TEWL (Carver et al. 2010), that are more pronounced at the terminal stages of the disease. However mechanisms of impairments of the normal homeostasis epidermis functions still remains unclear. The study of Rosenblum et al. (2008) supports the role of fungal toxins in the pathogenesis of *Bd*, which may be driven by zoospores (immature stage) and zoosporangia (mature stage) secretions. More interestingly, the recent in vitro study of Brutyn et al. 2012 reports rapid (< 4 hours) alterations of the *Xenopus laevis* epidermis structural integrity after the exposure with *Bd* zoospore secretions. Because amphibian epidermis is the key organ involved in maintaining homeostasis functions, disruption of the epidermis structure can compromise a number of critical active water and electrolytic pathways (Voyles et al. 2009, Carver et al. 2010, Marcum et al. 2010, Rosenblum et al. 2012, Voyles et al. 2012). To date the strongest evidence available suggests disruption of epithelial electrolyte channels function. The study of Voyles et al. (2009) in infected White's tree frogs (*Litoria caerulea*) demonstrated reduced sodium and chloride channel activity in epidermis leading ultimately to death through deterioration of cardiac electrical function (Voyles et al. 2009). Furthermore the study of Rosenblum et al. (2012) demonstrated a decreased expression of sodium channel genes in infected *Rana muscosa* and *Rana sierrae*, and suggests an indirect electrolytes imbalance caused by physical disruption of the epidermis, probably via fungal toxins (Rosenblum et al. 2008).

These recent studies greatly support the epidermal dysfunction hypothesis through disruption of active electrolyte pathways via fungal toxins. No evidences show that epidermal thickening can physically block transepidermal mass transfers. Given that maintaining an osmotic gradient (allowing a TWA) is primarily accomplished by the active pathways of electrolyte transport (Box 1), such disruption seems able to diminishing the

osmotic potential of amphibians, and thus reduced their ability to absorb water from water and moist substrates (Carver et al. 2010). Additionally, the pathogen has the possibility to rapidly disrupt homeostasis function of the amphibian skin. However, the influence of *Bd* on amphibian water relations with their terrestrial environment will require further investigations to a better understanding of these underlying mechanisms.

Box 4. Towards an original approach to study the organism-environment water relations.

In wet-skinned ectotherms the exchange of water, electrolytes, energy, etc. takes place through a unit skin surface area. In amphibians, the overall skin surface can be divided in three main functional areas: the evaporative surface area that interacts with the atmosphere and that controls TEWL, the ventral surface area in contact with the substratum that controls TWA, and the skin surface area in contact with other skin surfaces, which could be used by the animal when expressing water-conserving postures to limit TEWL rates (Tracy 1976). Currently, no practicable non-invasive methods are available to precisely estimating these functional surface areas (e.g. McClanahan and Baldwin 1969, Tracy 1976) because of the complex morphology of amphibians, especially when they express water-conserving postures (see Alvarado 1967, Gehlbach et al. 1969, Pough et al. 1983). Scanner-based non-invasive virtual sectioning techniques (whole-body Computed Tomography (CT) scanning, and Magnetic Resonance Images (MRI) (see Laforsh et al. 2012 for details) represent potentials appropriate digital imaging methods to model the complex outer morphology of an organism (Fig. 5). Both CT and MRI contain two-dimensional information (from each single slice of the image stacks produced by CT and MRI), as well as three-dimensional information of the scanned object, that consist of 3D pixels (called voxels, or volume

elements) which accurately reflect its volume and surface information. However, the generation of 3D-views of the data sets requires indispensable methodology of computerized 3D-reconstruction with appropriate computer softwares (Jacinto et al. 2012, Kéchichian et al. 2011, Laforsh et al. 2012). The 3D data are obtained in standard format that makes them suitable for simulation applications. Thus, these 3D geometries may be incorporated in modelling tools (e.g. multiphysics engineering modelling and simulation software) to develop 3D numerical analyses of any physics-based system (water evaporation process, water transfers in porous media etc.) carrying the surface areas and volume information of the scanned object. Digital imaging and computerized 3D-modeling is a promising technique in biophysical ecology, which would open original ways to study water, as well as energy, exchanges between an organism and its physical environment.

Concluding remarks and future research needs

Our goal here was to review understandings of the major mechanisms and phenomena (abiotic and biotic) in amphibians implicated in the physical organism-environment water relations. We highlighted the future research needs in the field of the biophysical ecology concerning the water transfers in amphibians and other wet-skinned taxa, i.e. i) the necessity to develop mathematical model of TEWL in quiescent air in order to provide a complementary model to the Tracy's one, but also to determine if the free advection is a necessary phenomenon to explain TEWL rate in calm air, ii) the requirement to revisit the model of TWA on soil substrate in the light of the large number of equations that have been derived to predict hydraulic properties of unsaturated soils, and especially in the light of the critical physiological processes involved in TWA (electrolyte and aquaporin epithelial channels, vascular perfusion), and iii) the necessity to understand how biotic factors (such as

skin pathogens) might affect the water relations (TEWL, TWA) of wet-skinned organisms with their environment, which are important factors to take into account in the regulation of homeostasis. In a context of climate change, these topics are critical to predict how amphibians might be affected in their physical relations with the environment, and represent an urgent interdisciplinary challenge in the field of biological conservation. Furthermore, the accessibility to modern modelling tools and recent technological and algorithmic advances (e.g. scanner-based non-invasive virtual sectioning techniques, multiphysics engineering modelling and simulation software) (Box 4) may allow to model and simulate these water transfers taking into account the specific intrinsic characteristics (skin resistance to water evaporation and absorption, hydraulic conductivity, postures etc.) and the active mechanisms of these wet-skinned organisms, involved in water transfers. This would contribute to open original modelling approaches to study the wet-skinned organism-environment relations and considerably improve our knowledge of the effects of local and global environmental changes on individuals and populations.

Thesis aim

Focusing on an amphibian species, the palmate newt (*Lissotriton helveticus*), my thesis aims at:

i) Evaluating the intrinsic characteristics of this species involved in and influencing TEWL (i.e. skin resistance to evaporation, water-conserving postures) [chapters 1, 2, 3]

ii) Setting up innovative approaches to measure and model accurately the functional surface areas of their skin that contribute to TEWL and TWA [chapters 1, 2]

iii) Establishing laws of water transfers between *L. helveticus* and its physical environment in quiescent air, including effects related to changes in environmental parameters (temperature, RH) in order to model and predict TEWL in a large range of temperature and relative humidity [chapter 2]

iv) Improving our understandings on the physiological responses to the potentially lethal emergent skin pathogen *Batrachochytrium dendrobatidis* [chapter 3].

The Palmate newt constitutes an excellent model for such studies because this species corresponds to a semiterrestrial amphibian which may spend considerable amounts of time in the terrestrial environment (but return to water in order to breed), and are active during the warmest months of the year. Moreover, this species is highly sensitive to TEWL due to its elongated shape and small size, which defined a high body surface to volume ratio (all things being equal, smaller species lose water through a greater area, relative to their body volume, than larger species). Finally, Palmate newts are known to be affected by the skin pathogen *Batrachochytrium dendrobatidis* in the wild (Dejean et al. 2010).

Symbols / S.I. Units

A_e = evaporative skin surface area [m²]

A_{v} = ventral skin surface area in contact with the substratum [m²]

D = diffusion coefficient of the water vapour in air [$m^2.s^{-1}$]

φ = relative humidity [$0 > \varphi > 1$]

g = gravitational acceleration [$m.s^{-2}$]

h = mass transfer coefficient [$m.s^{-1}$]

J = mass flux [$kg.s^{-1}$]

K = soil hydraulic conductivity [$m.s^{-1}$]

K' = mass transfer coefficient [$kg.s^{-1}.m^{-2}.kPa^{-1}$]

L = characteristic length [m]

v = kinematic viscosity of the air [$m².s^{-1}$]

R_{bl} = resistance to TEWL provided by the boundary layer [$s.m^{-1}$]

R_s = skin resistance to TEWL [$s.m^{-1}$]

U = air flow velocity [$m.s^{-1}$]

θ = soil water content [$0 > \theta > 1$]

ρ = humid air density [$kg.m^{-3}$]

ρ_v = water vapour density [$kg.m^{-3}$]

$\vec{\nabla}\rho_v$ = local vapour density gradient [$kg.m^{-3}.m^{-1}$]

$\rho_{vs}(T)$ = water vapour density in air at saturation [$kg.m^{-3}$], dependents from temperature (T)

Ψ = soil water potential [kPa]

Ψ_a = amphibian water potential [kPa]

Subscripts

A = advection

D = diffusion

v = water vapour

Glossary Box

Arginine vasotocin (AVT) is an antidiuretic hormone (ADH) released from the neurohypophysis (in the central nervous system) in the regulation of water and electrolyte balance and other homeostatic functions.

Capillarity expresses the tendency of a liquid to enter into the narrow pores within a porous media, due to the combination of the cohesive forces within the liquid (expressed in its **surface tension**) and the adhesive forces between the liquid and the solid (expressed in their **contact angle**).

Ectotherms by definition are organisms that obtain heat primarily from the external environment. All ectotherms generate at least some heat from internal physiological reactions but are relatively small or negligible in controlling body temperature.

Forced advection is a mechanism in which fluid motion is generated by an external source.

Free advection termed also natural advection is a mechanism in which the fluid motion is only generated by density difference in the fluid due to the humid air density gradient.

Homeostasis represents the stability of physiological systems that maintain life; such as body temperature, body water, pH level etc. that are maintained over a narrow range, as a result of their critical role in survival.

Hysteresis is defined as the difference in the relationship between, for example, the water content of the soil and the corresponding water potential obtained under wetting and drying processes.

Saturation of a soil expresses the water volume present in the soil relative to the pore space. The degree of saturation of a soil ranges from zero in completely **unsaturated** dry soil to unity in a completely **saturated** soil.

LITERATURE CITED

Alvarado RH (1967) The significance of grouping on water conservation in *Ambystoma*. *Copeia* 3:667-668

Alvarado RH (1972) The effects of dehydration on water and electrolytes in *Ambystoma tigrinum*. *Physiol Zool* 45:43-53

Audette M, Rivière D, Ewend M, Enquobahrie A, Valette S (2011) Approach-guided controlled resolution brain meshing for FE-based interactive neurosurgery simulation. Workshop on Mesh Processing in Medical Image Analysis, in conjunction with MICCAI 2011, Toronto, Canada, 176-186

Barari A, Omidvar M, Ghotbi AR, Ganji DD (2009) Assessment of wáter penetration problema in unsaturated soils. *Hydrol Earth Sci Discuss* 6:3811-3833

Bellard C, Bertelsmeier C, Leadley P, Thuiller W, Courchamp F (2012) Impacts of climate change on the future of biodiversity. *Ecol let* 15:365-377

Berger L, Hyatt AD, Speare R, Longcore JE (2005) Life cycle stages of the amphibian chytrid *Batrachochytrium dendrobatidis*. *Dis Aquat Org* 68:51-63

Berger L, Speare R, Daszak P, Green DE and 10 others (1998) Chytridiomycosis causes amphibian mortality associated with population declines in the rain forests of Australia and Central America. *Proc Natl Acad Sci USA* 95:9031-9036

Blaustein AR, Gervasi SS, Johnson PTJ, Hoverman JT, Belden LK, Bradley PW, Xie GY (2012) Ecophysiology meets conservation: understanding the role of disease in amphibian population declines. *Phil Trans R Soc B* 367:1688-1707

Bozinovic F, Calosi P, Spicer JI (2011) Physiological correlates of geographic range in animals. *Anu Rev Ecol Evol Syst* 42:155-179

Browne CL, Paszkowski CA (2010) Hibernation sites of western toads (*Anaxyrus boreas*): characterization and management implications. *Herpetol Cons Biol* 5:49-63

Brutyn M, D'Herde K, Dhaenens M, Van Rooij P and 8 others (2012) *Batrachochytrium dendrobatidis* zoospore secretions rapidly disturb intercellular junctions in frog skin. *Fungal Genet Biol* 49:830–837

Campbell CR, Voyles J, Cook DI, Dinudom A (2012) Frog skin epithelium: electrolyte transport and chytridiomycosis. *Inter J Biochem Cell Biol* 44:431-434

Carver S, Bell BD, Waldman B (2010) Does chytridiomycosis disrupt amphibian skin function? *Copeia* 2010:487-495

Datta AK (2002) Diffusion mass transfer: unsteady-state. In: Biological and bioenvironmental heat and mass transfer. Cornell University, New York pp. 285-305

Debbissi C, Orfi J, Nasrallah SB (2003) Evaporation of water by free or mixed convection into humid air and superheated steam. *Int J Heat Mass transfer* 46:4703-4715

Dejean T, Miaud C, Ouellet M (2010) La chytridiomycose : une maladie émergente des amphibiens. *Bull Soc Herp Fr* 134:27-46

Dobkins DS, Gettinger RD, O'Connor MP (1989) Importance of retreat site for hydration state in *Bufo marinus* during dry rainy season. *Am Zool* 29:88A

Farquhar M, Palade GE (1965) Cell junctions in amphibian skin. *J Cell Biol* 26:263-291

Feder ME, Burggren WW (1985) Cutaneous gas exchange in vertebrates: design, patterns, control and implications. *Biol Rev* 60:1-45

Fisher MC, Garner TWJ, Walker SF (2009) Global emergence of *Batrachochytrium dendrobatidis* and amphibian chytridiomycosis in space, time, and host. *Annu Rev Microbiol* 63:291-310

Fisher MC, Henk DA, Briggs CJ, Brownstein JS, Madoff LC, McCraw SL, Gurr SJ (2012) Emerging fungal threats to animal, plant and ecosystem health. *Nature* 484:186-194

Gehlbach FR, Kimmel JR, Weems WA (1969) Aggregations and body water relations in tiger salamanders (*Ambystoma tigrinum*) from the Grand Canyon rims, Arizona. *Physiol Zool* 42:173-182

Guo P, Hillyard SD, Fu BM (2003) A two-barrier compartment model for volume flow across amphibian skin. *Am J Physiol Integr Comp Physiol* 285:R1384-R1394

Hillel D (1998) Flow of water in unsaturated soil. In: Hillel D (ed.) Environmental soil physics pp. 203-242

Hillman SS, Withers PC, Drewes RC, Hillyard SD (2009) Ecological and environmental physiology of amphibians. Oxford University Press

Hillyard SD, Willumsen NJ (2011) Chemosensory function of amphibian skin: integrating epithelial transport, capillary blood flow and behaviour. *Acta Physiol* 202:533-548

IPCC (2007) Working group I report, climate change 2007: "the physical science basis". The fourth assessment report of the intergovernmental panel on climate change, Paris

Jacinto H, Kéchichan R, Desvignes M, Prost R, Valette S (2012) A Web Interface for 3D Visualization and Interactive Segmentation of Medical Images, Web3D 2012, Los-Angeles, USA, 2012. RTF Tagged XML BibTex Google Scholar

Jaynes DB, Rogowski AS (1983) Applicability of Fick's law to gas diffusion. *Soil Sci Soc Am J* 47:425-430

Jehle R, Arntzen JW (2000) Post-breeding migration of newts (*Triturus cristatus* and *T. marmoratus*) with contrasting ecological requirements. *J Zool London* 251:297-306

Jodat A, Moghiman M (2012) An experimental assessment of the evaporation correlation for natural, forced and combined convection regimes. *Proc IME C J Mech Eng Sci* 226:145-153

Kearney M, Porter W (2009) Mechanistic niche modelling: combining physiological and spatial data to predict species'ranges. *Ecology Letters* 12:334-350

Kéchichan R, Valette S, Desvignes M, Prost R (2011) Efficient Multi-Object Segmentation of 3D Medical Images Using Clustering and Graph Cuts. IEEE International Conference on Image Processing, Brussels, Belgium, 2196-2200

Kilpatrick AM, Briggs CJ, Daszak P (2010) The ecology and impact of chytridiomycosis: an emerging disease of amphibians. *Trends Ecol Evol* 25:109-118

Kosugi K, Hopmans JW, Dane JH (2002) Parametric models. In: Dane JH, Topp GC (eds.) Methods of soil analysis, part I, Physical methods, 3rd edn. Madison: SSSA, pp. 739-757

Laforsh C, Imhof H, Sigl R, Settles M, Heß M, Wanninger A (2012) Application of computational 3D-modeling in organismal biology. In: Alexandru C (ed), Modeling and simulation in engineering. InTech, Rijeka, pp. 117–142

Leij FJ, Russel WB, Lesh SM (1997) Closed-form expression for water retention and conductivity data. *Ground Water* 35:848-858

Lillywhite HB (2006) Water relations of tetrapod integument. J Exp Biol 209:202-226

Maclean IMD, Wilson RJ (2011) Recent ecological responses to climate change support predictions of high extinction risk. *PNAS* 108:12337-12342

Marangio MS, Anderson JD (1977) Soil moisture preference and water relations of the marbled salamander, *Abystoma opacum* (Amphibia, Urodela, Ambystomatidae). J Herpetol 11:169-176

Marcum RD, St-Hilaire S, Murphy PJ, Rodnick KJ (2010) Effects of *Batrachochytrium dendrobatidis* infection on ion concentrations in the boreal toad *Anaxyrus (Bufo) boreas boreas*. *Dis Aquat Org* 91:17-21

McClanahan L, Baldwin R (1969) Rate of water uptake through the integument of the desert toad, *Bufo punctatus*. *Comp Biochem Physiol* 28:381-389

Parmesan C (2006) Ecological and Evolutionary responses to climate change. *Annu Rev Ecol Evol Syst* 37:637-669

Pessier AP, Nichols DK, Longcore JE, Fuller MS (1999) Cutaneous chytridiomycosis in poison dart frogs (*Dendrobates spp.*) and white's tree frogs (*Litoria caerulea*). *J Vet Diagn Invest* 11:194-199

Pough FH, Taigen TL, Stewart MM, Brussard PF (1983) Behavioural modification of evaporative water loss by a Puerto Rican frog. *Ecology* 64:244-252

Rachowicz LJ, Hero JM, Alford RA, Taylor JW, Morgan JAT, Vredenburg VT, Collins JP, Briggs CJ (2005) The novel and endemic pathogen hypotheses: competing explanations for the origin of emerging infectious diseases of wildlife. *Conserv Biol* 19:1441-144

Ray C (1958) Vital limits and rates of desiccation in salamanders. *Ecology* 39:75-83

Richard BG, Peth S (2009) Modelling soil physical behavior with particular reference to soil science. *Soil and Tillage Research* 102:216-224

Rollins-Smith L, Woodhams D (2011) Amphibian immunity: Staying in tune with the environment. In: Demas GE, Demas G, Nelson RJ (eds.) Ecoimmunology. Oxford, United Kingdom: Oxford University Press; pp. 92143.

Rosenblum EB, Poorten TJ, Settles M, Murdoch GK (2012) Only skin deep: shared genetic response to the deadly chytrid fungus in susceptible frog species. *Mol Ecol* 21:3110–3120

Rosenblum EB, Stajich JE, Maddox N, Eisen MB (2008) Global gene expression profiles for life stages of the deadly amphibian pathogen *Batrachochytrium dendrobatidis*. *Proc Nat Acad Sci USA* 105:17034-17039

Schabetsberger R, Jehle R, Maletzky A, Pesta J, Sztatecsny M (2004) Delineation of terrestrial reserves for amphibians: post-breeding migrations of Italian crested newts (*Triturus c. carnifex*) at high altitude. *Biol Cons* 117: 95-104

Schwarzkopf L, Alford RA (1996) Desiccation and shelter-site use in a tropical amphibian: comparing toads with physical models. *Functional Ecology*. 10:193-200

Seebacher F, Alford (2002) Shelter microhabitats determine body temperature and dehydration rates of a terrestrial amphibian (*Bufo marinus*). *J Herpetol* 36:69-75

Shahidzadeh-Bonn N, Rafai S, Azouni A, Bonn D (2006) Evaporating droplets. *J Fluid Mech* 549:307-313

Shoemaker VH, Hillman SS, Hillyard SD, Jackson DC, McClanahan LL, Withers PC, Wygoda ML (1992) Exchange of water, ions, and respiratory gases in terrestrial amphibians. In: Feder E, Burggren WW (ed) Environmental Physiology of the Amphibians. University of Chicago Press, Chicago

Shoemaker VH, Nagy KA (1977) Osmoregulation in amphibians and reptiles. *Ann Rev Physiol* 39:449-471

Skerrat LF, Berger L, Speare R, Cashins S, McDonald KR, Phillott AD, Hines HB, Kenyon N (2007) Spread of chytridiomycosis has caused the rapid global decline and extinction of frogs. *EcoHealth* 4:125-134

Spight TM (1967) The water economy of salamanders: exchange of water with the soil. *Biol Bull* 132:126-132

Spight TM (1968) The water economy of salamanders: evaporative water loss. *Physiol Zool* 41:195-203

Spotila JR (1972) Role of Temperature and Water in the Ecology of Lungless Salamander. *Ecol Monogr* 1:95-125

Spotila JR, Berman EN (1976) Determination of skin resistance and the role of skin in controlling water loss in amphibians and reptiles. *Comp Biochem Physiol* 55A**:**407-411

Spotila JR, O'Connor MP, Bakken GS (1992) Biophysics of heat and mass transfert. In: Feder E, Burggren WW (ed) Environmental Physiology of the Amphibians. University of Chicago Press, Chicago

Stuart SN, Chanson JS, Cox NA, Young BE, Rodrigues ASL, Fishman DL, Waller RW (2004) Status and trends of amphibian declines and extinctions worldwide. *Science* 306:1783-1786

Suzuki M, Hasegawa T, Ogushi Y, Tanaka S (2007) Amphibian aquaporins and adaptation to terrestrial environments: a review. *Comp Biochem Physiol* 148A:72-81

Suzuki M, Tanaka S (2009) Molecular and cellular regulation of water homeostasis in anuran amphibians by aquaporins. *Comp Biochem Physiol* A 153:231-241

Thomas CD, Cameron A, Green RE, Bakkenes M and 15 others (2004) Extinction risk from climate change. *Nature* 427:145-148

Tracy CR (1976) A model of the dynamic exchange of water and energy between a terrestrial amphibian and its environment. *Ecol Monogr* 46:293-326

Tracy CR, Welch WR, Porter WP (1980) Properties of air: a manual for use in biophysical ecology. Third Edition, University of Wisconsin Technical Report

van Genuchten MT (1980) A closed-form equation for predicting the hydraulic conductivity of unsaturated soils. *Soil Sci Soc Am J* 44:892-898

van Genuchten MT, Pachepsky YA (2011) Hydraulic properties of unsaturated soils. In: Glinski J, Horabik J, Lipiec J (eds.) Encyclopedia of agrophysics pp. 368-376

van Rooij P, Martel A, D'Herde K, Brutyn M, Croubels S, et al. (2012) Germ Tube Mediated Invasion of *Batrachochytrium dendrobatidis* in Amphibian Skin Is Host Dependent. *PLoS ONE* 7(7): e41481. doi:10.1371/journal.pone.0041481

Voyles J, Berger L, Young S, Speare R, Webb R, Warner J, Rudd D, Campbell R, Skerratt LF (2007) Electrolyte depletion and osmotic imbalance in amphibians with chytridiomycosis. *Dis Aquat Org* 77:113-118

Voyles J, Vredenburg VT, Tunstall TS, Parker JM, Briggs CJ, Rosenblum EB (2012) Pathophysiology in Mountain Yellow-Legged Frogs (*Rana muscosa*) during a Chytridiomycosis Outbreak. *PLoS One* 7(4):e35374

Voyles J, Young S, Berger L, Campbell C and 7 others (2009) Pathogenesis of chytridiomycosis, a cause of catastrophic amphibian declines. *Science* 326:582-585

Weon BM, Je JH, Poulard C (2011) Convection-enhanced water evaporation. *AIP Advances* 012102

Withers PC, Hillman SS (2001) Allometric and ecological relationships of ventricle and liver mass in anuran amphibians. *Funct Ecol* 15:60-69

Young JE, Christian KA, Donnellan S, Parry D (2005) Comparative analysis of cutaneous evaporation water loss in frogs demonstrates correlation with ecological habits. *Physiol Biochem Zool* 78:847-856

CHAPTER ONE

Article submitted to *Frontiers in Zoology*

Article 1: **Modelling skin surface areas involved in water transfer in amphibians**

Thomas Wardziak[1]*, Laurent Oxarango[2], Sebastien Valette[3], Laurent Mahieu-Williame[3], and Pierre Joly[1]

[1] Université de Lyon; UMR 5023 Ecologie des Hydrosystèmes Naturels et Anthropisés; Université Lyon 1 ; ENTPE; CNRS; 6 rue Raphaël Dubois, 69622 Villeurbanne, France

[2] LTHE, Université de Grenoble, BP 53, 38041 Grenoble Cedex, France

[3] CREATIS-LRMN, Lyon, France

* Corresponding author (thomas.wardziak@orange.fr)

ABSTRACT: Magnetic resonance imaging (MRI)-based three dimensional (3D) reconstructions were used to derive accurate quantitative data on body volume and functional skin surface areas involved in water transfer in the palmate newt *Lissotriton helveticus*. Body surface area can be functionally divided into evaporative surface area that interacts with the atmosphere and controls the transepidermal evaporative water loss (TEWL), the ventral surface area in contact with the substratum that controls transepidermal water absorption (TWA), and the skin surface area in contact with other skin surfaces. That last surface area allows the evaporative surface area to be reduced when the animal adopts water-conserving postures. We generated 3D geometries of the newts via volume-rendering by a "segmentation" process carried out using a graph-cuts algorithm and a web-based interface. Our 3D geometries reproduced the two postures adopted by the palmate newt, i.e. an "I"-shaped posture characterized by a straight body without tail coiling, and a stereotyped "S"-shaped water-conserving posture, where the body is huddled up with the tail coiling along it. As a guide to the quality of the surface area estimations, we compared measurements of TEWL rates between living newts and their agar replicas reproducing the two postures. Whereas the newts did not show any physiological adaptations to restrain evaporation, they expressed an efficient "S"-shaped water-conserving posture with a resulting water economy of about 22.1 %, which is very close to the 23.6 % reduction in evaporative surface area measured using 3D analysis.

KEY WORDS: Amphibians; Evaporative water loss; Water-conserving behaviour; Water relations; Modelling; Image processing; Magnetic resonance imaging

INTRODUCTION

Understanding and predicting how environmental changes might affect amphibian relationships with the physical environment is a serious challenge to conservation biology. These wet-skinned ectotherms have a highly permeable, heavily vascularized and physiologically active skin across which a considerable amount of heat, gas and water are exchanged (Tracy 1976, Shoemaker and Nagy 1977, Feder and Burggren 1984, Spotila et al. 1992, Shoemaker et al. 1992, Lillywhite 2006, Hillman et al. 2009). They are thus closely linked to their physical environment by their skin surface, and are also highly sensitive to rapid environmental changes, when living on land, because of permanent and obligatory transepidermal water losses (TEWL). Modelling energy and water balance on the organism scale needs interdisciplinary knowledge of the physical laws that govern the conservation of energy and mass, the physiological and behavioural processes regulating (or not) the transfer, and the morphology of the organism under study. Models of dynamic exchanges of energy and mass were first established for the frog *Rana pipiens*, and are readily generalizable to other amphibian species (Tracy 1976, Shoemaker et al. 1992, Spotila et al. 1992, Hillman et al. 2009). These models consist of a set of equations involving both environmental and organismal variables and parameters, i.e. the intrinsic characteristics of the animal (body weight, hydration level, postures and thus the surface area across which mass transfer occurs, skin resistance to TEWL, etc.). When using these models, some variables are straightforward to measure (e.g. air temperature and relative humidity, wind speed, hydration level of the animal, skin resistance to TEWL, etc.), while others, such as skin surface area across which heat and water are exchanged with the environment, provide a real challenge. The total skin surface of an amphibian can be divided into three main

functional areas (Tracy 1976): the evaporative surface area that interacts with the atmosphere and controls TEWL, the ventral surface area in contact with the substratum, which controls trans-epidermal water absorption (TWA), and skin surface areas in contact with other skin surfaces, which could be used by the animal when adopting water-conserving postures to limit TEWL rates.

Currently, no feasible methods are available to directly and precisely estimate these functional surface areas, because of the complex morphology of amphibians, especially when they adopt water-conserving postures (see Alvarado 1967, Gehlbach et al. 1969, Spotila and Berman 1976, Pough et al. 1983, Wardziak et al. 2013). In some studies, euthanized amphibians were skinned and the area of each piece of skin determined by tracing its outline on graph paper (McClanahan and Baldwin 1969, Maina 1989). Other studies have used a electrolytic bath technique to evaluate the total surface area of model frogs cast in aluminium (Porter et al. 1973, Tracy 1976), as well as a planimeter to evaluate the impression of the ventral surface area made by frogs sitting on a clear surface (Tracy 1976). Recent technological advances in medical image acquisition and processing, e.g. whole-body computed tomography (CT) scanning and magnetic resonance imaging (MRI) adapted for small animals (see Laforsch et al. 2012) open up new possibilities for modelling complex morphologies and estimating functional surface areas in amphibians, thus providing new ways for studying the biophysical ecology and autecology of organisms.

On the other hand, in order to evaluate skin resistance to TEWL, agar replicas made from individual casts are commonly used and have proved to be useful for water loss studies (Spotila and Berman 1976, Buttemer 1990, Amey and Grigg 1995, Shwartzkopf and Alford 1996, Navas and Araujo, 2000, Tracy et al. 2007, Wardziak et al. 2013). Models made of 3% agar (97% water) have the advantage of evaporating water at the same rate as free water

surfaces (i.e. with no skin resistance to TEWL) (Spotila and Berman 1976, Amey and Grigg 1995) and thus represent closely the surface area of living animals.

In this paper, we present a MRI-based 3D reconstruction method to generate 3D geometries of amphibians, as shown here with the palmate newt, *Lissotriton helveticus*, in order to derive accurate quantitative data about the total surface area, volume, surface/volume ratio and the three functional skin surface areas (defined above) involved in water transfer. Our 3D geometries reproduce all the postures expressed by palmate newts when subjected to desiccation stress. We also attempt to quantify skin resistance to TEWL and the influence of water-conserving postures on TEWL rates for this species during its terrestrial phase, using agar replicas (following Spotila and Berman, 1976), in order to improve our knowledge on water exchange for this species with its physical environment.

MATERIALS AND METHODS

Animal collection

Adult male palmate newts *Lissotriton helveticus* (n = 10) were collected in May 2011 during their aquatic phase in forest ruts near Mépieu, France (05°26’28’’E, 45°43’56’’N). They were housed in aquaria providing both aquatic and terrestrial environments allowing them to leave the water. When they entered the terrestrial stage, they were housed individually in plastic boxes (19.0 x 16.5 x 9.5 cm) lined with moistened paper, renewed weekly. The boxes were kept in climate-controlled rooms at 20 ± 1°C, 60 ± 10 % of relative humidity under a 16:8 light:dark photoperiod. The newts were fed with small crickets *ad libitum*. All the experimental newts were released in their respective environments at the end of the experiments.

Acquisition of 3D geometries of living newts

As demonstrated by Wardziak et al. (2013), the palmate newt adopted two types of posture: the "I"-shaped posture characterized by a straight body with no tail coil, and the "S"-shaped posture when the body is huddled up with the tail coiled along it, which is considered as a stereotypic water-conserving posture. The aim of the experiment was to acquire 3D geometries of all the experimental newts in their two postures using MRI equipment. One day before MRI scanning, we standardized the water balance of the newts by installing each individual in a plastic Petri dish (h = 2.5 cm, Ø = 9 cm) filled with 15 mL of tap water for 24 h, thus allowing it to reach a standard weight (W_0) through TWA. W_0 was defined as the weight of a fully hydrated animal. A few minutes before the MRI scan, each newt was individually weighed (mean W_0 ± standard error (se): 0.5761 ± 0.0370 g) and then anesthetized in a solution of MS222. Each newt was then placed in the MRI system a first time to obtain a scan of its "I"-shaped posture, and a second time for its "S"-shaped posture. ^{1}H magnetic resonance images were carried out at 4.7 Tesla (200 MHz) using a Bruker Biospec MRI system equipped with Magnex gradient (100 mm i.d.), 400 mT/m maximum gradient strength and 390 µs rise time. Radio-frequency (RF) excitation and signal reception were accomplished using a quadrature coil (32 mm i.d., Rapid Biomedical GmBH). High-resolution MRI datasets were acquired using a T_1 weighted 3D FLASH sequence (TR = 15 ms, TE = 6 ms, flip angle = 15°). To avoid image distortion and surface calculation errors, an isotropic resolution of 200 x 200 x 200 μm^3 was used for a field of view of 50 x 30 x 20 mm^3 and a matrix encoding of 250 x 150 x 100 voxels for a total acquisition time of 3 min and 45 sec. The sequence was optimized to provide the best acquisition-time/resolution ratio. No image filtering was applied.

3D geometry segmentation and meshing

The purpose of the experiment was to analyse the volumes obtained by MRI (n = 20) to generate 3D geometries of living newts (thereafter numerical newts) (Fig. 1a) following two consecutive steps: for each volume, we segmented the newt image and generated a 3D triangular mesh representing its external surface. Segmentation was carried out with a graph-cuts algorithm. We used the approach proposed by Kéchichan et al. (2011), which is an improvement over Boykov and Jolly (2001), allowing for interactive segmentation of large volume images. For each volume, we manually labelled some parts belonging to the newt, and some parts belonging to the outside, thus providing the algorithm with clues as to what to extract from the image. The interactive nature of the approach made it easy to perform corrections whenever segmentation errors were found. Once the segmentation had been done, we obtained a volume with voxels labelled as inside or outside the animal. From this volume, we extracted the external surface of the newt, which was the surface between the two different labels. This was done using the approach proposed by Audette et al. (2011), which generates meshes suitable for simulations and guarantees the generated meshes to be manifold. We used a web-based interface (Jacinto et al. 2012) for the segmentation and meshing. Final "I" and "S" 3D geometries were converted to 1253 $\pm$ 4, and 1250 $\pm$ 5 mesh elements (means ± se), respectively.

Surface areas and volumes of the 3D geometries

The commercial package COMSOL Multiphysics 4.2 was used for the 3D analyses of the surface areas, volumes and surface/volume ratios of the numerical newts in their two postures. These 3D geometries were imported into COMSOL. The total surface area (A) and volume (V) of each numerical newt was estimated, as well as its total surface area/volume

ratio (AVR) and its three main functional surface areas (A_e : the evaporative surface area that interacts with the atmosphere, A_v : the ventral area in contact with the substratum, A_s : the skin surfaces in contact with other skin surfaces when the animals adopt the "S"-shaped water-conserving posture. COMSOL Multiphysics can evaluate the total surface area A and the total volume V of a numerical newt by using a surface integral taken over its external boundary and a volume integral over the domain shaped by this external boundary, respectively. The AVR ratio was deduced from the A and V values. The surface area A_e was computed using the same surface integration methodology, including a trigonometric criterion for mesh element selection. Comsol Multiphysics provided the Cartesian components (nx, ny, nz) of the normal vector n associated with each mesh element. The angle between this normal vector and the horizontal plane θ was calculated as

$$\theta = \arctan\left(\frac{n_z}{\sqrt{{n_x}^2 + {n_y}^2}}\right)$$

A mesh element was included in the surface integral if it satisfied the criterion $\theta \geq \Theta$. For this purpose, a trigonometric method was used with 10 numerical newts adopting the "I"-shaped posture for detecting, on a virtual transverse section of the body, the limit angle Θ between the sub-circular shape of the dorsal body perimeter in contact with air and the horizontal straight shape of the ventral part of body perimeter in contact with the substratum. This was performed using ImageJ software (v1.4). The limit angle Θ measured was about -0.955 radian (n = 10, 95% confidence interval, -0.984; -0.925). The mean limit angle Θ was applied to all the numerical newts in order to estimate their surface areas A_e. The surface area A_v was deduced from the total surface area A and the evaporative surface A_e as $A_v = A - A_e$. The surface area A_s was deduced from the difference in evaporative surface areas A_e between the "I"- and "S"-shaped postures. Finally, the different estimations

corresponding to intrinsic characteristics of the newts (i.e. A, V, RAV, A_e and A_v) were plotted as a function of W_0.

TEWL measurements with living newts

The purpose of this experiment was to acquire gravimetrically the cumulative TEWL over a 60 min period for the 10 individuals. Measurements were carried out in a climate-controlled room at 20.3 ± 0.4°C and 62.2 ± 1.1% RH. One day before these TEWL measurements, newt body weights were standardized as described above (mean W_0 ± se: 0.5773 ± 0.0367 g). The standardized newts were placed individually in a webbed cage (h = 3 cm, Ø = 6 cm) laid on a microbalance (Scaltec sbc 31; 0.0001 g sensitivity). The webbed cage aimed to limit biases due to individuals remaining in close contact with the sides of the cage, and thus reducing TEWL. Body weight loss for each newt was measured every 2 minutes over a 60 min period. Simultaneously, we monitored the percentage of time spend in activity and in a given posture (when inactive) using JWatcher (1.0 version software).

TEWL measurements for agar replicas

Our aim was to compare the cumulative TEWL kinetics of living newts with that of a free water surface using agar replicas, and evaluate the influence of the "S" water-conserving posture on TEWL rate. For each experimental newt (n = 10), we created agar replicas of their "I" and "S" postures (Fig. 1b) using the method of Spotila & Berman (1976). We created agar models of the experimental newts by immersing each previously anesthetized individual into fluid alginate in a small plastic container. Before moulding, we made the anesthetized newt adopt one of the two desired postures. After alginate hardening, we gently removed the animal before filling the mould with a solution of 3% agar, 97% water. We thus obtained 10

"I"-shaped agar replicas (mean body weight ± se: 0.5785 ± 0.0343 g) and 10 "S"-shaped agar replicas (mean body weight ± se: 0.5785 ± 0.0357 g), each of them being a copy of one experimental newt. Measurements of TEWL kinetics of agar replicas were carried out under conditions identical to those for living newts.

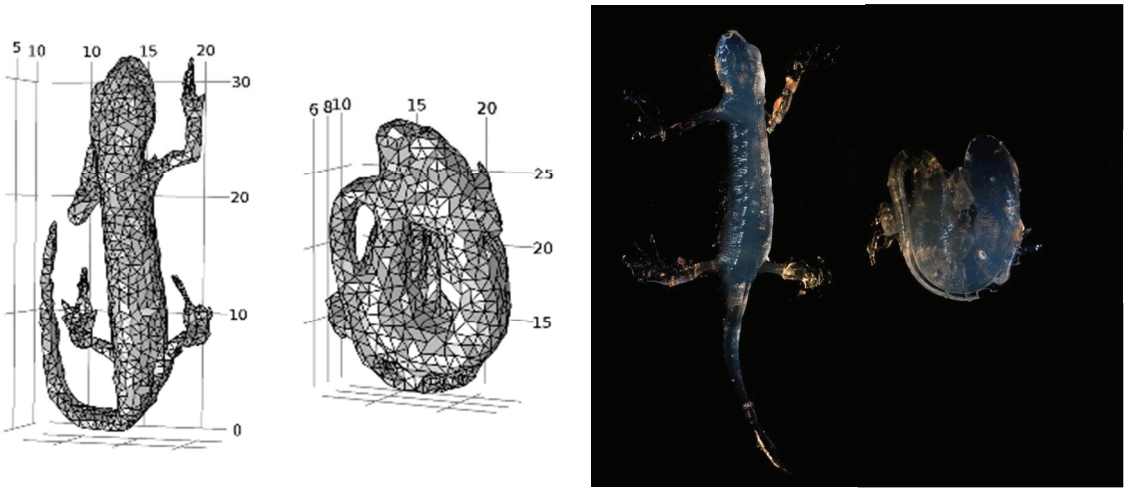

Fig. 1. (a) 3D meshed geometries representing the "I"-shaped posture and the "S"-shaped water-conserving posture of *Lissotriton helveticus* obtained via a magnetic resonance imaging (MRI)-based 3D reconstruction method (Pictures from COMSOL Multiphysics v4.2); (b) Agar replicas of the "I"- and "S"- shaped postures of a newt obtained following the method of Spotila and Berman (1976) (photograph taken by T. Colin).

Statistical analyses

In order to test the significance of the interactions between the intrinsic newt characteristics (i.e. A, V, AVR, A_e and A_v) and their standard body weight W_0 (for the two postures "I" and "S"), linear models were used. Given that the relationships between standard body weight and surfaces areas (A, A_e and A_v) and the AVR ratio follow a power relationship (McClanahan and Baldwin 1969, Tracy 1976), the data were previously log-transformed in order to use linear models.

We used linear mixed models to evaluate the effect of W_0 and the "S"-shaped posture on A, V, AVR, A_e and A_v. As explained above, relationships following a power relationship were previously log-transformed. The mixed models included two fixed effects (W_0 and postures) together with the interactions between these factors. Non-significant interactions were excluded from the final model. The model took into account the correlated error between measurements made on a same individual as a random effect.

In order to evaluate the influence of posture on the TEWL rate, we investigated the effects of W_0, posture, time (time spent since the beginning of the desiccation experiment, form 0 to 60 min) and their interactions with the TEWL rates of agar replicas using the linear mixed model. W_0, posture and time were considered as fixed effects. The model took into account the correlated error between measurements made on a same individual as a random effect. The covariance structure for the model was selected using the Akaike information criterion (AIC): a first order autoregressive correlation between measurements was selected. Estimates were computed using a restricted maximum likelihood (REML) approach. Factor significance was tested using Wald t tests (Bolker et al. 2009). Non-significant interactions were then successively removed to obtain the final model.

Residual normality, independence and variance homogeneity were checked. All the models were calculated using R 3.0.1 software (R Development Core Team 2013) with the 'nlme' package for linear mixed models (Pinheiro et al. 2009).

RESULTS

Surface areas, volume and surface/volume ratios of the 3D geometries

We plotted the estimations of the total surface area A and volume V of each numerical newt according to posture as a function of W_0 (Figs. 2a, 2b). The least-squares best-fit equations for these relationships are: "I"-shaped posture: $A = 11.003\, W^{0.6112}$ (linear model log(A)-log(W): R^2 = 0.804, *P-value (P)* = 4.394 x 10^{-4}) and $V = 1.1623\, W - 0.0356$ (linear model: R^2 = 0.849, *P* = 1.516 x 10^{-4}); "S"-shaped posture: $A = 8.3541\, W^{0.5725}$ (linear model log(A)-log(W): R^2 = 0.8162, *P* = 3.38 x 10^{-4}) and $V = 1.1177\, W - 0.0153$ (linear model: R^2 = 0.8462, *P* = 1.636 x 10^{-4}). The mixed models showed that the "S"-shaped posture significantly reduced the total surface area A, but had no significant effect on newt volume. Moreover, it showed that heavier newts had higher total surface areas and volumes than lighter ones (Table 1 and Fig. 2a). Based on the measured data, total surface area was significantly reduced about 22.2 per cent (n = 10, 95% confidence interval, 17.8-26.5).

We plotted the surface/volume ratio (AVR, calculated from the total surface area and volume) of the numerical newts according to their postures as a function of W_0 (Fig. 2c). The least-squares best-fit equations for the relationships are $AVR = 9.5849\, W^{-0.474}$ ("I"-shaped posture; linear model log(AVR)-log(W): R^2 = 0.6118, *P* = 0.007501) and $AVR = 7.4201\, W^{-0.493}$ ("S"-shaped posture; linear model log(AVR)-log(W): R^2 = 0.5549, *P* = 0.01343). The mixed model showed that the "S"-shaped posture significantly reduced the surface/volume ratio of the newts. We estimated a reduction of about 21.6 per cent (n = 10, 95% confidence interval, 17.6-26.5). The model also suggests that lighter newts have a higher AVR than heavier ones (Table 1 and Fig. 2c).

Table 1. Effect of standard weight (W_0) and postures ("I" and "S") on total surface area (A), volume (V) and total surface area/volume ratios (AVR) of *Lissotriton helveticus*. The mixed model includes two fixed effects (W_0 and posture) together with the interactions between them. Non-significant interactions were excluded from the final model. The model takes into account the correlated error between measurements made on a single individual as a random effect.

	Estimates	Std. error	Degrees of Freedom	*Wald t test-value*	*P-value*
log(A) [cm²]					
Intercept	1.0366419	0.01883305	9	55.04377	< 0.0001
log(W_0)	0.5916482	0.06989435	8	8.46489	< 0.0001
posture	-0.1099800	0.01069923	9	-10.27925	< 0.0001
V [cm³]					
Intercept	-0.022773	0.09768150	9	-0.233135	0.8209
W_0	1.140013	0.16633097	8	6.853885	0.0001
posture	-0.005380	0.00839893	9	-0.640558	0.5378
log(AVR)					
Intercept	0.9792335	0.03354972	9	29.187527	< 0.0001
log(W_0)	-0.4837496	0.12845365	8	-3.765947	0.0055
posture	-0.1064800	0.00985183	9	-10.808140	< 0.0001

We also plotted estimations of the evaporative surface area A_e and the ventral surface area A_v of each numerical newt according to posture as a function of W_0 (Figs. 2d, 2e). The least-squares best-fit equations for the relationships are: "I"-shaped posture: $A_e = 9.3347\ W^{0.631}$ (linear model log(A_e)-log(W): R^2 = 0.7165, P = 0.002012) and $A_v = 1.6558\ W^{0.5093}$("I"-shaped posture; linear model log(A_v)-log(W): R^2 = 0.4226, P = 0.04187); "S"-shaped posture: $A_e = 6.8155\ W^{0.559}$ (linear model log(A_e)-log(W): R^2 = 0.761, P = 9.936 x 10^{-4}) and $A_v = 1.5325\ W^{0.631}$(linear model log(A_v)-log(W): R^2 = 0.7593, P = 0.001022). The mixed model shows that the "S"-shaped posture significantly reduces both the evaporative

surface area in contact with the atmosphere and the ventral surface area in contact with the substrate (Table 2 and Figs. 2d, 2e). The average reduction of A_e (i.e. A_s) represents a reduction of about 23.6 per cent (n = 10, 95% confidence interval, 17.7-29.4), and a reduction of about 14.3 per cent (n = 10, 95% confidence interval, 8.2-20.4) for A_v. As expected, the model suggests that heavier newts have a higher evaporative and ventral surface area than lighter ones (Table 2 and Figs. 2d, 2e). Additional analyses reveal that the average reduction in ventral surface area is significantly less pronounced than the average reduction in evaporative surface area (*paired t-test: t* = 6.2554, *Degrees of Freedom (DF)* = 9, *P* = 0.0001487).

Table 2. Effect of standard weight (W_0) and postures ("I" and "S") on evaporative surface area (A_e) and ventral surface area in contact with the substratum (A_v) of *Lissotriton helveticus.* The mixed model includes two fixed effects (W_0 and posture), together with the interactions between them. Non-significant interactions were excluded from the final model. The model takes into account the correlated error between measurements made on a single individual as a random effect.

	Estimates	Std. error	Degrees of Freedom	*Wald t test-value*	*P-value*
log(A_e) [cm²]					
Intercept	0.9611769	0.02348505	9	40.92718	< 0.0001
log(W_0)	0.5948308	0.08713454	8	6.82658	0.0001
posture	-0.1187800	0.01338492	9	-8.87417	< 0.0001
log(A_v) [cm²]					
Intercept	0.2339527	0.03473335	9	6.735679	0.0001
log(W_0)	0.5700032	0.13044947	8	4.369533	0.0024
posture	-0.0636600	0.01680443	9	-3.788286	0.0043

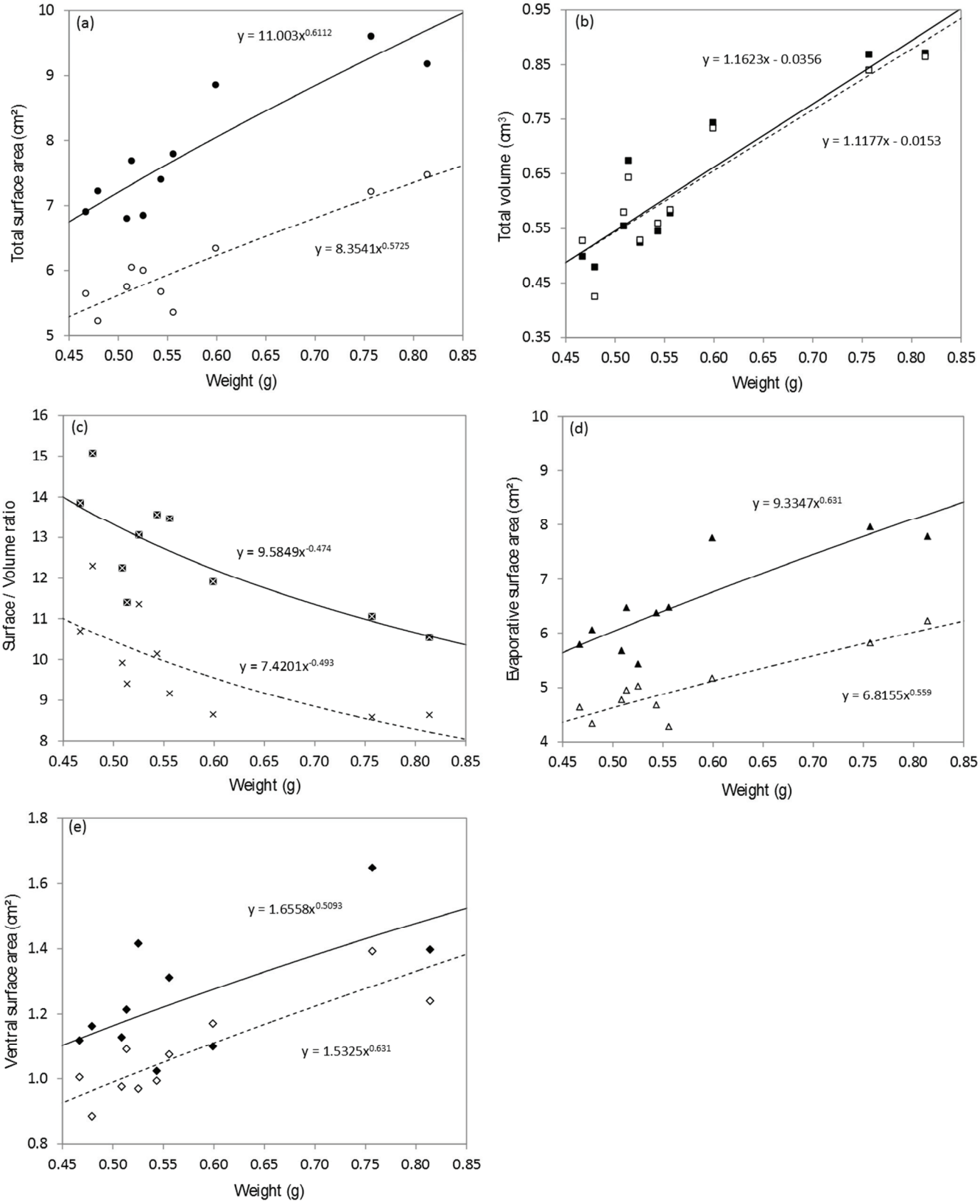

Fig. 2. Relationships between standard body weight and (a) total surface area, (b) volume, (c) surface/volume ratio (calculated from the total surface area and volume), (d) evaporative surface area, and (e) ventral surface area in contact with the substratum for both the "I"-(filled dots) and "S"-shaped posture (open dots) for *Lissotriton helveticus*.

TEWL measurements with living newts and agar models

The linear mixed model suggests that the “S”-shaped posture is related to a significantly lower TEWL rate than the “I”-shaped posture (Table 3 and Fig. 3). The reduction in cumulative TEWL measured over the 60 min period in this “S”-shaped posture is about 22.1 per cent (n = 10, 95% confidence interval, 18.4-25.9). The model also shows that the TEWL rate of agar models also decreases throughout the experiment (Table 3 and Fig. 3). However, this reduction is less pronounced for the “S”-shaped agar replicas and for heavier ones (Table 3). Furthermore, the water loss from agar replicas, in both “I”- and “S”-shaped postures, was not significantly different from living newts (Fig. 3). TEWL data for living newts are included within the “free water surface” 95% confidence intervals formed by “I”- and “S”-shaped agar replicas, which is consistent with the general behaviour of live newts during desiccation, knowing that newts evaporate water at the same rate as free water surfaces. In fact, during the desiccation experiment, the experimental newts were essentially inactive: 10.4 per cent only of the dehydration time was spent moving (n = 10, 95% confidence interval, 6.7-14.2). When inactive, newts predominantly adopted the “I” posture for 53.4 per cent of the dehydration time (n = 10, 95% confidence interval, 40.0-66.8) versus 36.2 per cent (n = 10, 95% confidence interval, 21.3-51.0) for the “S” posture.

Table 3. Mixed model analyses for transepidermal evaporative water loss (TEWL) rates based on posture in agar models. The model includes three fixed effects (standardized body weight (W_0), posture ("I" and "S") and successive measurements made within the desiccation period (time)) together with the interactions between these factors. Non-significant interactions were excluded from the final model. The model takes into account the correlated error between measurements made on a single individual as a random effect.

	Estimates	Std. error	Degrees of Freedom	*Wald t test-value*	*P-value*
TEWL rate [mg/min]					
Intercept	0.7003237	0.11959004	585	5.856037	< 0.0001
posture	-0.2321315	0.01949989	585	-11.904247	< 0.0001
W_0	0.3146214	0.20190047	585	1.558299	0.1197
time	-0.0058739	0.00112429	585	-5.224559	< 0.0001
W_0 × time	0.0044680	0.00187986	585	2.376755	0.0178
posture × time	0.0017241	0.00041279	585	4.176809	< 0.0001

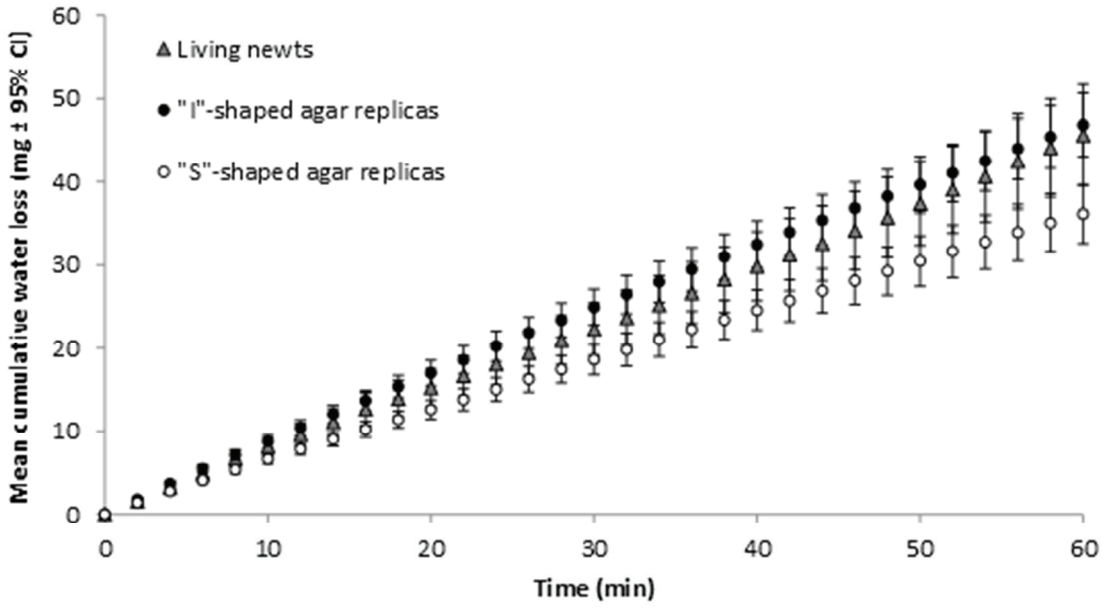

Fig. 3. Mean cumulative transepidermal evaporative water loss (TEWL, ± 95% confidence interval (CI)) over a 60 min period for live palmate newts (n = 10) in comparison with both their "I" and "S" agar replicas (n = 10 for each). Filled dots: "I"-shaped agar model; open dots: "S"-shaped agar model; triangles: living *Lissotriton helveticus*.

DISCUSSION

The MRI-based 3D reconstruction method used in this paper, generates accurate quantitative data about some important intrinsic characteristics of an amphibian (i.e. surface areas) concerning water evaporation, as well as heat transfer. In fact, given the precision of the MRI system used (i.e. 0.2/0.1/0.15 mm), our 3D geometries generated a root mean square error < 0.15 mm and a Hausdorff distance < 0.8 mm, meaning that these geometries have an error inferior to one pixel compared to images obtained by MRI, giving robust estimations of total surface area, volume, surface/volume ratios, and their relationships with the standard weight. However, the trigonometric method presented here to obtain estimations of the evaporative surface area may show bias since we had to obtain a measure of the representative threshold angle Θ of the numerical newts. Further experiments are needed to develop a more accurate method. Nonetheless, our results on the evaporative surface areas, according to the postures expressed by the newts, are consistent with the data obtained from agar replicas and the surface/volume ratio. In fact, when the palmate newt adopted the "S"-shaped water-conserving posture, the evaporative surface area was reduced by about 23.6 $\pm$ 5.8 per cent, an amount very close to the reduction in measured TEWL rate (with agar replicas), i.e. 22.1 $\pm$ 3.7 per cent over the 60 min period, knowing that the TEWL rate is proportional to the evaporative surface area in contact with the atmosphere (Tracy 1976, Spotila et al. 1992, Shoemaker et al. 1992, Lillywhite 2006, Hillman et al. 2009). Furthermore the reduction in surface/volume ratio measured imposed by the "S"-shaped posture is also of the same order. These results suggest that the postures adopted by urodeles may have significant consequences on TEWL rates and thus on survival in the terrestrial environment (Pough et al. 1983). In contrast, when applying a similar agar

replica protocol, Tracy et al. (2007) found that the water-conserving posture in the anuran *Cyclorana australis* did not lead to significant reduction in TEWL (compared to their upright posture, the equivalent of the "I"-shaped posture in the palmate newt), suggesting that the efficiency of water-conserving postures depends on the general morphology of the animal (i.e. spherical vs. elongated), which could determine the proportion of skin surfaces being in contact with other skin surfaces. Interestingly, the "S"-shaped posture in the palmate newt also leads to a reduction in the ventral surface area, probably because body huddling increases internal pressure, which in turn reduces the scope for belly flattening. This suggests that the water-conserving posture reduces the skin surface area in contact with the atmosphere, and also reduces skin surface area in contact with the substratum controlling water absorption, but to a significantly lesser extent. Furthermore, we found that the palmate newt's skin surface evaporates water at the same rate as a free water surface. Consequently, the skin characteristics (e.g. composition and physical state of the epidermal structure, see Farquahar and Palade, 1965 and Lillywhite 2006) of this species during the terrestrial phase do not constitute an efficient barrier to water evaporation, and thus presents a negligible skin resistance to TEWL, as observed in most amphibian species (Lillywhite 2006). Such results indicate that palmate newts do not show any physiological adaptations to restrain evaporation, and that the ways adopted for reducing the TEWL rate in their terrestrial phase rely on behavioural adaptations, such as microhabitat selection (Shwartzkopf and Alford 1996) and/or the adoption of water-conserving postures (Alvarado 1967, Gehlbach et al. 1969, Pough et al. 1983, Wardziak et al. 2013) as shown in these studies.

Here, we have presented an original non-destructive approach to accurately measure the intrinsic characteristics of live amphibians involved in both water and heat transfer. In

addition, the method of Spotila and Berman (1976) proved efficient in acquiring the essential understanding of water transfer in an amphibian. However, agar replicas are useful only for short duration assays. As these shrink as they lose water (Tracy et al. 2007, Wardziak et al. 2013), long-term measurements of TEWL rates become questionable. More interestingly, the resulting 3D geometries of newts are suitable for simulation applications. These 3D geometries may be used and incorporated into modelling tools, such as multiphysics engineering modeling and simulation software, making it possible to model and simulate any physics-based system, based on the fundamental physical laws that govern the conservation of energy and mass. Using 3D geometries of live amphibians represents the first important step in an original approach to studying water, as well as energy exchanges between an amphibian and its physical environment.

Acknowledgements. We warmly thank Théotime Colin and Marion Javal for their help and support in the laboratory. We also thank Théotime Colin for providing the *L. helveticus* agar models picture. We finally thank Patricia Hulmes, a native English speaker, who helped to improve this manuscript. This study was supported by a grant from the French *Ministère de l'Enseignement Supérieur et de la Recherche* and was conducted with the approval of the Préfecture de l'Isère (decision 2011-1710) and the Ethics Committee of University Lyon 1 in accordance with current French laws.

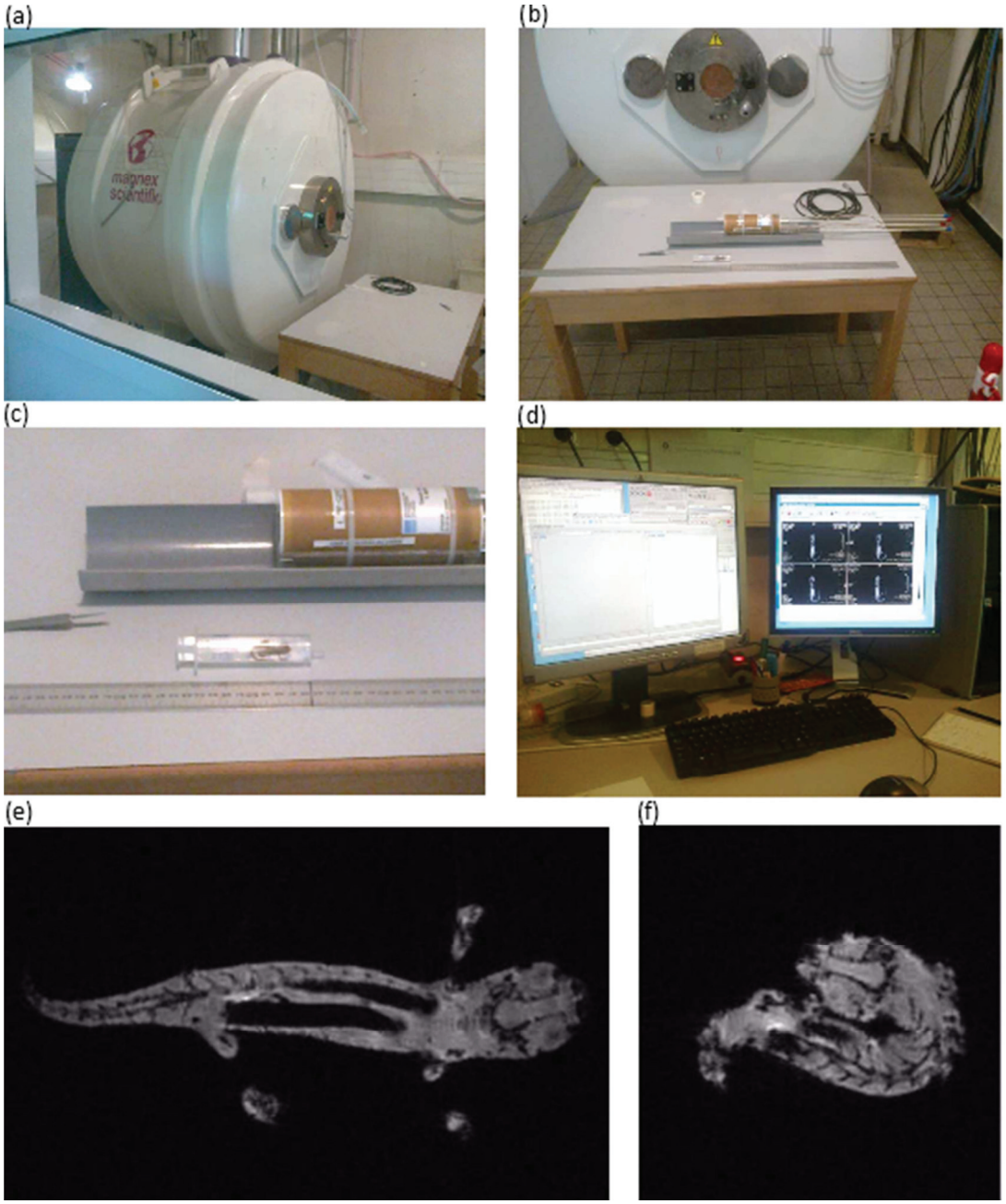

Figure S1. (a) The Bruker Biospec ^{1}H MRI System (CREATIS-LRMN laboratory, Unversity of Lyon, France); (b) and (c) anesthetized palmate newts were placed inside the quadrature coil (32 mm i.d., Rapid Biomedical GmBH) which is then placed inside the MRI system for imaging acquisitions; (d) after a total acquisition time of 3 min 45 sec we obtained a 3D volume of the newt; € and (f) examples of acquisition for a newt in the "I"- and "S"-shaped posture, respectively. The MRI signal intensity is a function of the newt characteristics, such as proton density which is linearly proportional to the number of mobile protons in water in the tissues. High signal intensity (bright) corresponds to high water content. In contrast, low signal intensity (dark) corresponds to low water content.

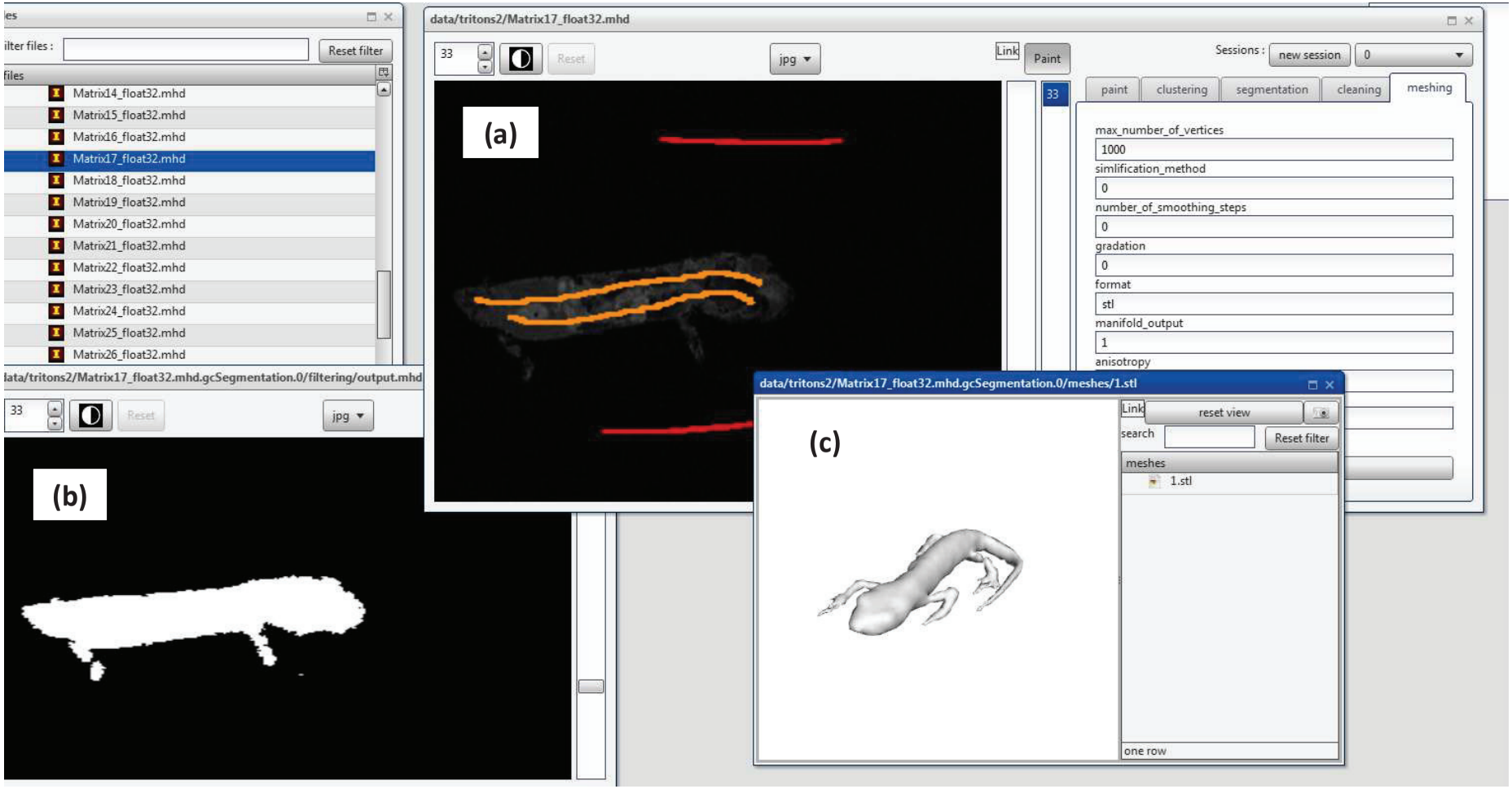

Figure S2. The segmentation and meshing steps to generate 3D geometries using the 3D volumes obtained by MRI system. (a) We have to manually label some parts belonging to the newt and to the outside, which provide clues to the algorithm of what to extract from the image. (b) We obtain a volume with voxels labeled as inside (white) or outside the newt (dark). (c) From this volume the external surface of the newt was extracted and meshed. The segmentation and meshing steps were performed via a web-based interface (Jacinto et al. 2012).

LITERATURE CITED

Alvarado RH (1967) The significance of grouping on water conservation in *Ambystoma*. *Copeia* 3:667-668

Amey AP, Grigg GC (1995) Lipid-reduced evaporative water loss in two arboreal hylid frogs. *Comp Biochem Physiol* 111:283-291

Audette M, Rivière D, Ewend M, Enquobahrie A, Valette S (2011) Approach-guided controlled resolution brain meshing for FE-based interactive neurosurgery simulation. Workshop on Mesh Processing in Medical Image Analysis, in conjunction with MICCAI 2011, Toronto, Canada, 176-186

Boykov Y, Jolly MP (2001) Interactive graph cuts for optimal boundary and region segmentation of objects in N-D images. *International Conference on Computer Vision (ICCV)* 1:105-112

Buttemer A (1990) Effect of temperature on evaporative water loss of the Australian tree frogs *Litoria caerulea* and *Litoria chloris*. *Physiol Zool* 63:1043-1057

Farquhar M, Palade GE (1965) Cell junctions in amphibian skin. *J Cell Biol* 26:263-291

Feder ME, Burggren WW (1985) Cutaneous gas exchange in vertebrates: design, patterns, control and implications. *Biol Rev* 60:1-45

Gehlbach FR, Kimmel JR, Weems WA (1969) Aggregations and body water relations in tiger salamanders (*Ambystoma tigrinum*) from the Grand Canyon rims, Arizona. *Physiol Zool* 42:173-182

Hillman SS, Withers PC, Drewes RC, Hillyard SD (2009) Ecological and environmental physiology of amphibians. Oxford University Press

Jacinto H, Kéchichan R, Desvignes M, Prost R, Valette S (2012) A Web Interface for 3D Visualization and Interactive Segmentation of Medical Images, Web3D 2012, Los-Angeles, USA, 2012. RTF Tagged XML BibTex Google Scholar

Kéchichan R, Valette S, Desvignes M, Prost R (2011) Efficient Multi-Object Segmentation of 3D Medical Images Using Clustering and Graph Cuts. IEEE International Conference on Image Processing, Brussels, Belgium, 2196-2200

Laforsh C, Imhof H, Sigl R, Settles M, Heß M, Wanninger A (2012) Application of computational 3D-modeling in organismal biology. In: Alexandru C (ed), Modeling and simulation in engineering. InTech, Rijeka, pp. 117–142.

Lillywhite HB (2006) Water relations of tetrapod integument. *J Exp Biol* 209:202-226

Maina JN (1989) The morphology of the lung of the East African tree frog *Chiromantis petersi* with observations on the skin and the buccal cavity as secondary gas exchange organs. A TEM and SEM study. *J Anat* 165:29-43

McClanahan L, Baldwin R (1969) Rate of water uptake through the integument of the desert toad, *Bufo punctatus*. *Comp Biochem Physiol* 28:381-389

Navas CA, Araujo C (2000) The use of agar models to study amphibian thermal ecology. *J Herpetol* 32:330-334

Porter WP, Mitchell JW, Beckman WA, DeWitt CB (1973) Behavioral implications of mechanistic ecology, Thermal and behavioural modelling of desert ectotherms and their microenvironment. *Oecologia* 13:1-54

Pinheiro JC, Bates DM, DebRoy S, Sarkar D, The R Core Team (2009) nlme: linear and nonlinear mixed effects models. *R package version* 3: 1-96

Pough FH, Taigen TL, Stewart MM, Brussard PF (1983) Behavioural modification of evaporative water loss by a Puerto Rican frog. *Ecology* 64:244-252

R Development Core Team (2013) R: a language and environment for statistical computing. R Foundation for Statistical Computing, Vienna

Schwarzkopf L, Alford RA (1996) Desiccation and shelter-site use in a tropical amphibian: comparing toads with physical models. *Funct Ecol* 10:193-200

Shoemaker VH, Hillman SS, Hillyard SD, Jackson DC, McClanahan LL, Withers PC, Wygoda ML (1992) Exchange of water, ions, and respiratory gases in terrestrial amphibians. In: Feder E, Burggren WW (ed) Environmental Physiology of the Amphibians. University of Chicago Press, Chicago

Shoemaker VH, Nagy KA (1977) Osmoregulation in amphibians and reptiles. *Ann Rev Physiol* 39:449-471

Spotila JR, Berman EN (1976) Determination of skin resistance and the role of skin in controlling water loss in amphibians and reptiles. *Comp Biochem Physiol* 55A**:**407-411

Spotila JR, O'Connor MP, Bakken GS (1992) Biophysics of heat and mass transfer. In: Feder E, Burggren WW (ed) Environmental Physiology of the Amphibians. University of Chicago Press, Chicago

Tracy CR (1976) A model of the dynamic exchange of water and energy between a terrestrial amphibian and its environment. *Ecol Monogr* 46:293-326

Tracy CR, Betts G, Tracy CR, Christian KA (2007) Plaster models to measure operative temperature and evaporative water loss of amphibians. *J Herpetol* 41:597-603

Wardziak T, Luquet E, Plenet S, Léna JP, Oxarango L, Joly P (2013) Impact of both desiccation and exposure to an emergent skin pathogen on transepidermal water exchange in the palmate newt (*Lissotriton helveticus*). *Dis Aquat Org* 104:215-224

CHAPTER TWO – PART 1

Article in preparation

Article 2: **Numerical analysis of transepidermal evaporative water loss driven by diffusion in an urodele amphibian**

Thomas Wardziak*[a], Pierre Joly[a] and Laurent Oxarango[b]

[a] Université de Lyon; UMR 5023 Ecologie des Hydrosystèmes Naturels et Anthropisés; Université Lyon 1 ; ENTPE; CNRS; 6 rue Raphaël Dubois, 69622 Villeurbanne, France

[b] LTHE, Université de Grenoble, BP 53, 38041 Grenoble Cedex, France

* Author for correspondence (thomas.wardziak@orange.fr)

ABSTRACT: A diffusion-controlled evaporation (DCE) model in calm air based on the Fick's first law was developed to simulate transepidermal evaporative water loss (TEWL) in a terrestrial amphibian (*Lissotriton helveticus*) at various conditions of temperature (15 – 30°C) and relative humidity (40 – 80%). The finite element method was used to solve the differential equations over 3D geometries of *L. helveticus* obtained using Magnetic Resonance Imaging (MRI)-based 3D reconstruction method. Our DCE model was shown to be adequate to predict experimental TEWL rates of living newts, as well as their agar replicas in a large range of climatic conditions under a lack of advection phenomenon. It also highlighted the minimal threshold of air flow velocity that authorizes the application of the advection-diffusion model of Tracy developed for wet-skinned organisms. Additionally, using the DCE model, a new methodology to estimate accurately the functional surface areas of an amphibian, i.e. the evaporative surface area that interacts with the atmosphere, and the ventral surface area in contact with the substratum, was developed. This method is based on a robust physical concept since it takes into account all the surface elements of a 3D geometry that effectively contribute to the desiccation. The modelling approach provides a promising technique in biophysical ecology, which would open original ways to study water, as well as energy, exchanges between an organism and its physical environment.

KEY-WORDS: Amphibian; Magnetic resonance imaging; Diffusion; Advection; Water evaporation; Model; Skin surface area

INTRODUCTION

Organisms are closely coupled to their environment through exchanges of energy and mass (e.g. water, electrolytes, and respiratory gases). Under the selective pressure of continuous variation of environment over time and space, organisms have evolved physiological, morphological and behavioural adaptations to maintain homeostasis (e.g. water and electrolyte equilibrium, energy balance) (Kearney and Porter 2009, Biozinovic et al. 2011). However, in a climate change context, speed, frequency and intensity of variation over time and space of thermal and/or hydric conditions (IPCC 2007) may overpass the plasticity capacities of organisms, leading thus to detrimental physiological and functional consequences resulting in homeostasis breaking (Spotila & Berman 1976, Spotila et al. 1992, Shoemaker et al. 1992). In such a context, predicting how ecological changes might affect organisms in their relations with physical environment is a critical and urgent interdisciplinary challenge for developing effective conservation strategies. For this purpose, the interdisciplinary field of biophysical ecology combines fundamental physical laws that govern heat, mass and momentum transfers. Ecophysiology, behavioural ecology, and biophysics (analysis of size, shape, skin characteristics, etc.) and environmental physics converge to derive mechanistic models of energy and mass balance at the organism scale (Tracy 1976, Biozinovic et al. 2011).

Amphibians represent an ideal biological model in this research field since these wet-skinned ectotherms are characterized by obligatory and permanent exchanges of water gases, heat and ions through their permeable skin (Shoemaker and Nagy 1977, Feder and Burggren 1984, Spotila et al. 1992, Shoemaker et al. 1992, Lillywhite 2006, Hillman et al. 2009). In the terrestrial habitat, their skin is an efficient pathway for the absorption of water

and electrolytes (transepidermal water absorption, TWA) but does not oppose a strong resistance to evaporation (transepidermal evaporative water loss, TEWL) (Shoemaker and Nagy 1977, Feder and Burggren 1984, Spotila et al. 1992, Shoemaker et al. 1992, Lillywhite 2006, Hillman et al. 2009). Consequently, the amphibians are particularly sensitive to their physical environment, and therefore represent the vertebrate taxon the most threatened by environmental changes (Stuart et al. 2004).

The fundamental physical laws of mass transfer and mass balance provide an extremely practical modelling framework to study and improve our understandings of physical amphibian-environment water exchanges (Tracy 1976, Spotila et al. 1992, Shoemaker et al. 1992). Currently, a model of TEWL has been established for the terrestrial leopard frog (*Rana pipiens*) and are sufficiently general to be applied (with some modifications) to other amphibians and other wet-skinned taxa (see Tracy 1976, Shoemaker et al. 1992, Spotila et al. 1992, Hillman et al. 2009). Tracy's model of TEWL describes the water vapour transport by molecular diffusion (as described by the Fick's first law; see Jaynes and Rogowski, 1983) and forced advection (wind) using a fully established air flow boundary layer. The TEWL through a unit of skin evaporative surface area is calculated as a function of the water vapour concentration gradient (between the amphibian skin surface and air). This mass flux depends on the ambient temperature and relative humidity (RH) that drive the molecular diffusion process (Tracy et al. 1980, Jaynes and Rogowski, 1983). It also depends on the wind speed due to the boundary layer assumption. This dependence is questionable since it implies that the amphibian's TEWL nullify as the wind speed nullify. According to the Fick's law, the TEWL should not nullify in a purely diffusive situation provided that a water vapour concentration gradient exists close to the evaporative surface. Furthermore, terrestrial amphibians express water-conserving behaviours that consist generally in avoiding unfavourable ambient

conditions (temperature, RH, and wind speed) by seeking shelters (e.g. Pough et al. 1983, Dobkins et al. 1987, Shoemaker et al. 1992, Seebacher and Alford 2002) that could prevent from air movements. In addition, considering a purely diffusive situation, it is known for water droplets that the evaporation rate is proportional to the perimeter of the droplet not to its evaporative surface area (Deegan et al. 1997, Shahidzadeh-Bonn et al. 2006, Weon et al. 2011). By analogy, in such a purely diffusive situation, it would be more relevant to reason with an equivalent perimeter for amphibians.

In order to tackle the problem of water transport estimation, recent technological, algorithmic and simulation tools advances (e.g. Bottomley et al. 1986, Xia et al. 1993, Nguyen et al. 2007, Wardziak et al. article [1], but see also Laforsh et al. 2012 for details) should open a new approach to study the physical amphibian-environment water relations. For example, in plant science, Bottomley et al. (1986) and Xia et al. (1993) have investigated the water transport in root systems using a Nuclear Magnetic Resonance (NMR) system. More recently, Nguyen et al. (2007) have developed a diffusion model of transient water profiles and water loss of pear fruit via Magnetic Resonance Imaging (MRI)-based 3D reconstruction method. In line with these studies, Wardziak et al. (article [1]) have generated, using a MRI-based 3D reconstruction method, 3D geometries of living palmate newts (*Lissotriton helveticus*) that can be used in simulation tools. In this context we attempt, using the 3D geometries generated by Wardziak et al. (article [1]), to perform 3D numerical simulation of TEWL of palmate newts in order to i) identify the physical processes involved in TEWL, ii) develop a general and accurate relationship to estimate amphibian TEWL rates in calm air for a large range of temperature and RH, and iii) develop a new methodology to estimate accurately the functional surface areas of an amphibian, i.e. the evaporative surface area that interacts with the atmosphere, and the ventral surface area in

contact with the substratum. The 3D numerical simulation of newt desiccation is validated against experiments on both living newts and their agar replicas.

MATERIALS AND METHODS

Experimental data acquisitions

Animal collection. Adult male palmate newts *Lissotriton helveticus* (n = 10) were collected in May 2011 during their aquatic phase in forest ruts near Mépieu, France (05°26'28''E, 45°43'56''N). All individuals from this population were housed in aquaria providing both aquatic and terrestrial environments allowing them to leave water. When the newts began their terrestrial stage, they were housed individually in plastic boxes (19 x 16.5 x 9.5 cm) lined with moistened cellulose paper, renewed weekly. The boxes were kept in climate-controlled rooms at 20 ± 1°C, 60 ± 10% of RH and a 16:8 light:dark cycle. Newts were fed with small crickets *ad libitum*.

Experiment 1. The purpose of the experiment was to acquire gravimetrically the TEWL along a 60 min period (and TEWL rates) of the 10 experimental newts for different conditions of temperature and RH. Three different conditions (15°C/80 % RH, 20°C/60 % RH, 30°C/40 % RH) were investigated using three different climate-controlled rooms (Table 1). Before TEWL measurements, body weight of the newts was standardized by placing them individually in plastic Petri dish (h = 2.5 cm, Ø = 9 cm) filled with 15 mL of tap water during 24 h allowing them to reach the standard weight (W_0) of a full hydrated animal. Mean W_0 (g) ± standard error (SE): 0.5774 ± 0.020; mean snout-vent length (SVL; cm) ± SE: 3.10 ± 0.05. The palmate newt expresses two postures (Wardziak et al. 2013, article [1]): the "I"-shaped posture is characterized by a relative straight body with no tail coil while the "S"-shaped

posture is a stereotyped water-conserving posture characterized by the body huddled up with the tail coiled along it. At each measurement, two fully hydrated newts were individually placed in a webbed cage (h = 3 cm, Ø = 6 cm) laid on a microbalance (Scaltec sbc 31; 0.0001 g sensitivity, dimensions: 170 x 170 x 240 mm). The webbed cage allows to avoid biases due to variation of TEWL when the newt remains in close contact with the sides of a cage. The meshes were sufficiently large (0.5 x 0.5 cm) to have a negligible impact on TEWL rate. Body weight loss for each newt was measured every 2 minutes along a 60 minutes period for each climatic condition. Simultaneously, we monitored the percentage of time spent moving (%Act), and in a given posture when inactive (%$Inact_I$ for the "I" posture and %$Inact_S$ for the "S" posture using JWatcher (1.0 version software).

Experiment 2. The purpose of the experiment was to acquire gravimetrically TEWL along a 60 min period (and TEWL rates) of agar replicas of each experimental newt in their "I"- and "S"-shaped postures. TEWL rates of agar replicas can be used as estimators of the quality of predicted TEWL rates of our numerical analyses (see details below). Agar replicas made of 3% agar (97% water) have the advantage to present the surface area of live animals closely and they evaporate water at the same rate as free water surface (Spotila and Berman 1976, Amey and Grigg 1995) as the adult palmate newts in terrestrial phase (article [2]). We used the method of Spotila & Berman (1976) for obtaining 10 "I"-shaped agar replicas (mean body weight ± SE: 0.5785 ± 0.0343 g) and 10 "S"-shaped agar replicas (mean body weight ± SE: 0.5785 ± 0.0357 g) of each of the 10 experimental newts. Measurements of TEWL kinetics of agar replicas were carried out with a protocol identical to experiment 1, under conditions similar to condition 2 experienced by the living newt (conditions 2a1 and 2a2 in Table 1).

Table 1. Average climatic conditions of desiccation (± standard deviation) experienced by the experimental newts *Lissotriton helveticus* (i.e. condition 1, 2 and 3) and their agar replicas in the "I"- and "S"-shaped postures (i.e. condition $2a_1$ and $2a_2$, respectively) over a 60 min period used for Diffusion-Controlled Evaporation models.

	Temperature, t [°C] and relative humidity, φ_0 [%] conditions				
Newt identity	Condition 1	Condition 2	Condition $2a_1$	Condition $2a_2$	Condition 3
P01 / P02	14.73 ± 0.53 °C 86.06 ± 5.72 %	19.96 ± 0.60 °C 62.58 ± 1.68 %	20.04 ± 0.18 °C 63.11 ± 0.44 %	20.55 ± 0.20 °C 62.75 ± 1.57 %	29.79 ± 0.11 °C 38.31 ± 0.39 %
P07 / P10	15.09 ± 0.43 80.77 ± 4.21	19.85 ± 0.31 62.43 ± 1.23	20.49 ± 0.07 63.97 ± 0.54	20.36 ± 0.15 62.81 ± 1.05	30.06 ± 0.06 41.18 ± 2.89
P04 / P05	14.76 ± 0.35 83.82 ± 3.34	20.82 ± 0.04 60.66 ± 0.36	20.57 ± 0.18 60.95 ± 1.47	20.80 ± 0.08 62.68 ± 1.94	30.08 ± 0.05 38.18 ± 0.39
P03 / P08	14.89 ± 0.16 86.95 ± 5.16	20.81 ± 0.04 61.46 ± 0.34	20.50 ± 0.09 60.84 ± 0.23	20.92 ± 0.06 63.37 ± 1.27	30.11 ± 0.03 42.18 ± 0.67
P06 / P09	15.26 ± 0.45 89.30 ± 7.11	20.36 ± 0.09 63.67 ± 0.22	20.13 ± 0.20 61.46 ± 0.90	20.47 ± 0.25 60.67 ± 0.22	29.92 ± 0.20 42.53 ± 0.51

The Diffusion-Controlled Evaporation (DCE) model

Mathematical model. The DCE model assumes that water vapour is dilute in air such as the Fick's first law is valid. The RH is defined as:

$$\varphi = \frac{\rho_v}{\rho_{vs}(T)} \quad (1)$$

where φ is the RH [-], ρ_v is the water vapor density [kg.m^{-3}] and ρ_{vs} is the saturated water vapour density [kg.m^{-3}] (see Table 2 for temperature dependence relationship).

Introducing the RH (equation 1), the local mass flux vector is expressed by the general form of the Fick's law as:

$$\vec{j} = -D(T)\rho_{vs}(T)\vec{\nabla}\varphi \quad (2)$$

where $\vec{j}$ is the 3D mass flux vector [kg.m^{-2}.s^{-1}], $\vec{\nabla}$ is the gradient operator and D is the molecular diffusion coefficient [m².s^{-1}]. D is assumed isotropic and depends on the temperature (see Table 2 for temperature dependence relationship).

The water vapour mass balance is defined as:

$$\frac{\partial \rho_v}{\partial t} = \vec{\nabla} \cdot \vec{j} \quad (3)$$

The term in the left side of the eq. (3) corresponds to the accumulation of the water vapour in air. The term in the right side describes the diffusive transport of the water vapour in all the directions, and accounts for molecular interactions between water vapour and air.

The temperature is assumed to be constant in the entire domain. This isothermal assumption is the main physical assumption of the proposed DCE model. Even if the thermal equilibrium between an ectotherm and its environment is very classical in biology, the physical implication is not trivial and should be considered with care. The evaporation of water on the animal skin should promote a local temperature decrease (due to the latent heat of vaporisation). Even a small temperature decrease may promote natural convection around the animal and then modify the vapour flux. However, as a first approach, this thermal behaviour is neglected in this study.

The eq. (3) simplifies using eqs. (1) and (2) with the isothermal assumption as:

$$\frac{\partial \varphi}{\partial t} = -D(T)\Delta\varphi \quad (4)$$

where Δ is the Laplace operator.

Calculation domain, initial and boundary conditions. The parallelepipedic calculation domain corresponds to the dimensions of the microbalance used in the exp. 1 and 2 (i.e. 170 x 170 x 240 mm) (Fig.1.a). It incorporates the 3D geometries of the 10 experimental newts (numerical newts) in their two postures obtained via a MRI-based 3D reconstruction method

(details in article [1]). Each numerical newt was placed at the bottom center of the domain (Fig. 1.b). Each test on experimental newts is simulated using the corresponding numerical newt and the experimental environmental conditions (T and φ_0) (Table 1). The simulated time is 1 hour. The initial condition is a constant value of RH φ_0.

Two different set of boundary conditions were considered. First, all the boundaries of the microbalance were considered totally impervious to water vapour (the DCE model 1). This boundary conditions correspond to a no-flux Neumann condition that reads:

$$\vec{j} \cdot \vec{n} = 0 \quad (5)$$

where $\vec{n}$ is the boundary normal unit vector.

In the second set of boundary conditions (the DCE model 2), a constant value of RH, such as $\varphi = \varphi_0$ (Dirichlet boundary condition) is applied on three boundaries of the microbalance. It aims at simulating the non-airtightness of the three sliding sides of the microbalance. The measured TEWL kinetics obtained in the exp. 1 and 2 were used in order to determine the DCE model that provides the best description of the water vapour diffusion behaviour of our experiments (i.e. Neumann *vs.* Dirichlet boundary condition). Since the palmate newt's skin surface area evaporates water as the same rate as free water surfaces (article [1]), their skin has no capacity to limit evaporation from its surface and can be considered as saturated in water (Tracy 1976, Shoemaker et al. 1992, Spotila et al. 1992, Hillman et al. 2009). Thus, the numerical newt boundary is defined with a constant RH condition, such as $\varphi = 1$, which corresponds to a free water surface boundary condition.

Numerical implementation. The 3D problem defined by eq. (6) and the set of boundary conditions is solved by the finite element method using the transport of diluted species interface of the commercial package COMSOL Multiphysics 4.2. The calculation domain was meshed using the "Normal" tetrahedral meshing of COMSOL Multiphysics (Fig. 1.c). It

consists in 40999 ± 2322 mesh elements (mean ± SE). It naturally presents a strong mesh refinement close to the newt surface since the MRI image analysis mesh is composed of 1252 ± 4 triangular mesh elements on average (see article [1]). Using a sensibility analysis of the meshing on the estimation of water flux (data not shown), we retained the "Normal" meshing since it provides the best compromise between time simulation and accuracy of the TEWL estimations. See also Table 2 for a description of the model parameters applied to simulate water vapour transport.

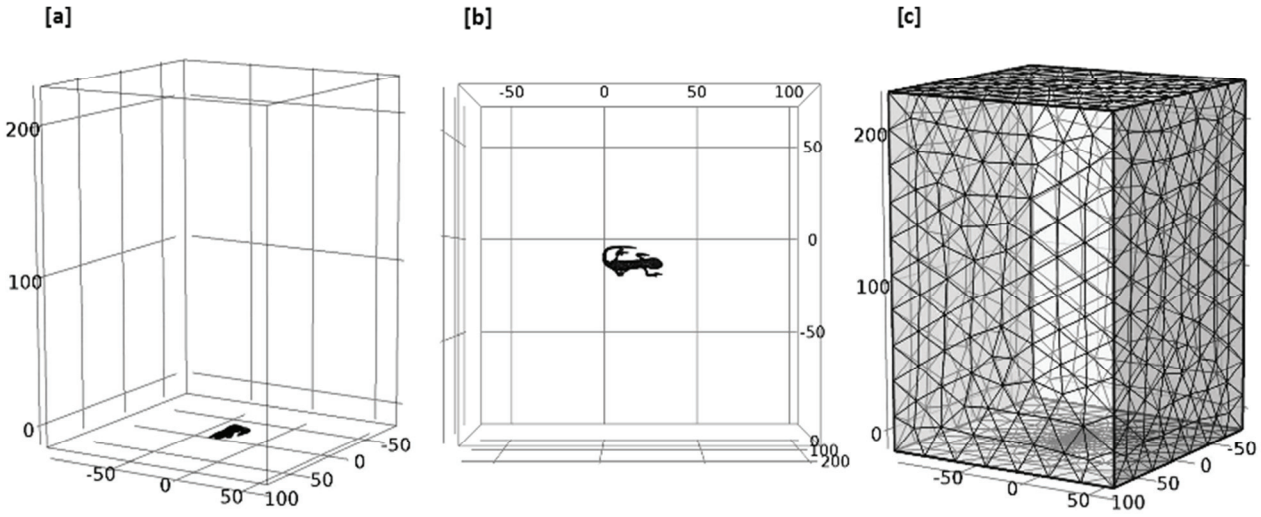

Fig. 1. [a] The calculation domain corresponds to the dimensions of the microbalance used in the experiments (i.e. 170 x 170 x 240 mm), and was defined for studying the evolution of water vapour transported by diffusion. [b] 3D geometries of the numerical newts were placed at the bottom center of the domain. [c] The calculation domain was meshed using the tetrahedral meshing. (Pictures from COMSOL Multiphysics v4.2).

Calculation of the TEWL. The TEWL rate ($\dot{m}$) [in kg.s^{-1}] is calculated as the surface integral of the local mass flux on the numerical newt total surface area A [m²] as:

$$\dot{m} = \iint_A d\dot{m} = \iint_A \vec{j} \cdot \vec{n} dA \quad (6)$$

One should note that the treatment of Dirichlet condition on the newt boundary is performed using the weak constraint advanced option of Comsol Multiphysics in order to prevent unbearable errors on the flux integration.

Evaporative and ventral surface area estimation of the numerical newts

Wardziak et al. (article [1]) proposed a methodology to estimate the total newt surface area (A) and two functional surface areas, i.e. the evaporative surface area that interact with the atmosphere (A_e), and the ventral surface area in contact with the substratum (A_v). The calculation of A was based on a surface integral of the meshed numerical newt:

$$A = \iint_A dA \quad (7)$$

The estimation of A_e used the same surface integral including a trigonometric criterion to select mesh elements contributing to the evaporative surface area.

The proposed methodology based on the DCE model (termed here the flux method) uses a physical criterion for mesh element selection: a mesh element is included in the surface area A_e if it presents a positive normal diffusive flux, i.e. $\vec{j} \cdot \vec{n} > 0$.

In both methods, the surface area A_v is deduced from the total surface area (A) (see article [1], figure 2a) and the evaporative surface A_e as:

$$A_v = A - A_e \quad (8)$$

Comparison of the experimental data with the DCE model

Because agar replicas and numerical newts are designed from the same individual newt, and because agar replicas loss water at the same rate as free water surface (Spotila and Berman 1976, Amey and Grigg 1995), TEWL rates ($\dot{m}$) of these models can be used as

estimators of the quality of the DCE model. We thus compared predicted and measured TEWL rates over the 60 min period for both the "I"-and "S"-shaped agar replicas and for living newts. Furthermore, for living newts, the comparison was carried out in relation with their behaviours. To better observe how the measured TEWL rates for living newts diverge from the predicted values of the "I"- and "S"-shaped postures, a TEWL dimensionless index μ was calculated for each experimental newt as:

$$\mu = \left[\frac{2 \times (\dot{m}_L - \dot{m}_S{}^*)}{(\dot{m}_I{}^* - \dot{m}_S{}^*)}\right] - 1 \qquad (9)$$

where $\dot{m}_L$ is the measured TEWL rate for the living newt, and $\dot{m}_I{}^*$, $\dot{m}_s{}^*$ are the predicted TEWL rate of the newt in the "I"- and "S"-shaped postures, respectively. If the measured values were in agreement with the predicted values of the "I"- or the "S"-shaped posture, then μ would be equal to $+1$ or -1, respectively. Such values would correspond to a living newt that spent 100 % of its dehydration time either in the "I"-or in the "S"-shaped posture, respectively. The value 0 would correspond to a newt with an intermediate behaviour.
The values of TEWL rate values are given by the slopes of linear regression models between TEWL and time.

Setting up models to estimate TEWL rates in a large range of temperature and RH.

Once the DCE model developed and its predictive accuracy verified with the agar replicas and the living newts, we used it to simulate TEWL rates in calm air under different combinations of temperature and RH to propose a physical model to estimate TEWL rates in a large range of climatic conditions. All the possible combinations between the three temperatures (15, 20 and 30°C) and RH (80, 60 and 40 %) were simulated (under a 60 min period) for each numerical newt according to posture. Following the formalism proposed by

Tracy (1976) and classical empirical expressions for diffusive or convective fluxes, the TEWL rate [kg.s^{-1}] in calm air can be defined with this first empirical relation (the empirical model 1):

$$\dot{m}_1 = A_e\, D\, \rho_{vs}\, h_1\, (1 - \varphi_0) \quad (10)$$

However, in a purely diffusive situation, it would be more relevant to impose a dependency of the TEWL rate with an equivalent perimeter $\sqrt{A_e}$ (Deegan et al. 1997, Shahidzadeh-Bonn et al. 2006, Weon et al. 2011). In such consideration, a second empirical relation can be defined (the empirical model 2):

$$\dot{m}_2 = \sqrt{A_e}\, D\, \rho_{vs}\, h_2\, (1 - \varphi_0) \quad (11)$$

where h_1 [m^{-1}] and h_2 [-] are mass transfer coefficients which describe a water vapour transfer in a purely diffusive situation (from the real evaporative surface area of the numerical newts, and in a semi-infinite domain), D (diffusion coefficient of water vapour in air) and ρ_{vs} (density of saturated water vapour) were calculated from eqs. presented in Table 2. The eqs. (10) and (11) constitute empirical models that describes TEWL rate in steady state with skin physically acting as a free water surface, and at thermal equilibrium.

Once TEWL rates for each numerical newt were calculated from the DCE model (for the nine combinations of temperature and RH), and their evaporative surface area A_e evaluated from the flux method (see above), an average mass transfer coefficient under calm air (i.e. without any air movement) can be evaluated using eqs. (10) and (11).

Because the evaporative surface area A_e of an urodele may be difficult to obtain without an appropriate methodology, the empirical model (eq. (11)) should be modified introducing an average coefficient α_i defined as $\alpha_i = \sqrt{A_e}/W_0$ (i = posture I or S) (the useful model):

$$\begin{cases} \dot{m}_{3,I} = \alpha_I\, W_0\, D\, \rho_{vs} * h_2\, (1 - \varphi_0) & (11.1) \\ \dot{m}_{3,S} = \alpha_S\, W_0\, D\, \rho_{vs} * h_2\, (1 - \varphi_0) & (11.2) \end{cases}$$

where α_i is an equivalent perimeter per standard body weight ratio ($m^2.kg^{-1}$) and is assumed to be characteristics of experimental *L. helveticus*.

Table 2. Model parameters applied in the Diffusion-Controlled Evaporation (DCE) models in order to simulate the water vapor transport by diffusion at the climatic conditions of desiccation experienced by experimental newts of *Lissotriton helveticus* and their agar replicas. Equation of diffusion coefficient provided from Tracy, Welch and Porter (1980); equation of saturated water vapor density provided from Markowski and Richardson (2011).

Symbol	Meaning / S.I. units	Equation / Value
t	Ambient air temperature [°C]	(see values presented in Table 1)
T	Ambient air temperature [K]	$t + T_0$
T_0	Temperature of reference [K]	273.15
P	Air pressure [Pa]	101325
P_0	Air pressure of reference [Pa]	101325
φ_0	Ambient relative humidity of reference [-]	(see values presented in Table 1)
D	Diffusion coefficient of water vapor in air [$m^2.s^{-1}$]	$2.26 \cdot 10^{-5} \times \left(\frac{T}{T_0}\right)^{1.81} \times \left(\frac{P_0}{P}\right)$
ρ_{vs}	Saturated water vapor density [$kg.m^{-3}$]	$\frac{\left[611.2 \exp\left(\frac{17.67t}{t+243.5}\right)\right]}{R_v T}$
R_v	Gas constant for water vapor [$J.kg^{-1}.K^{-1}$]	461.51

Comparison of Tracy's model with our empirical model 1

Under the range of climatic conditions and newt size used in this study, and using our model described by eq. (10), it is possible to evaluate the minimal threshold of air flow velocity that authorizes the application of Tracy's model: considering an amphibian skin surface saturated in water vapour at thermal equilibrium, Tracy's model can be written as (Tracy 1976):

$$\dot{m}' = A_e \, D \, \rho_{vs} \, h'(1 - \varphi_0) \qquad (12)$$

where h' is a mass transfer coefficient [m^{-1}] defined as:

$$h' = \left(\frac{0.3}{L}\right)\left(\frac{UL}{v}\right)^{0.6} \qquad (13)$$

where L is the snout-vent length (SVL) [m], U is the velocity of air flow [$m.s^{-1}$], and v is the kinematic viscosity of the air [$m^2.s^{-1}$] (See Tracy, Welch and Porter 1980 for calculation of the kinematic viscosity of the air according to temperature).

As explain by the eqs. (12) and (13), Tracy's model describes specifically a water vapour transport by molecular diffusion coupled with a forced advection leading to the mass transfer coefficient nullifying as the wind velocity nullifies. The mass transfer coefficient h_1 (from eq. (10)) was compared with h' (eq. (13)) under a range of air flow velocity from 0.001 to 0.1 $m.s^{-1}$, for the minimal and maximal values of SVL obtained in our experimental newts (i.e. 0.029 and 0.034 m), and of temperature (i.e. 15 and 30°C). For the range of air flow velocity, two different h' were thus calculated from eq. (13): $h'1$ for minimal temperature and minimal SVL, and $h'2$ maximal temperature and maximal SVL.

Statistical analyses

To analyse how each DCE model (model 1 or 2, i.e. Neumann *vs.* Dirichlet boundary condition) fits the data, we checked if the two models present the same driving force of water vapour evaporation by diffusion at least during the first 10 minutes. We compared TEWL rates between the two models using a mixed model. The mixed model including the boundary condition as fixed effect.

To evaluate the climatic condition on TEWL dimensionless index μ (eq. (9)), a mixed model including the conditions (1, 2 and 3, see Table 1) as fixed effect was used. In addition,

to evaluate the effect of percentage of time spent moving (%Act) and in a given posture (%$Inact_I$ and %$Inact_S$) on μ, three mixed models were used. The mixed models include %Act, %$Inact_I$ and %$Inact_S$ as fixed effect, respectively.

To evaluate the functional dependence on temperature, RH and posture of mass transfer coefficients h_1 and h_2, we also used a mixed model that includes three fixed effects (temperature, RH, and postures) and the interaction between temperature and RH.

For all the mixed models, estimates were computed using a restricted maximum likelihood (REML) approach. We tested factor significance using Wald t tests (Bolker et al. 2009). Non-significant interactions were then successively removed to obtain the final model. All the models took into account the correlated error between measurements made on a same individual as a random effect. We also checked for residual normality, independence and variance homogeneity. All the models were run using R 3.0.1 (R Development Core Team 2013) with the 'nlme' package for linear mixed models (Pinheiro et al. 2009).

RESULTS AND DISCUSSION

Diffusion-Controlled Evaporation (DCE) models 1 and 2. Within each of the three conditions of temperature and relative humidity (Table 1), TEWL remained constant since the dynamics of water is linearly related to time (Fig. 2a). This dynamics is similar to that observed with agar replicas (article [1]). These results diverge from the TEWL rates predicted by the DCE model 1 when the boundaries of the microbalance obey to Neumann's condition (Fig. 2b – we show only results for condition 2, but identical results were obtained for conditions 1 and 3). The DCE model 1 predicted a decrease of the water vapour loss rate

over time (Figs. 2b). This behaviour is in agreement with the physical principle of molecular diffusion. Since the microbalance is perfectly sealed, the mathematical problem tends to an asymptotic solution with RH constant and equal 1 on the whole calculation domain. At this point, the TEWL rate nullifies since the animal is in equilibrium with ambient air. The evolution of TEWL for model 2 presents a linear trend as observed during the experiment. In this case, the water vapour is able to leak out of the microbalance. This first qualitative observation seems to support the non-airtightness of the microbalance and the DCE model 2 seems to describe more accurately the experiment. The figure 3 presents 3D RH spatial distribution (colours) and flux vectors fields (arrows). The RH gradient that establishes around the animal is the driving force of the desiccation (Tracy 1976, Jaynes and Rogowski 1983, Shoemaker et al. 1992, Spotila et al. 1992). One should note that, a steady state establishes after few minutes in the DCE model 2. The RH and flux distributions are very similar for both models after 2 minutes. This observation is supported by a statistical analysis comparing the results of the two model during the first 10 minutes in condition 2: TEWL rates between DCE models 1 and 2 for both the posture “I” and “S” are not significantly different (mixed model, Neumann vs. Dirichlet with “I”-shaped posture: *Degrees of Freedom (DF)* = 9, *Wald t test-value (t)* = -1.41, *P-value (P)* = 0.1934; “S”-shaped posture: *DF* = 9, *t* = -1.67, *P* = 0.1302). After a longer period, the water vapour accumulates in the DCE model 1. It leads to an increase of the average value of RH and a decrease of the flux vectors magnitude. The description of water vapour leaks using Dirichlet conditions may not be fully realistic since the faces of the microbalance were not wide open during the experiment. Nevertheless, the DCE model 2 will be used for comparison with experiments on agar replicas and living animals since it seems to present a good general trend agreement with experiment. One should note that both DCE model 1 and 2 represent realistic physical

situations: a perfectly impervious cavity and a widely open cavity respectively. Since a refuge (such as burrows, natural cavities) may provide shelter from harsh environmental conditions (Pough et al. 1983, Scharzkopf and Alford 1996), these results show the importance of the shelter selection on TEWL rates: more a shelter provides an enclosed space (which presents a low leak of water vapour), more TEWL rates are reduced.

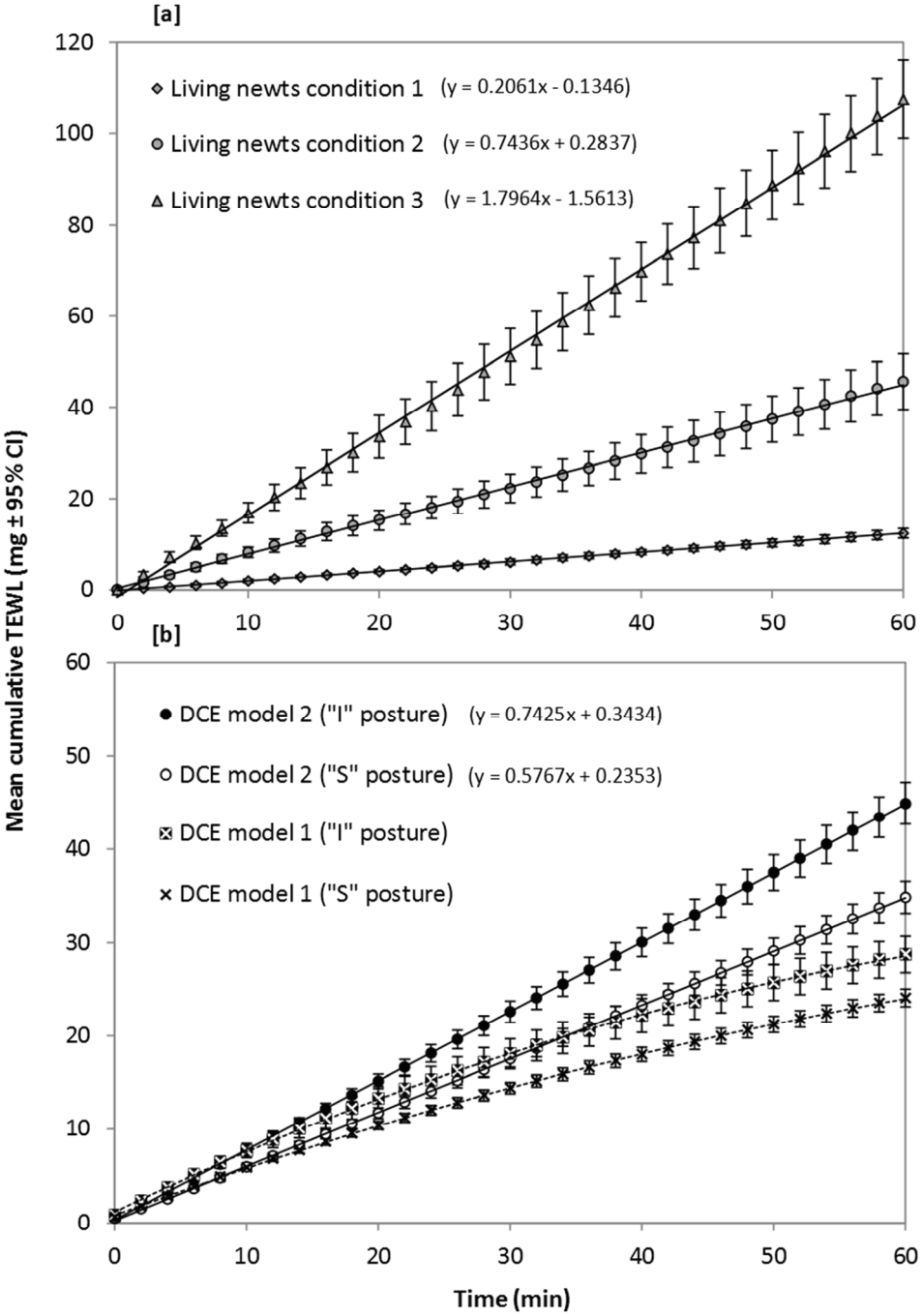

Fig. 2. Mean cumulative transepidermal evaporative water loss (TEWL, ± 95% confidence interval (CI)) under a 60 min period [a] for living palmate newts (n = 10) in the three conditions of desiccation (see Table 1); [b] for numerical newts in their two postures (“I” and “S”) from the diffusion-controlled

evaporation (DCE) model 1 (Neumann boundary condition) and 2 (Dirichlet boundary condition) only presented for the climatic condition 2 (see Table 1).

Comparison of the experimental agar replicas data with the DCE model 2. Measured TEWL rates of agar replicas according to "I"- and "S"-shaped postures were compared to those predicted by the DCE model 2 (Table 3, Fig. 4). The main observation that can be made from these results is the very good agreement of the model and the experiment. The average errors in TEWL predictions were about 3.3 per cent for the "I"-shaped posture (n=10, 95% Confidence Interval (CI), −5.8 - 12.4) and 1.2 per cent for the "S"-shaped posture (n=10, 95% CI, −7.3 - 9.7), let an average error about 0.0344 $mg.min^{-1}$ (n = 10, 95% CI, −0.0368 - 0.1056) and 0.0158 $mg.min^{-1}$ (n = 10, 95% CI, −0.0359 - 0.0675), respectively. Consequently, the measured reductions in TEWL rates between the "I"- and the "S"-shaped postures (22.9 %) were closely similar to those of the predictions from the model (21.1 %) (Table 4). The average error is about 3.7 per cent (n = 10, 95% CI, −29.9 – 37.3), let an average error about 0.0189 $mg.min^{-1}$ (n = 10, 95% CI, −0.0298 - 0.0676). The strong variability observed in the results between some agar replicas and their corresponding numerical newts (Tables 3, 4) most probably reflects postural variations when experimental newts were placed in a desired posture for the MRI and the casting (for creating their agar replicas). Nonetheless, difference in TEWL rates between predicted and measured values did not exceed 0.10 $mg.min^{-1}$, which means that the DCE model 2 precisely predicts TEWL rates measured on the agar replicas. In addition, the agar replicas are purely passive physical models, i.e. they have no mean to prevent the temperature decrease that should occur during desiccation. The agreement between results from the DCE model and agar replicas may validate the assumption of isothermal conditions or expresses the negligible effect of thermal natural convection on the vapour flux around the animal.

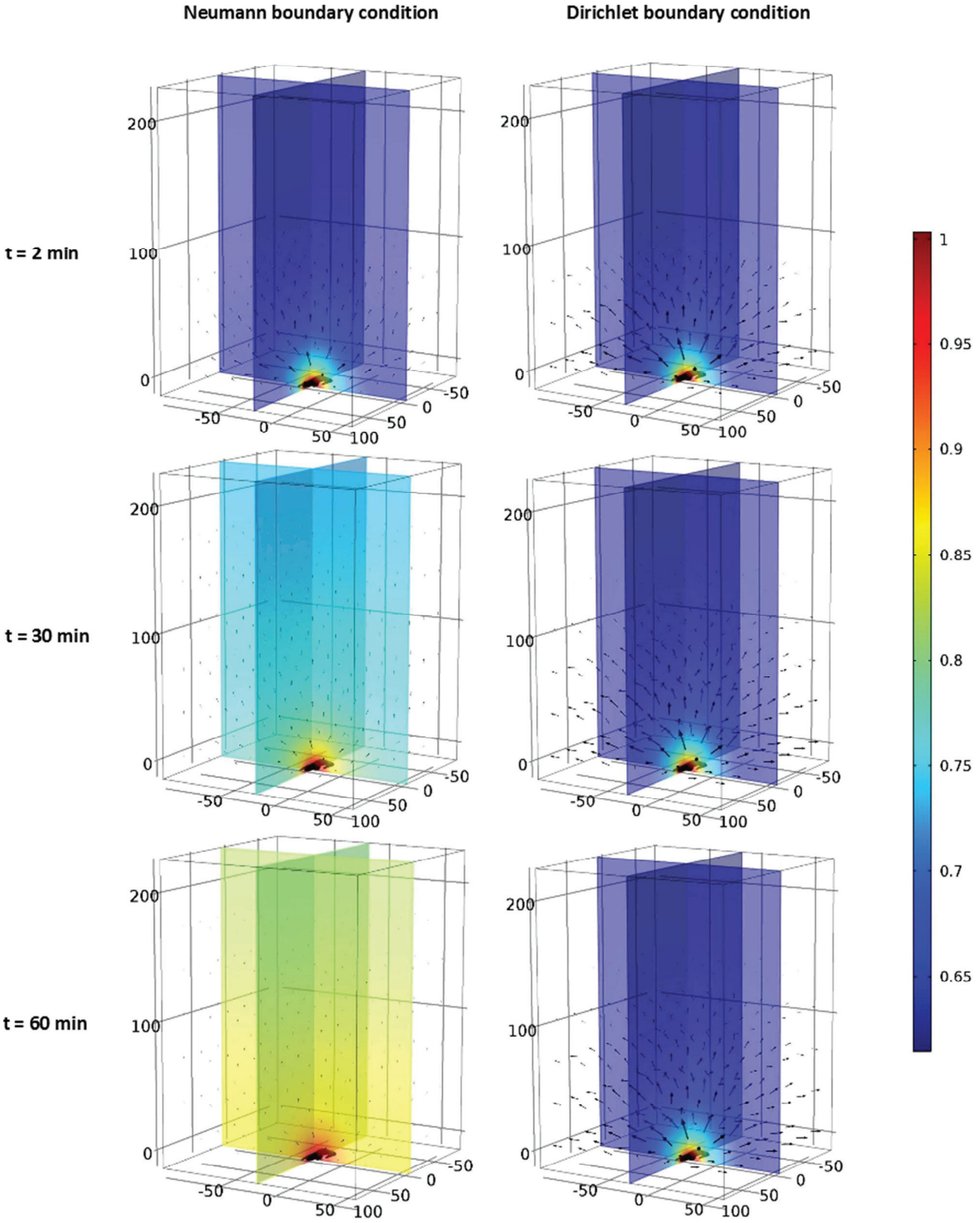

Fig. 3. Three-dimensional relative humidity (RH) distribution (colors) and flux vectors fields (arrows) only presented for the climatic condition 2 (see Table 1). It represents the evolution of RH in the calculation domain at three different times: 2, 30 and 60 min according to boundary conditions from the diffusion-controlled evaporation (DCE) model 1 (Neumann) and 2 (Dirichlet). (Pictures from COMSOL Multiphysics v4.2).

Table 3. Comparison of predicted and measured transepidermal evaporative water loss (TEWL) rates (mg.min^{-1}) over a 60 min period for both the "I"-and "S"-shaped agar replicas of *Lissotriton helveticus*. The values correspond to the slopes of the linear regression models between TEWL and time. Predictions calculated from the DCE model 2 using measured climatic **conditions 2a** presented in Table 1. $\dot{m}_I$ = TEWL for "I"-shaped postures; $\dot{m}_S$ = TEWL for "S"-shaped postures; $*$ = numerical newt

Agar replicas	$\dot{m}_I$	$\dot{m}_I{}^*$	$(\dot{m}_I - \dot{m}_I{}^*)$	$\%\,(\dot{m}_I - \dot{m}_I{}^*)$	$\dot{m}_S$	$\dot{m}_S{}^*$	$(\dot{m}_S - \dot{m}_S{}^*)$	$\%\,(\dot{m}_S - \dot{m}_S{}^*)$
P01	0.8485	0.7348	+ 0.1137	+ 13.4	0.7181	0.6336	+ 0.0845	+ 11.8
P02	0.6442	0.7124	− 0.0682	− 10.6	0.5285	0.5588	− 0.0303	− 5.7
P03	0.8492	0.7225	+ 0.1267	+ 14.9	0.6757	0.5494	+ 0.1263	+ 18.7
P04	0.8526	0.7732	+ 0.0794	+ 9.3	0.6284	0.5794	+ 0.049	+ 7.8
P05	0.7403	0.8168	− 0.0765	− 10.3	0.5540	0.5995	− 0.0455	− 8.2
P06	0.7970	0.7343	+ 0.0627	+ 7.9	0.5739	0.5792	− 0.0053	− 0.9
P07	0.9240	0.7452	+ 0.1815	+ 19.6	0.7354	0.6334	+ 0.1020	+ 13.9
P08	0.6718	0.7798	− 0.1080	− 16.1	0.5596	0.5487	+ 0.0109	+ 2.0
P09	0.7000	0.7387	− 0.0387	− 5.5	0.4820	0.5762	− 0.0942	− 19.5
P10	0.7256	0.6510	+ 0.0746	+ 10.3	0.5289	0.5683	− 0.0394	− 7.5
Mean	**0.7753**	**0.7409**	**+ 0.0344**	**+ 3.3**	**0.5984**	**0.5826**	**+ 0.0158**	**+ 1.2**
± 95% CI	**± 0.0660**	**± 0.0317**	**± 0.0712**	**± 9.1**	**± 0.0619**	**± 0.0220**	**± 0.0517**	**± 8.5**

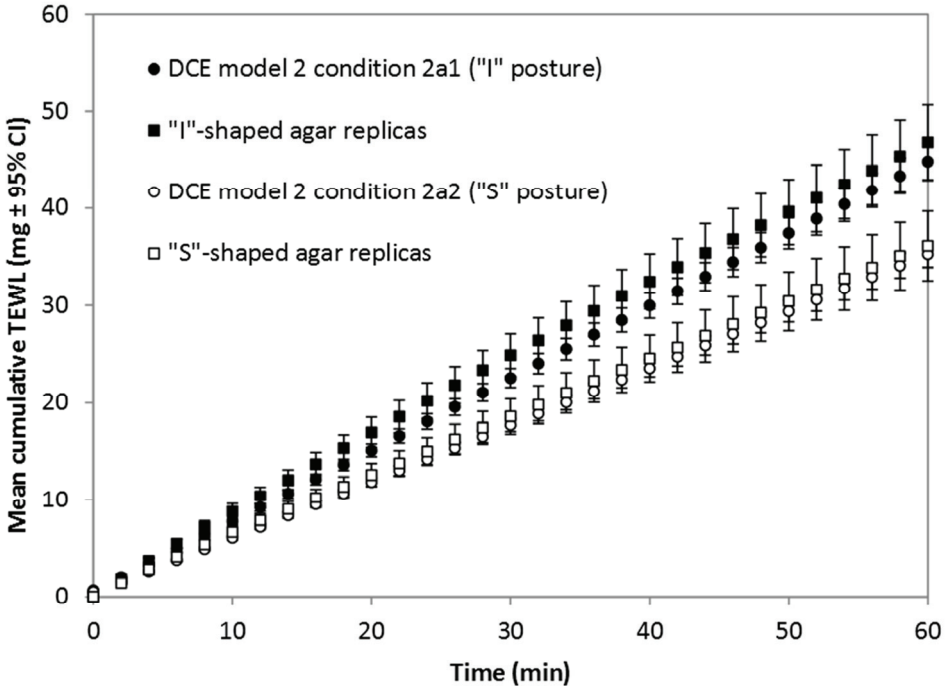

Fig. 4. Mean cumulative transepidermal evaporative water loss (TEWL, ± 95% confidence interval (CI)) under a 60 min period in the climatic condition 2a (see Table 1), measured for the "I"- and "S"-shaped agar replicas of the experimental palmate newts (n = 10) in comparison with the predicted TEWL rates for the "I"- and "S"-shaped postures from the diffusion-controlled evaporation (DCE) model 2.

Estimations of functional surface areas by the flux method. The predicted and measured reductions in TEWL rates provided by the "S"-shaped posture are closely related to our estimated reduction of evaporative surface area A_e by the flux method (Table 4). The estimations of the surface areas A_e and A_v of each numerical newt according to posture were plotted as a function of standard weight, in comparison with those obtained by Wardziak et al. (article [1]) via the trigonometric method (Figs. 5a,b). The least-squares best-fit equations of these relationships are represented in Figure 5, and follow a power relation as previously demonstrated by Tracy (1976), McClanahan and Baldwin (1969) and Wardziak et al. (article [1]). They could be used practically to estimate the functional surface area of palmate newts knowing their standard body weight W_0. The trigonometric method

systematically leads to under-estimations of the evaporative surface areas A_e. However, the agreement between the two methods is reasonable (lower than 4 % in average). Since the ventral surface area is small compared to the evaporative surface area (A_v/A_e = 0.1495), the estimation of A_v presents more uncertainty. The flux method, presented in this paper, is based on a robust physical concept since it takes into account all the surface elements that effectively contribute to the desiccation. Thus, we recommend to use the flux method to estimate the functional surface areas even if its implementation requires a more complex numerical effort. Additionally, via the evaporative surface areas estimated by the flux method, average A_e/W_0 ratios (α_I and α_S, see eqs. (11.1), (11.2)) according to the newt postures ("I" and "S") were calculated. The "I"- and "S"-shaped postures present an average ratio about 1.20 m².kg^{-1} (n = 10, 95% CI, 1.11 - 1.29) and 0.93 m².kg^{-1} (n = 10, 95% CI, 0.86 - 1.01), respectively.

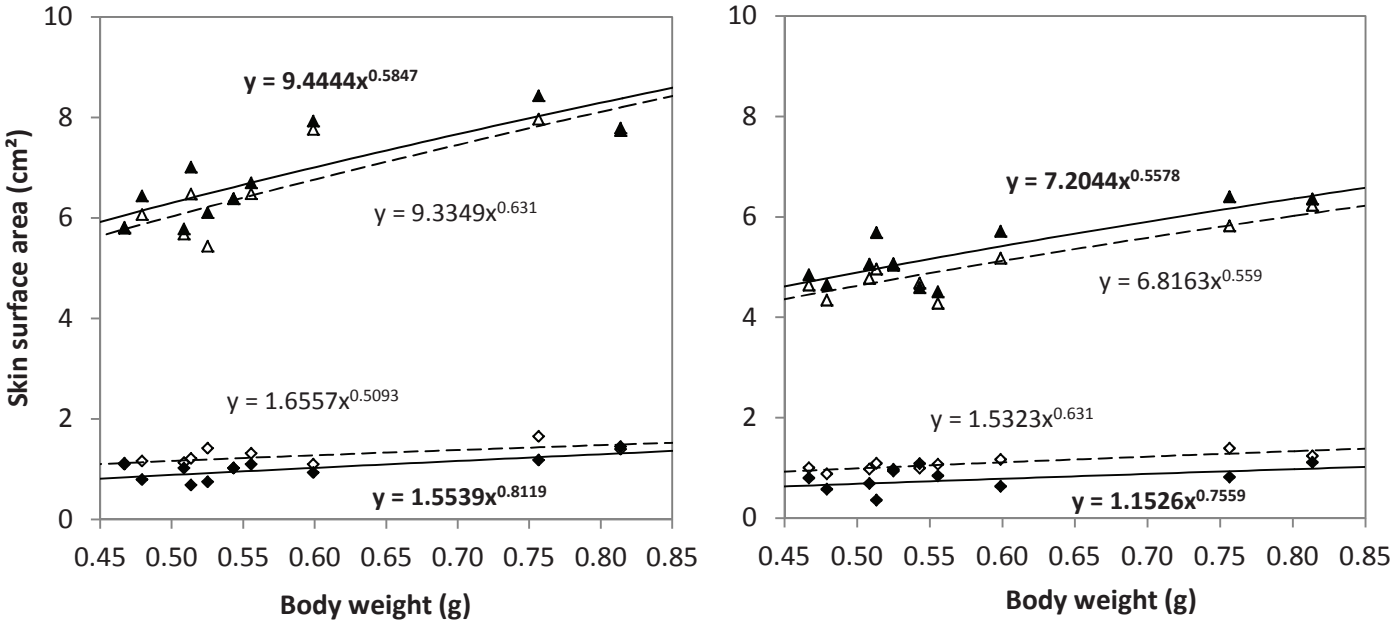

Fig. 5. Relationships between standard body weight (W_0; g) and evaporative and ventral surface areas (cm²) of experimental *Lissotriton helveticus* [a] for their "I"-shaped posture (triangles), and [b] for their "S"-shaped posture (diamonds), according to the method used, i.e. the flux method (black signs) or the trigonometric method (white signs). Solid and dashed lines represent the least-squares best-fit equations of these relationships for the flux and the trigonometric method, respectively. (Data of the trigonometric method from article [1]).

Table 4. Comparison of predicted and measured transepidermal evaporative water loss (TEWL) rate differences (mg.min^{-1}) over a 60 min period between the "I"-and "S"-shaped agar replicas of *Lissotriton helveticus*. Values calculated from the slopes of the linear regression models presented in Table 3. Data of the evaporative surface areas (A_e ; cm²) estimated via the flux method are presented. $\dot{m}_I$ = TEWL for "I"-shaped postures; $\dot{m}_S$ = TEWL for "S"-shaped postures; A_{e_I} = evaporative surface area for "I"-shaped postures; A_{e_S} = evaporative surface area for "S"-shaped postures; $*$ = numerical newt

Newt	$(\dot{m}_I - \dot{m}_S)$	% $(\dot{m}_I - \dot{m}_S)$	$(\dot{m}_I{}^* - \dot{m}_S{}^*)$	% $(\dot{m}_I{}^* - \dot{m}_S{}^*)$	A_{e_I}	A_{e_S}	$(A_{e_I} - A_{e_S})$	% $(A_{e_I} - A_{e_S})$
P01	+ 0.1304	+ 15.4	+ 0.1012	+ 13.8	7.74	6.36	+ 1.38	+ 17.8
P02	+ 0.1157	+ 18.0	+ 0.1536	+ 21.6	7.01	5.69	+ 1.32	+ 18.8
P03	+ 0.1735	+ 20.4	+ 0.1731	+ 24.0	5.81	4.85	+ 0.96	+ 16.5
P04	+ 0.2242	+ 26.3	+ 0.1938	+ 25.1	6.69	4.51	+ 2.18	+ 32.6
P05	+ 0.1863	+ 25.2	+ 0.2173	+ 26.6	7.93	5.71	+ 2.22	+ 28.0
P06	+ 0.2231	+ 28.0	+ 0.1551	+ 21.1	6.10	5.07	+ 1.04	+ 17.0
P07	+ 0.1886	+ 20.4	+ 0.1091	+ 14.7	8.43	6.40	+ 2.03	+ 24.1
P08	+ 0.1122	+ 16.7	+ 0.2311	+ 29.6	6.43	4.65	+ 1.78	+ 27.7
P09	+ 0.2180	+ 31.1	+ 0.1625	+ 22.0	6.38	4.59	+ 1.79	+ 28.1
P10	+ 0.1967	+ 27.1	+ 0.0827	+ 12.7	5.78	5.06	+ 0.72	+ 12.5
Mean	**+ 0.1769**	**+ 22.9**	**+ 0.1580**	**+ 21.1**			**+ 1.54**	**+ 22.3**
± 95% CI	**± 0.0309**	**± 3.8**	**± 0.0351**	**± 4.1**			**± 0.38**	**± 4.7**

Comparison of the experimental living newt data with the DCE model 2. The measured TEWL rates of living newts were compared to those of the DCE model 2 for the "I"- and "S"-shaped postures at each condition of desiccation (Tables 5-7; Figs. 6a-c). The variation of the TEWL index μ according to the conditions of desiccation is presented in Figure 7. The index decreases significantly when the desiccation condition became warmer (mixed model: *DF* = 19, *t* = -2.61, *P* = 0.0172). In other words, the living newts expressed more the "S"-shaped water-conserving posture in the warmer and drier condition, while they expressed dominantly an "I"-shaped posture in the colder and wet climatic conditions (Tables 5-7). This observation is supported by a statistical analysis, which reveals that μ significantly increases with the percentage of time spent in the "I"-shaped posture (mixed model: DF = 19, *t* = 2.87, *P* = 0.0098), and significantly decreases with the percentage of time spent in the "S"-shaped posture (mixed model: *DF* = 19, t = -2.71, *P* = 0.0138). Surprisingly, we detect no significant influence of the percentage of time spent moving on μ (mixed model: DF = 19, t = -2.02, *P* = 0.0579). Our results also show that the index μ presents important variations, i.e. between -2 and $+4$ according to the climatic condition. Given that our DCE model 2 has been validated experimentally for TEWL rates, these results suggest that newt's behaviours may have complex influences on TEWL rates (and thus on the index μ) that are not taken into account by DCE model. For example, according to our results, an "I"- and/or an 'S"-shaped posture (for living newts) could present great variation in their effective evaporative surface area; in particular when the newt exhibits an erected "I"-shaped postures (but also when it is moving), the belly can participate to TEWL if it comes in contact with air. Nonetheless, overall, the DCE model provides good predictions of living newts TEWL (Tables 5-7; Figs. 6a-c). For all the climatic conditions, the average TEWL index closely follows the newt's average behaviour observed (Tables 5-7).

Table 5. Comparison of predicted and measured transepidermal evaporative water loss (TEWL) rates (mg.min^{-1}) over a 60 min period for living *Lissotriton helveticus* in relation with their behaviors. The values correspond to the slopes of the linear regression models between TEWL and time. Predictions calculated from the DCE model 2 using measured climatic **conditions 1** presented in Table 1. $\dot{m}_L$ = TEWL for living newts; $\dot{m}_I$ = TEWL for "I"-shaped postures; $\dot{m}_S$ = TEWL for "S"-shaped postures; μ = TEWL index = $[2 \times (\dot{m}_L - \dot{m}_S{}^*)/(\dot{m}_I{}^* - \dot{m}_S{}^*)] - 1$; % $Act, Inact_I, Inact_S$ = percentage of time spent in moving, and in the "I"-and "S"-shaped postures, respectively; $*$ = numerical newt

Newt	$\dot{m}_L$	$\dot{m}_I{}^*$	$\dot{m}_S{}^*$	$(\dot{m}_L - \dot{m}_I{}^*)$	$(\dot{m}_L - \dot{m}_S{}^*)$	μ	% Act	% $Inact_I$	% $Inact_S$
P01	0.2116	0.1956	0.1612	+ 0.0160	+ 0.0504	+ 1.9	4.1	70.3	25.6
P02	0.1582	0.1891	0.1438	− 0.0309	+ 0.0144	− 0.4	4.5	86.7	8.8
P03	0.2060	0.1665	0.1315	+ 0.0395	+ 0.0745	+ 3.3	14.6	85.4	0.0
P04	0.2115	0.2196	0.1684	− 0.0081	+ 0.0431	+ 0.7	3.2	89.3	7.5
P05	0.2072	0.2302	0.1765	− 0.0230	+ 0.0307	+ 0.1	1.4	74.6	24.0
P06	0.1902	0.1478	0.1116	+ 0.0424	+ 0.0786	+ 3.3	5.1	94.9	0.0
P07	0.2439	0.2775	0.2310	− 0.0336	+ 0.0129	− 0.5	8.4	91.6	0.0
P08	0.2188	0.2209	0.1795	− 0.0021	+ 0.0393	+ 0.9	8.7	91.3	0.0
P09	0.2067	0.1486	0.110	+ 0.0581	+ 0.0957	+ 4.1	16.0	81.6	2.4
P10	0.2070	0.2431	0.2072	− 0.0361	− 0.0002	− 1.0	2.3	24.5	73.2
Mean	**0.2061**	**0.2039**	**0.1622**	**− 0.0022**	**+ 0.0439**	**+ 1.3**	**6.8**	**79.0**	**14.1**
± 95% CI	**± 0.0155**	**± 0.0302**	**± 0.0280**	**± 0.0249**	**± 0.0224**	**± 1.3**	**± 3.6**	**± 14.8**	**± 16.4**

Table 6. Comparison of predicted and measured transepidermal evaporative water loss (TEWL) rates (mg.min^{-1}) over a 60 min period for living *Lissotriton helveticus* in relation with their behaviors. The values correspond to the slopes of the linear regression models between TEWL and time. Predictions calculated from the DCE model 2 using measured climatic **conditions 2** presented in Table 1. $\dot{m}_L$ = TEWL for living newts; $\dot{m}_I$ = TEWL for "I"-shaped postures; $\dot{m}_S$ = TEWL for "S"-shaped postures; μ = TEWL index = $[2 \times (\dot{m}_L - \dot{m}_S{}^*)/(\dot{m}_I{}^* - \dot{m}_S{}^*)] - 1$; % $Act, Inact_I, Inact_S$ = percentage of time spent in moving, and in the "I"-and "S"-shaped postures, respectively; $*$ = numerical newt

Newt	$\dot{m}_L$	$\dot{m}_I{}^*$	$\dot{m}_S{}^*$	$(\dot{m}_L - \dot{m}_I{}^*)$	$(\dot{m}_L - \dot{m}_S{}^*)$	μ	% Act	% $Inact_I$	% $Inact_S$
P01	0.6090	0.7415	0.6128	− 0.1325	− 0.0038	− 1.1	7.8	40.5	51.7
P02	0.5598	0.7415	0.5431	− 0.1817	+ 0.0167	− 0.8	6.1	71.4	22.5
P03	0.8761	0.7254	0.5739	+ 0.1507	+ 0.3022	+ 3.0	8.3	83.2	8.5
P04	0.7082	0.7916	0.6114	− 0.0834	+ 0.0968	+ 0.1	11.5	23.7	64.8
P05	0.8842	0.8363	0.6330	+ 0.0479	+ 0.2512	+ 1.5	14.6	49.2	36.2
P06	0.8995	0.7026	0.5313	+ 0.1969	+ 0.3682	+ 3.3	10.0	44.2	45.7
P07	0.9129	0.7455	0.6191	+ 0.1674	+ 0.2938	+ 3.7	8.3	44.9	46.8
P08	0.7407	0.7829	0.5584	− 0.0422	+ 0.1823	+ 0.6	12.9	65.3	21.8
P09	0.7086	0.7064	0.5284	+ 0.0022	+ 0.1802	+ 1.0	22.0	72.8	5.3
P10	0.5373	0.6513	0.5555	− 0.1140	− 0.0182	− 1.4	2.8	38.9	58.3
Mean	**0.7436**	**0.7425**	**0.5767**	**+ 0.0011**	**+ 0.1669**	**+ 1.0**	**10.4**	**53.4**	**36.2**
± 95% CI	**± 0.1032**	**± 0.0372**	**± 0.0280**	**± 0.0966**	**± 0.0993**	**± 1.3**	**± 3.8**	**± 13.4**	**± 14.8**

Table 7. Comparison of predicted and measured transepidermal evaporative water loss (TEWL) rates (mg.min^{-1}) over a 60 min period for living *Lissotriton helveticus* in relation with their behaviors. The values correspond to the slopes of the linear regression models TEWL and time. Predictions calculated from the DCE model 2 using measured climatic **conditions 3** presented in Table 1. $\dot{m}_L$ = TEWL for living newts; $\dot{m}_I$ = TEWL for "I"-shaped postures; $\dot{m}_S$ = TEWL for "S"-shaped postures; μ = TEWL index = $[2 \times (\dot{m}_L - \dot{m}_S{}^*)/(\dot{m}_I{}^* - \dot{m}_S{}^*)] - 1$; $\%\, Act, Inact_I, Inact_S$ = percentage of time spent in moving, and in the "I"- and "S"-shaped postures, respectively; $*$ = numerical newt

Newt	$\dot{m}_L$	$\dot{m}_I{}^*$	$\dot{m}_S{}^*$	$(\dot{m}_L - \dot{m}_I{}^*)$	$(\dot{m}_L - \dot{m}_S{}^*)$	μ	$\%\, Act$	$\%\, Inact_I$	$\%\, Inact_S$
P01	1.6667	2.2526	1.8521	− 0.5859	− 0.1854	− 1.9	31.7	12.6	55.7
P02	1.6184	2.1784	1.6670	− 0.5600	− 0.0486	− 1.2	45.5	1.5	53.0
P03	1.8079	1.9422	1.5397	− 0.1343	+ 0.2682	+ 0.3	79.1	0.3	20.6
P04	1.9010	2.2360	1.6717	− 0.3350	+ 0.2293	− 0.2	0.8	6.4	92.7
P05	1.7976	2.3208	1.7869	− 0.5232	+ 0.0107	− 1.0	18.1	44.3	37.6
P06	1.7454	1.9759	1.5242	− 0.2305	+ 0.2212	− 0.0	66.4	13.0	20.6
P07	2.1943	2.2100	1.8360	− 0.0157	+ 0.3583	+ 0.9	57.5	13.1	29.4
P08	1.9212	2.0955	1.5007	− 0.1743	+ 0.4205	+ 0.4	31.7	4.2	64.1
P09	1.4944	2.0318	1.5116	− 0.5374	− 0.0172	− 1.1	43.8	2.1	54.1
P10	1.8172	1.9207	1.6476	− 0.1035	+ 0.1696	+ 0.2	50.3	19.5	30.2
Mean	**1.7964**	**2.1164**	**1.6537**	**− 0.3200**	**+ 0.1427**	**− 0.3**	**42.5**	**11.7**	**45.8**
± 95% CI	**± 0.1365**	**± 0.1021**	**± 0.0966**	**± 0.1546**	**± 0.1393**	**± 0.6**	**± 16.5**	**± 9.4**	**± 16.2**

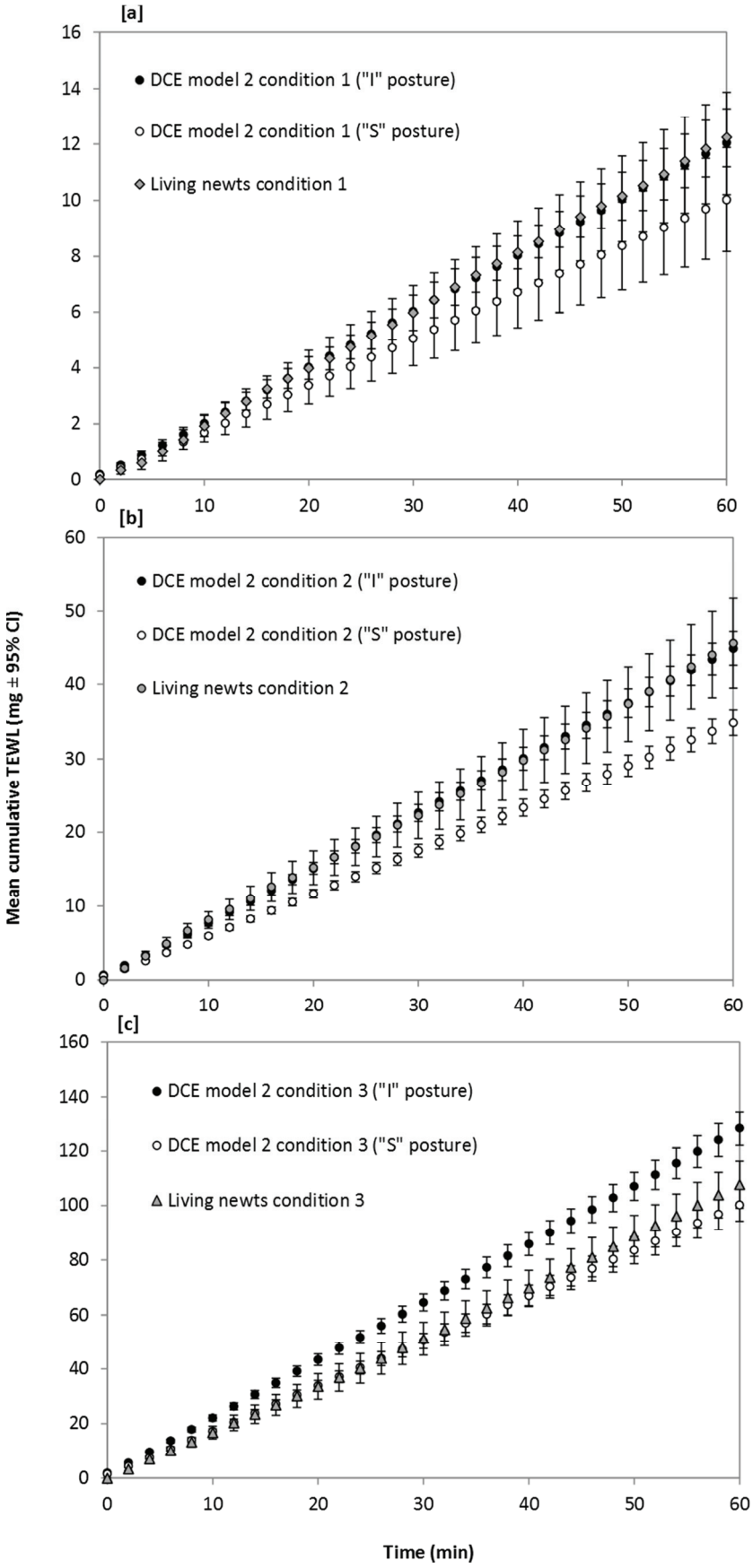

Fig. 6. [a], [b], [c] Mean cumulative transepidermal evaporative water loss (TEWL, ± 95% confidence interval (CI)) under a 60 min period in the three climatic condition (see Table 1), for the living newts (n = 10) in comparison with the predicted TEWL rates for the "I"- and "S"-shaped postures from the diffusion-controlled evaporation (DCE) model 2.

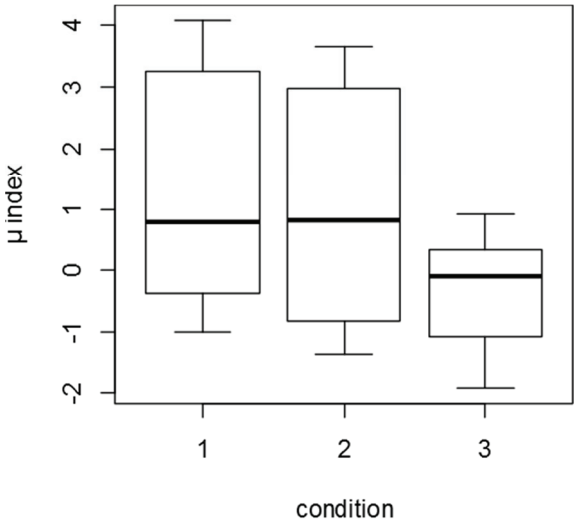

Fig. 7. Variation of the transepidermal evaporative water loss (TEWL) dimensionless index μ (see details in main text, and eq. (9)) according to the three climatic conditions (1 to 3). Boxplots represent the median, the first and the third quartile and range.

Setting up a model to estimate TEWL rates in a large range of temperature and RH. From our empirical models (eqs. (10), (11)), values of the mass transfer coefficients h_1 and h_2 were calculated for the nine combinations of temperature and RH, for each numerical newt according to its posture. The overall average h_1 and h_2 coefficients in calm air were about 106.22 m^{-1} (n = 180, 95% CI, 104.98 - 107.49) and 2.59 (n = 180, 95% CI, 2.57 – 2.61), respectively. Statistical analyses reveal that h_1 is independent from temperature, HR, and postures, contrarily to h_2 that is significantly influenced by postures with average values about 2.75 (“I”-shaped posture, n = 180, 95% CI, 2.73 – 2.77) and 2.43 (“S”-shaped posture, n = 180, 95% CI, 2.42 – 2.46) (Table 8).

Table 8. Effect of temperature, relative humidity (RH) and postures (“I” and “S”) on mass transfer coefficients h_1 (from eq. (10)) and h_2 (from eq. (11)) at all the combinations of temperature and RH simulated (see main text). The mixed model includes three fixed effects (temperature, RH, and postures) and the interaction between temperature and RH. Non-significant interaction was

excluded from the final model. The model takes into account the correlated error between measurements made on a same individual as a random effect.

h_1 [m^{-1}]	Estimates	Std. error	Degrees of Freedom	*Wald t test-value*	*P-value*
Intercept	106.22158	2.9485747	167	36.02472	< 0.0001
posture	0.43786	0.5167099	167	0.84739	0.3980
RH	-0.52483	1.5820946	167	-0.33173	0.7405
temperature	0.00498	0.0414290	167	0.12023	0.9044
h_2 [-]					
Intercept	2.7549876	0.028029425	167	98.28913	< 0.0001
posture	-0.3173838	0.008527509	167	-37.21882	< 0.0001
RH	-0.0125817	0.026110056	167	-0.48187	0.6305
temperature	0.0001253	0.000683722	167	0.18331	0.8548

From our empirical model 1 (eq. (10)), these results validate the choice of a single coefficient h_1 independent from the newt posture:

$$\dot{m}_1 = A_e\, D\, \rho_{vs} * 106.22(1 - \varphi_0) \quad (14)$$

It is worth noticing that such a result implies that the posture effect is fully explained by the reduction of surface area in "S"-shape. The topology of the newt evaporative surface does not influence the evaporative process.

By contrast, from our empirical model 2 (eq. (11)), these results invalidate such a choice of a single coefficient h_2 independent from the newt posture:

$$\begin{cases} \dot{m}_{2,I} = \sqrt{A_e}\, D\, \rho_{vs} * 2.75(1 - \varphi_0) & (15.1) \\ \dot{m}_{2,S} = \sqrt{A_e}\, D\, \rho_{vs} * 2.43(1 - \varphi_0) & (15.2) \end{cases}$$

Nonetheless, given that the general newt's behaviour in the three different climatic conditions (Tables 5, 6 and 7) is characterized by a composite behaviour of "I"- and "S"-shaped postures, this allows the choice of a single average coefficient:

$$\dot{m}_2 = \sqrt{A_e}\, D\, \rho_{vs} * 2.59(1 - \varphi_0) \quad (15.3)$$

Additionally, average α ratios were estimated for each newt's posture (see above) in order to propose a useful model to estimate the newts' TEWL rates without knowing A_e. Thus, from eqs. (11.1, 11.2) our useful TEWL model for *L. helveticus* in calm air can be written as:

$$\begin{cases} \dot{m}_{3,I} = 46.31 * W_0 \, D_v \, \rho_{vs} * 2.59 \left(1 - \varphi_0\right) & (16.1) \\ \dot{m}_{3,S} = 40.76 * W_0 \, D_v \, \rho_{vs} * 2.59 \left(1 - \varphi_0\right) & (16.2) \end{cases}$$

The TEWL rates obtained from the DCE model 2 were plotted against the TEWL rates predicted by the empirical relationships (eqs. (14) , (15.3) and (16.1-16.2)) for all the postures, temperature and RH combinations (Fig.8). Our results show that the TEWL rates predicted by our empirical model 1 (eq. (14)) explain approximately 97% of the variance of the calculated values with the DCE model 2, while our empirical model 2 (eq. (15.3)), that takes into account the skin surface area square root, explain approximately 98% of the variance. Moreover, this last model presents a better satisfactory precision in estimating TEWL rates with an overall relative error that does not exceed -10 and +10 % (mean: 0.40 %, n = 180, 95% CI, -0.59 - $+1.39$) against -10 and +20% for the empirical model 1 (mean: 0.68 %, n = 180, 95% CI, -0.55 - $+1.91$). Additionally, the use of an average α ratio as described in eqs. (11.1, 11.2) or (16.1, 16.2) leads to an acceptable loss of precision in the estimation of TEWL rates. In fact, our useful model explains approximately 91% of the variance of the measured values with DCE model 2, and presents a higher overall relative error between -20 to +40 % (mean: 2.20 %, n = 180, 95% CI, -0.18 - $+4.58$). These results suggest that both our empirical and the useful models appear to be suitable to the prediction of TEWL rates under the range of tested climatic conditions, and especially our empirical model 2 which attests that it is more relevant to reason with equivalent perimeter than skin surface areas. Since it has a robust physical base, it may even be used with a small extrapolation of the driving parameters (T, φ and W_0).

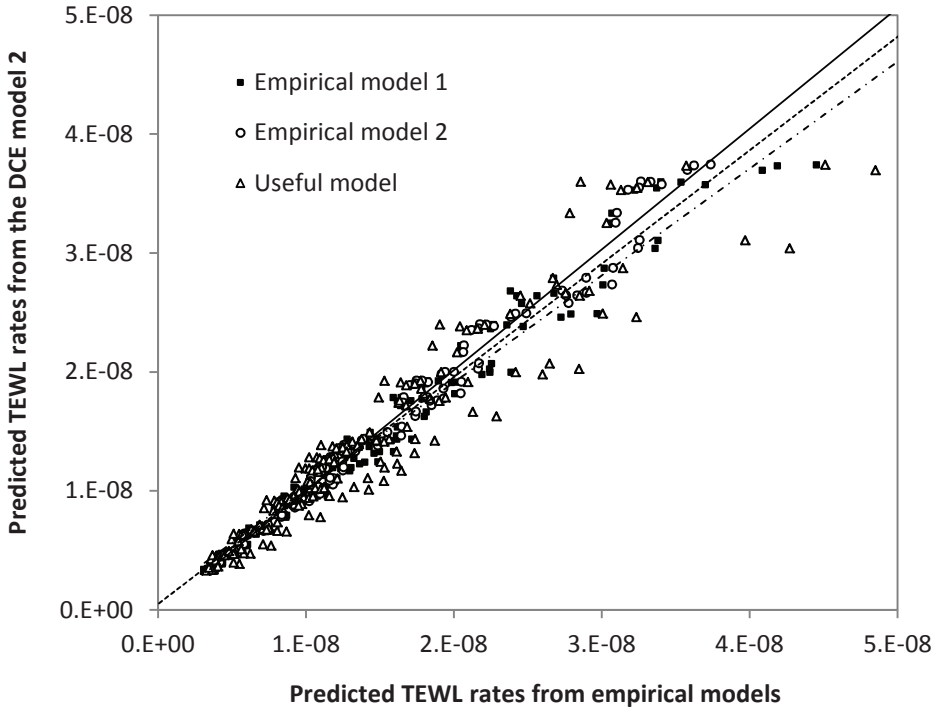

Fig. 8. TEWL rates (kg.s^{-1}) obtained from the DCE model 2 as a function of the predicted TEWL values from the empirical relationships (eqs. (10), (15.3) and (16.1-16.2)) for each numerical newt at all the postures, temperature and RH combinations. (Linear regressions: *Empirical model 1*: y = 0.954x + 5.10^{-10}, R² = 0.9745; *Empirical model 2*: y = 1.0149x - 1.10^{-10}, R² = 0.9844; *Useful model*: y = 0.8995 + 1.10^{-09}, R² = 0.9079).

Comparison of Tracy's model with our empirical model 1. The average value of our mass transfer coefficient h_1 (from eq. (10), i.e. 106.22 m^{-1}) corresponds to a coefficient at null air flow velocity. This result means that the mass transfer coefficient does not nullify under a lack of wind situation, contrarily to the prediction of the Tracy's model (eq. (12)). The variation of the mass transfer coefficients of Tracy (eq. (13)) $h'1$ and $h'2$ were plotted as function of air flow velocity (Fig. 9). In the figure 9, our value h_1 is presented as a point of reference. Under the range of temperature (15-30°C) and RH (40-80 %) studied in this paper, and the range of our experimental newt's size (0.029-0.034 m), these results show that for all the values of air flow velocity inferior to 2.5-3 cm.s^{-1}, the model of Tracy leads to under

estimations of the TEWL. Furthermore, these results suggest that Tracy's model should be revisited under the light of this study, for modelling and simulating water transfers between an amphibian and the air under forced advection. Our methodology may be applied to study slow wind boundary layer situations and may bring significant modifications to Tracy's model.

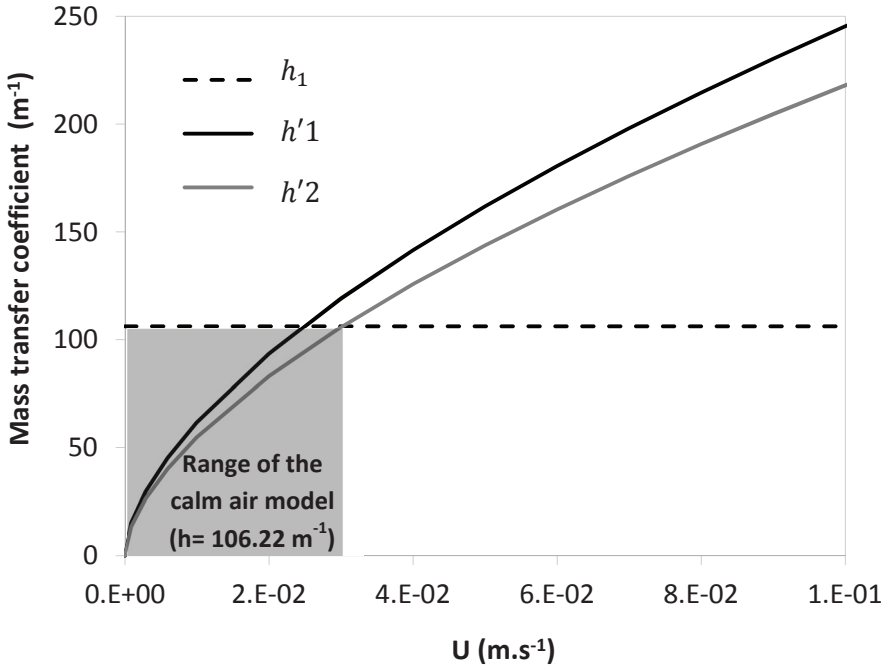

Fig. 9. Tracy's mass transfer coefficients h' (eq. (13)) as function of the air flow velocity U. Two different h' were calculated: $h'1$ for minimal temperature and SVL; $h'2$ for maximal temperature and SVL. The minimal and maximal values of SVL obtained in our experimental newts are 0.029 and 0.034 m, respectively; and those for temperatures are 15 and 30°C, respectively. Our value h_1 (from eq. (10)) is presented as a point of reference.

CONCLUSION

Using 3D geometries of living amphibians combined with a recent modelling tool, we successfully performed 3D numerical analysis of TEWL and proposed an accurate general and a simplified (useful) diffusion-controlled evaporation (DCE) models to estimate TEWL

rates in a large range of temperature and humidity under a lack of advection phenomenon. Moreover, in a purely diffusion situation it appears more relevant to reason with the skin surface area square root (perimeter) than the skin surface that interacts with atmosphere. For the experimental climatic conditions of this study, the models were shown to be adequate to predict TEWL rates of the living experimental newts, as well as their agar replicas, and highlighted the minimal threshold of air flow velocity that authorizes the application of the advection-diffusion Tracy's model. In addition, using our DCE model, a robust methodology to estimate accurately the functional surface areas of an amphibian was developed, since it takes into account all the surface elements of the newt's 3D geometries that effectively contribute to the desiccation. One should note that recent engineering and physical papers have described a natural autonomous free advection phenomenon as a potential water evaporation driving phenomena in calm air (Debbissi et al 2003, Shahidzadeh-Bonn et al. 2006, Weon et al. 2011, Jodat and Moghiman 2012). So, in such situation, water vapour molecules can be theoretically transported away from the evaporative skin surface area (saturated in water vapour) through air motion generated by buoyancy (gravitational forces) because, all things being equal, humid air is lighter than dry air. However, our results suggest that this phenomenon, as well as natural thermal convection, would be absent in our experimental conditions; if not, it should be negligible in comparison with the molecular diffusion driving by RH gradient that establishes around the animal. It is hoped that our general model developed in this paper will be used and improved to give a new quantitative basic overview, and a new firm theoretical framework, of the interrelatedness of amphibian's physical interaction with their terrestrial environment. Finally, it is hoped that the original approach used in this paper would open

new ways in the field of the biophysical ecology for comparative study of water and temperature relations in amphibians and other wet-skinned taxa.

Acknowledgements. We warmly thank Théotime Colin and Marion Javal for their help and support in the laboratory. This study was supported by a grant from the French *Ministère de l'Enseignement Supérieur et de la Recherche* and was conducted with the approval of the Préfecture de l'Isère (decision 2011-1710) and the Ethical Committee of University Lyon 1 in accordance with the current French laws.

LITERATURE CITED

Amey AP, Grigg GC (1995) Lipid-reduced evaporative water loss in two arboreal hylid frogs. *Comp Biochem Physiol* 111:283-291

Bolker BM, Brooks ME, Clark CJ, Geange SW, Poulsen JR, Stevens MHH, White JSS (2009) Generalized linear mixed models: a practical guide for ecology and evolution. Trends *Ecol Evol* 24:127-135

Bottomley PA, Roger HH, Foster TH (1986) NMR imaging shows water distribution and transport in plant root systems in situ. *Proc Natl Acad Sci USA* 83:87–89

Bozinovic F, Calosi P, Spicer JI (2011) Physiological correlates of geographic range in animals. *Anu Rev Ecol Evol Syst* 42:155-179

Debbissi C, Orfi J, Nasrallah SB (2003) Evaporation of water by free or mixed convection into humid air and superheated steam. *Int J Heat Mass transfer* 46:4703-4715

Deegan RD, Bakajin O, Dupont TF, Huber G, Nagel SR, Witten TA (1997) Capillary flow as the cause of ring stains from dried liquid drops. *Nature* 389:827-829

Dobkins DS, Gettinger RD, O'Connor MP (1989) Importance of retreat site for hydration state in *Bufo marinus* during dry rainy season. *Am Zool* 29:88A

Feder ME, Burggren WW (1985) Cutaneous gas exchange in vertebrates: design, patterns, control and implications. *Biol Rev* 60:1-45

Hillman SS, Withers PC, Drewes RC, Hillyard SD (2009) Ecological and environmental physiology of amphibians. Oxford University Press

IPCC (2007) Working group I report, climate change 2007: "the physical science basis". The fourth assessment report of the intergovernmental panel on climate change, Paris

Jaynes DB, Rogowski AS (1983) Applicability of Fick's law to gas diffusion. *Soil Sci Soc Am J* 47:425-430

Jodat A, Moghiman M (2012) An experimental assessment of the evaporation correlation for natural, forced and combined convection regimes. *Proc IME C J Mech Eng Sci* 226:145-153

Kearney M, Porter W (2009) Mechanistic niche modelling: combining physiological and spatial data to predict species'ranges. *Ecol Let* 12:334-350

Laforsh C, Imhof H, Sigl R, Settles M, Heß M, Wanninger A (2012) Application of computational 3D-modeling in organismal biology. In: Alexandru C (ed), Modeling and simulation in engineering. InTech, Rijeka, pp. 117–142

Lillywhite HB (2006) Water relations of tetrapod integument. *J Exp Biol* 209:202-226

McClanahan L, Baldwin R (1969) Rate of water uptake through the integument of the desert toad, *Bufo punctatus*. *Comp Biochem Physiol* 28:381-389

Markowski P, Richardson Y (2011) Mesoscale meteorology in midlatitudes. Penn State University, University Park, PA, USA.

Nguyen TA, Dresselaers T, Verboven P, D'hallewin G, Culeddu N, Van Hecke P, Nicolaï (2006) Finite element modelling and MRI validation of 3D transient water profiles in pears during postharvest storage. *J Sci Food Agric* 86:745-756

Pinheiro JC, Bates DM, DebRoy S, Sarkar D, The R Core Team (2009) nlme: linear and nonlinear mixed effects models. *R package version* 3:1-96

Pough FH, Taigen TL, Stewart MM, Brussard PF (1983) Behavioural modification of evaporative water loss by a Puerto Rican frog. *Ecology* 64:244-252

R Core Team (2013) R: A language and environment for statistical computing. R Foundation for Statistical Computing, Vienna, Austria. URL http://www.R-project.org/

Schwarzkopf L, Alford RA (1996) Desiccation and shelter-site use in a tropical amphibian: comparing toads with physical models. *Funct Ecol*. 10:193-200

Seebacher F, Alford RA (2002) Shelter microhabitats determine body temperature and dehydration rates of a terrestrial amphibian (*Bufo marinus*). *J Herpetol* 36:69-75

Shahidzadeh-Bonn N, Rafai S, Azouni A, Bonn D (2006) Evaporating droplets. *J Fluid Mech* 549:307-313

Shoemaker VH, Hillman SS, Hillyard SD, Jackson DC, McClanahan LL, Withers PC, Wygoda ML (1992) Exchange of water, ions, and respiratory gases in terrestrial amphibians. In: Feder E, Burggren WW (ed) Environmental Physiology of the Amphibians. University of Chicago Press, Chicago

Shoemaker VH, Nagy KA (1977) Osmoregulation in amphibians and reptiles. *Annual Review of Physiology*. 39:449-471

Spotila JR, Berman EN (1976) Determination of skin resistance and the role of skin in controlling water loss in amphibians and reptiles. *Comp Biochem Physiol* 55A**:**407-411

Spotila JR, O'Connor MP, Bakken GS (1992) Biophysics of heat and mass transfert. In: Feder E, Burggren WW (ed) Environmental Physiology of the Amphibians. University of Chicago Press, Chicago

Stuart SN, Chanson JS, Cox NA, Young BE, Rodrigues ASL, Fishman DL, Waller RW (2004) Status and trends of amphibian declines and extinctions worldwide. *Science* 306:1783-1786

Tracy CR (1976) A model of the dynamic exchange of water and energy between a terrestrial amphibian and its environment. *Ecol Monogr* 46:293-326

Tracy CR, Welch WR, Porter WP (1980) Properties of air: a manual for use in biophysical ecology. Third Edition, University of Wisconsin Technical Report

Wardziak T, Luquet E, Plenet S, Léna JP, Oxarango L, Joly P (2013) Impact of both desiccation and exposure to an emergent skin pathogen on transepidermal water exchange in the palmate newt (*Lissotriton helveticus*). *Dis Aquat Org* 104:215-224

Weon BM, Je JH, Poulard C (2011) Convection-enhanced water evaporation. *AIP Advances* 012102

Xia Y, Sarafis V, Campbell EO, Callaghan PT (1993) Non-invasive imaging of water flow in plants by NMR microscopy. *Protoplasma* 173:170–176

CHAPTER TWO – PART 2

Numerical analysis of transepidermal evaporative water loss driven by diffusion and free advection in an urodele amphibian

Remarques préliminaires

Cette partie de ma thèse représente la tentative de modéliser un phénomène encore mal connu dans le domaine de la mécanique des fluides : l'advection naturelle (free advection). Il s'agit d'une partie de ma thèse qui nécessiterait un développement complémentaire à une fin de publication. Au début de nos tentatives de modélisations de la perte en eau par évaporation chez L. helveticus, notre modèle de transepidermal evaporative water loss (TEWL ; article [2]) ne prenait pas en compte l'option avancée en contrainte faible (weak constraint) du logiciel Comsol Multiphysics pour l'estimation des flux. Il s'avère que dans notre cas (avec nos tritons numériques), résoudre l'équation (6) du flux de surface (cf. article [2]) sans prendre en compte cette option conduit à une sous-estimation non négligeable du flux de surface (d'un facteur 2 à 3) et donc des valeurs de TEWL chez nos tritons numériques. Nos premiers résultats prédisaient donc des valeurs de TEWL 2 à 3 fois moins importante de ce qui avait été observé expérimentalement. Ces résultats suggéraient alors la présence d'une variable que notre modèle de TEWL ne prenait pas en compte. Pour expliquer de telles différences, la présence d'un phénomène se superposant à la diffusion moléculaire - en l'occurrence la présence d'un flux d'air (advection) - a été envisagée. Des essais numériques, incluant l'erreur de calcul de flux, ont montré qu'une vitesse d'écoulement d'air d'environ 2 $cm.s^{-1}$ permettait de retrouver des valeurs de flux compatibles avec nos expériences. Cependant, le fait que les expérimentations (mesures de TEWL) se sont déroulées dans un environnement sans vent, et que les tritons ont été placés dans une balance fermée, n'était pas très compatible avec cette approche. La récente littérature en mécanique des fluides portant sur l'étude de l'évaporation de gouttes d'eau de l'ordre du millimètre et du

centimètre (Debbissi et al 2003, Shahidzadeh-Bonn et al. 2006, Weon et al. 2011, Jodat and Moghiman 2012) mentionnaient cependant des résultats similaires aux nôtres. Les auteurs ont suggéré la présence d'un phénomène d'advection naturelle, pouvant théoriquement avoir lieu en environnement sans vent, susceptible d'expliquer la sous-estimation de leurs modèles d'évaporation par rapport à leurs observations. Le moteur de ce phénomène est la différence de densité d'air humide, entre la surface qui s'évapore et l'air ambiant, du simple fait que l'air sec est plus dense que l'air humide générant ainsi des flux d'air de l'ordre de 1 à 10 cm.s^{-1} (Shahidzadeh-Bonn et al. 2006, Weon et al. 2011).

C'est dans ce contexte, que nous avions décidé de modéliser ce phénomène chez L. helveticus avant de nous rendre compte de la sous-estimation du flux de surface par nos premières méthodes de résolution de l'eq. (6) (cf. article [2]). Cette partie de ma thèse vise à présenter notre modèle d'advection-diffusion, ainsi que quelques résultats de cette modélisation chez L. helveticus.

INTRODUCTION

A model of dynamic exchanges of water with atmosphere based on the Fick's law has been established for the leopard frog *Rana pipiens* (Tracy 1976, Shoemaker et al. 1992, Spotila et al. 1992, Hillman et al. 2009). As described by the mechanistic models of Tracy (Tracy 1976), the difference in saturated water vapour density (or the Relative Humidity (RH) gradient) across the amphibian skin, and the water vapour diffusion coefficient, are not the only physical factors determining TEWL. Under natural conditions, transport of water vapour by air motion, and the air flow regime (i.e. laminar or turbulent) are the most important environmental variables because they can considerably enhance TEWL rate compared to pure molecular diffusion (Debbissi et al 2003, Shahidzadeh-Bonn et al. 2006, Weon et al. 2011, Jodat and Moghiman 2012). Tracy's model describes specifically a water vapour transport by molecular diffusion coupled with forced advection mechanism, i.e. an external and permanent air flow governed by the Reynolds number. However, forced advection may not be the only process influencing the evaporation process (Debbissi et al 2003, Shahidzadeh-Bonn et al. 2006, Weon et al. 2011, Jodat and Moghiman 2012). Theoretically, WEDP can be caused by the superposition (coexistence) of two distinct mechanisms: a forced and a free (autonomous) mass transport mechanism, the dominant one primarily depends upon air flow velocity. However, forced advection may not be the only process influencing the evaporation process (Debbissi et al 2003, Shahidzadeh-Bonn et al. 2006, Weon et al. 2011, Jodat and Moghiman 2012). Theoretically, WEDP can be caused by an autonomous mechanism termed free advection. Water vapour molecules can be transported away from an evaporative surface area by the air motion generated by buoyancy because, all things being equal, humid air is lighter than dry air (Shahidzadeh-Bonn

et al. 2006, Weon et al. 2011, Jodat and Moghiman 2012). Thus, WEDP can be caused by the superposition (coexistence) of these two distinct mechanisms: the forced advection and the free (autonomous) advection mechanism. By analogy with thermal convection, forced advection should generally dominate free advection. However, in a quiescent air environment, the free advection mechanism should trigger and generate a WEDP. The dimensionless mass transfer Rayleigh number (Ra) approximates the ratio of the buoyant forces (causing free mass transport mechanisms) versus diffusive and viscous forces (working against it) (Shahidzadeh-Bonn et al. 2006, Weon et al. 2011, Jodat and Moghiman 2012):

$$\mathrm{Ra} = \frac{g L^3 \Delta\rho}{v\, D\, \rho} \qquad (1)$$

where g is the gravitational acceleration [m.s^{-2}], L is the characteristic length of the animal [m] (for amphibians this parameter is defined as the snout-vent length), v is the kinematic viscosity of the air [m².s^{-1}], D is the diffusion coefficient of the water vapor in air [m².s^{-1}], and $\Delta\rho/\rho$ [-] is the reduced humid air density [kg.m^{-3}] across the skin (see Tracy, et al. 1980 for calculation of v; and see Table 2 in article [2] for calculation of D and ρ). Situations providing a high Rayleigh number are likely to promote the free advection mechanism. In addition, the dimensional analysis of the equation (1) shows that free advection should increase as temperature and air humidity gradient (around the animal) increase, and especially with the size of the animal. Experimental evidences of free advection in quiescent atmosphere are currently scarce (Shahidzadeh-Bonn et al. 2006, Weon et al. 2011). The studies of Shahidzadeh-Bonn et al. (2006) and Weon et al. (2011) have focused on the evaporating behaviour of small water droplets (max diameter: 0.6 cm) at 20-25°C and 30-50% RH. Evaporation kinetics are evaluated by monitoring change in the radius of the

droplet along time (using imaging methods). It is then compared to empirical diffusion-controlled evaporation models. In all these studies, the theoretical predictions have recurrently under-estimated evaporation rate (by a factor from 2 to 5), thus suggesting that water evaporation in quiescent air is not purely diffusive. For these authors, the gradient in humid air density above water droplets could create an air flow susceptible to enhance water evaporation. The characteristic speed for this free advection is estimated within a range from 1 $cm.s^{-1}$ (Shahidzadeh-Bonn et al. 2006) to 10 $cm.s^{-1}$ (Weon et al. 2011), thus supporting the hypothesis of a strong contribution to WEDP, at least at the small scale considered. Consequently, humid air gradient surrounding the evaporative surface is likely able to create small autonomous air flows that could considerably enhance water evaporation by molecular diffusion (Shahidzadeh-Bonn et al. 2006, Weon et al. 2011). Under free advection, water evaporation rate depends on both the RH and the humid air gradient between evaporative surface and ambient air (Shahidzadeh-Bonn et al. 2006, Weon et al. 2011, Jodat and Moghiman 2012).

In the light of these recent studies, there is no reason to neglect this phenomenon in wet-skinned animals. Given that the skin surface of an amphibian is assumed to be an air film saturated in water vapour (i.e. 100% RH; actually slightly less than 99.5% depending on the osmotic concentration of the body fluids (Hillman et al. 2009)), the humid air density gradient across their skin could create non negligible air flow and thus potentially enhance their TEWL rate by molecular diffusion. Furthermore, terrestrial amphibians express water-conserving behaviours that generally consist in avoiding unfavourable ambient conditions (temperature, relative humidity, wind speed) by seeking shelters (e.g. Pough et al. 1983, Dobkins et al. 1989, Shoemaker et al. 1992, Schwarzkopf and Alford 1996, Seebacher and

Alford 2002) that could trigger free WEDP. In such a case, free WEDP would be likely to play a significant role in amphibian's TEWL in this kind of environment.

In this way, it would be interesting to consider now how the free advection would influence TEWL rate of amphibians by molecular diffusion in order to evaluate the relative weight of this phenomenon in a calm air situation (compared to pure molecular diffusion). Moreover, we explored how this phenomenon would be influenced by the organism's size. In this context we attempt, using the 3D geometries generated by Wardziak et al. (article [1]), to perform 3D numerical simulation of TEWL, driven by both the molecular diffusion and the free advection, of palmate newts (*Lissotriton helveticus*) in order to identify if such a physical process is involved in their TEWL when subjected to dehydration under lack of forced advection phenomenon. This was performed by comparison with the diffusion-controlled evaporation (DCE) model developed in article [2].

MATERIALS AND METHODS

Experimental data acquisitions

This part represents the protocols described in the article [2].

The Combined Advection-Diffusion (CAD) model

Mathematical model: the Advection-Diffusion equation. The CAD model follows the same assumptions that the DCE model (see article [2], equations (1) to (3)). Thus, our diffusion model with the isothermal assumption is:

$$\frac{\partial \varphi}{\partial t} = -D(T)\Delta\varphi \quad (2)$$

where φ is the Relative Humidity RH [-], the term in the left side of the eq. (2) corresponds to the accumulation of RH in air, D is the molecular diffusion coefficient [m².s^{-1}]. D is assumed isotropic and depends on the temperature T [K] (see article [2], Table 2 for temperature dependence relationship), and Δ is the Laplace operator.

Introducing an advection transport of RH due to air velocity field U in eq. (2) leads to:

$$\frac{\partial \varphi}{\partial t} + \nabla \cdot (U\varphi) = -D(T)\Delta\varphi \quad (3)$$

U is thus the air motion component [m.s^{-1}], and is assumed laminar and incompressible.

Mathematical model: the Navier-Stokes equation of air motion. The CAD model introduces the equation of continuity which represents the conservation of mass as:

$$\frac{\partial \rho}{\partial t} + \nabla \cdot (\rho U) = 0 \quad (4)$$

where ρ is the humid air density [kg.m^{-3}], and assumed constant. According to the ideal gas law the humid air density can be describes as:

$$\rho = \left\{\frac{P}{T} - \rho_{vs}(T)\varphi(R_v - R_d)\right\} \times \frac{1}{R_d} \quad (5)$$

where P is the air pressure [Pa], ρ_{vs} is the saturated water vapor density (kg.m^{-3}) (see article [2], Table 2 for temperature dependence relationship), and R_v, R_d are the gas constant for water vapor and for dry air (461.51 and 287.05J.kg^{-1}.K^{-1}), respectively.

The conservation of air motion equation is also introduces in the CAD model as:

$$\frac{\partial U}{\partial t} + (U \cdot \nabla)U = -\frac{1}{\rho}\nabla P + \frac{\mu}{\rho}\nabla^2 U + F \quad (6)$$

where μ is the dynamic viscosity of the air (Pa.s^{-1}), and μ/ρ represents the kinematic viscosity [m².s^{-1}]. The air viscosity is assumed constant. F is the volume force (N.m^{-3}). The term in the left side of the eq. (6) corresponds to the air acceleration, or the time rate of change of its velocity U. The terms in the right side account for the sum of the applied forces

per unit mass of air, determining the air acceleration: the first term describes the pressure force, the second term represents the viscous force, and the last term is the volume force F. The volume force represents the humid air density gradient force due to gravity force (buoyant force) since humid air is lighter than dry air. This is the term which considers the advection by buoyancy (free advection) in our CAD model. Following the Boussinesq approximation the volume force, assumed a linear relationship between the humid air densities at local and reference RH $(\rho - \rho_0)$ (see eq. (5)) to give

$$F = g(\rho - \rho_0) = g\rho_{vs}(T)\frac{R_v - R_d}{R_d}(\varphi - \varphi_0) \qquad (7)$$

where g is the acceleration of gravity (m.s-2). The CAD model assumes that variations in the humid air density have no effect on the air flow field that they give rise to buoyant forces. Thus, in the Navier-Stokes equation (eq. (4) and (6)), humid air density changes may be neglected except where they are coupled to the gravitational acceleration in the buoyant force. The reference is calculated using the reference RH φ_0

Calculation domain, initial and boundary conditions

Numerical implementation

Calculation of the TEWL

All these parts of this article are identical than those described in article [2]. However, given that the Dirichlet boundary condition, as defined in the DCE model 2 (see article [2]), presents a good general trend agreement with our TEWL experiments for both living newts and their agar replicas, only this boundary condition is presented for the CAD model.

Additionally, to explore the influence of newt's size on the free advection phenomenon the scale geometric object transform operation of COMSOL Multiphysics (v4.2) was used. This

was performed only for one numerical newt (from the adult male palmate newt P05; Snout-Vent Length (SVL) = 3.0 cm). The 3D geometry was transformed in all space dimensions using a scale factor equal to 0.4 and 2.5, respectively. This allows to the 3D geometry to present characteristic size close to a juvenile palmate newt and to an adult male of the biggest newt species (i.e. *Triturus cristatus*) of the Rhône-Alpes region, respectively (Fig. 1). In this study, the values of TEWL rate presented are given by the slopes of linear regression models between TEWL and time.

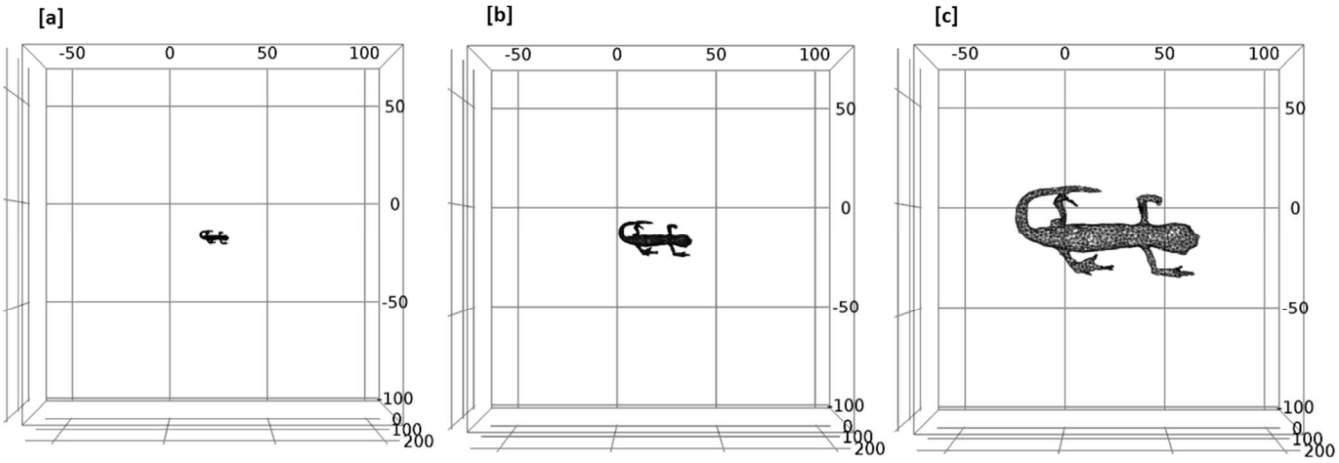

Fig. 1. [a, b, c] 3D geometries of the numerical newt P05 were placed at the bottom center of the calculation domain used for studying the evolution of water vapour transported by combined advection-diffusion. The initial 3D geometry [b] (scale factor equal to 1) was transformed in all space dimensions using a scale factor equal to 0.4 [a] and 2.5 [c]. (Pictures from COMSOL Multiphysics v4.2).

RESULTS AND DISCUSSION

Diffusion-Controlled Evaporation (DCE) and Combined Advection-Diffusion (CAD) model (Dirichlet condition). Predicted TEWL rates by the CAD model for the initial numerical newt P05 (Fig. 1b) was compared to those predicted by the DCE model 2 and the agar replicas (article [2]) (Table 1, Fig. 2). The predicted cumulative TEWL under a 60 min period according

to postures (“I” and “S”) and models (DCE and CAD) were presented in the Figure 2, but only for the climatic condition 2a (t = 20°C; φ_0, see Table 1 from article [2]). The main observation that can be made from these results is that our CAD model does not presents a good agreement with experiments. Combining the free advection to the molecular diffusion process leads to over-estimations of TEWL for both “I”- and “S”-shaped postures (Fig. 2) which increase with temperature (Table 1; data presented only for the “I”-shaped posture). These results strongly suggest that this phenomenon is absent in our experimental conditions, which corroborate what suggested Wardziak et al. (article [2]) given the good agreement of the DCE model with experiments.

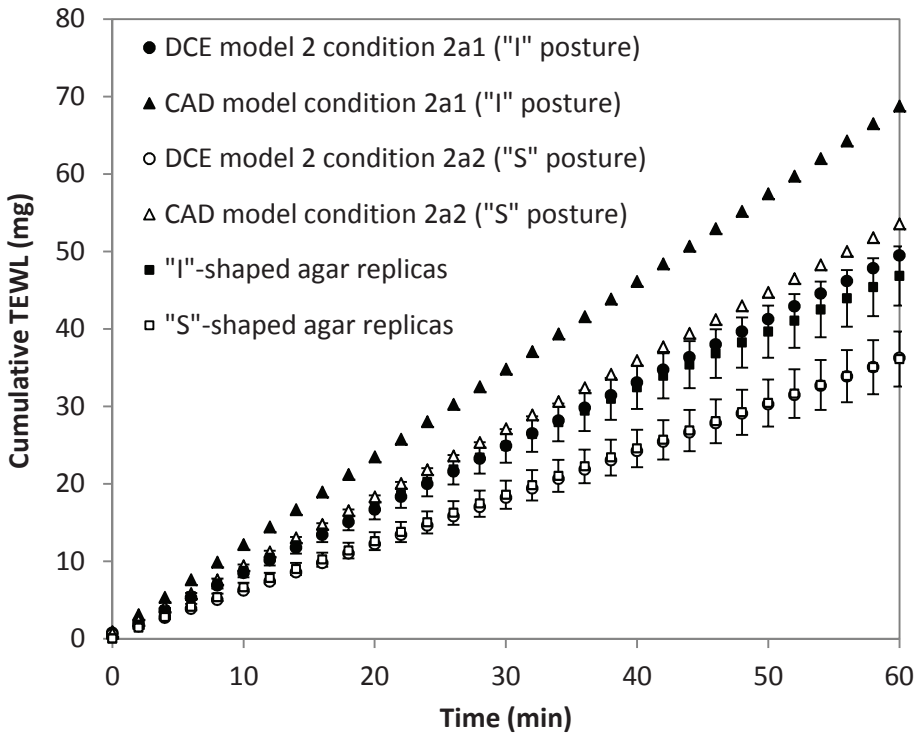

Fig. 2. Predicted cumulative transepidermal water loss for the palmate newt P05 (initial3D geometry, see Fig. 1b) in its two postures (“I” and “S”) under a 60 min period obtained from DCE model 2 (see article [2]) in comparison with predicted data from CAD model in the climatic condition 2a (seeTable 1 from article [2]). Mean measured cumulative TEWL (± 95% confidence interval (CI)) for the “I”- and “S”-shaped agar replicas of the experimental palmate newts (n = 10) are represented as a reference (data from article [2]).

Free advection and newt's size. Comparison of predicted TEWL rates over a 60 min period for the "I"-shaped numerical newt (P05) between the two models (DCE and CAD) according to the scale factor and climatic conditions were presented in Table 1. Although our results suggest a lack of free advection in our experimental conditions, they show (in the case where such a phenomenon occurs) that the gradient in humid air density above an amphibian could create small autonomous air flows. The figure 3 presents the RH spatial distribution (colours) and flux vectors fields (arrows), the diffusive and free advective flux streamlines, and the air flow velocities. After 60 min the RH gradient that establishes around the animal is the driving force of the TEWL through molecular diffusion and free advection. It generates through action of buoyant forces movements of the humid air gradient causing a free water vapour transport mechanisms through small air flow velocities (Shahidzadeh-Bonn et al. 2006, Weon et al. 2011, Jodat and Moghiman 2012). The pattern of advective flux streamlines suggests a kind of classical 3D Rayleigh-Bénard convection. The air flow velocities vary from 0.6 to 3.4 $cm.s^{-1}$ (according to the newt's size) which have considerably enhanced water evaporation by molecular diffusion (from 8 to 66 per cent) (Table 1). As expected, the results suggest a significant effect of the newt's size on the free advection force; more an amphibian is larger more the buoyant forces are important, due to their more important contribution (through their TEWL) to the ambient humid air than smaller animals.

Table 1. Comparison of predicted transepidermal evaporative water loss (TEWL) rates [mg.min^{-1}] over a 60 min period for the "I"-shaped numerical newt of *Lissotriton helveticus* (P05) between the diffusion-controlled evaporation (DCE) model 2 (from article [2]) and the combined free advection-diffusion (CAD) model (using a Dirichlet boundary condition). The values correspond to the slopes of the linear regression models between TEWL and time. Predictions calculated from the models using measured climatic **conditions 1, 2a and 3** (see Table 1 from article [2]) according to the **scale factor** (**1, 0.4 and 2.5**) applied on the initial numerical newt. Values of the maximal air flow velocities [cm.s^{-1}] predicted from the CAD model, and of the Rayleigh number (Ra, from eq. (1)) were also shown. $\dot{m}_I{}^*$ = predicted TEWL for "I"-shaped posture.

Newt (**scale factor**; climatic condition)	$\dot{m}_I{}^*{}_{\mathrm{DCE}}$	$\dot{m}_I{}^*{}_{\mathrm{CAD}}$	$(\dot{m}_I{}^*{}_{\mathrm{CAD}} - \dot{m}_I{}^*{}_{\mathrm{DCE}})$	% $(\dot{m}_I{}^*{}_{\mathrm{CAD}} - \dot{m}_I{}^*{}_{\mathrm{DCE}})$	Max air flow velocity	Ra
P05 (**0.4**; 1)	0.0966	0.1056	+ 0.0090	+ 8.5	0.6	46
P05 (**1**; 1)	0.2302	0.3012	+ 0.0710	+ 23.6	1.1	714
P05 (**2.5**; 1)	–	–	–	–	–	11160
P05 (**0.4**; 2a1)	0.3419	0.3909	+ 0.0490	+ 12.5	1.1	155
P05 (**1**; 2a1)	0.8168	1.1324	+ 0.3156	+ 27.9	2.2	2427
P05 (**2.5**; 2a1)	2.2022	6.4666	+ 4.2644	+ 66.0	3.4	37926
P05 (**0.4**; 3)	0.9820	1.0863	+ 0.1043	+ 9.6	2.1	173
P05 (**1**; 3)	2.3208	3.3438	+ 1.0230	+ 30.6	3.4	2702
P05 (**2.5**; 3)	–	–	–	–	–	42221

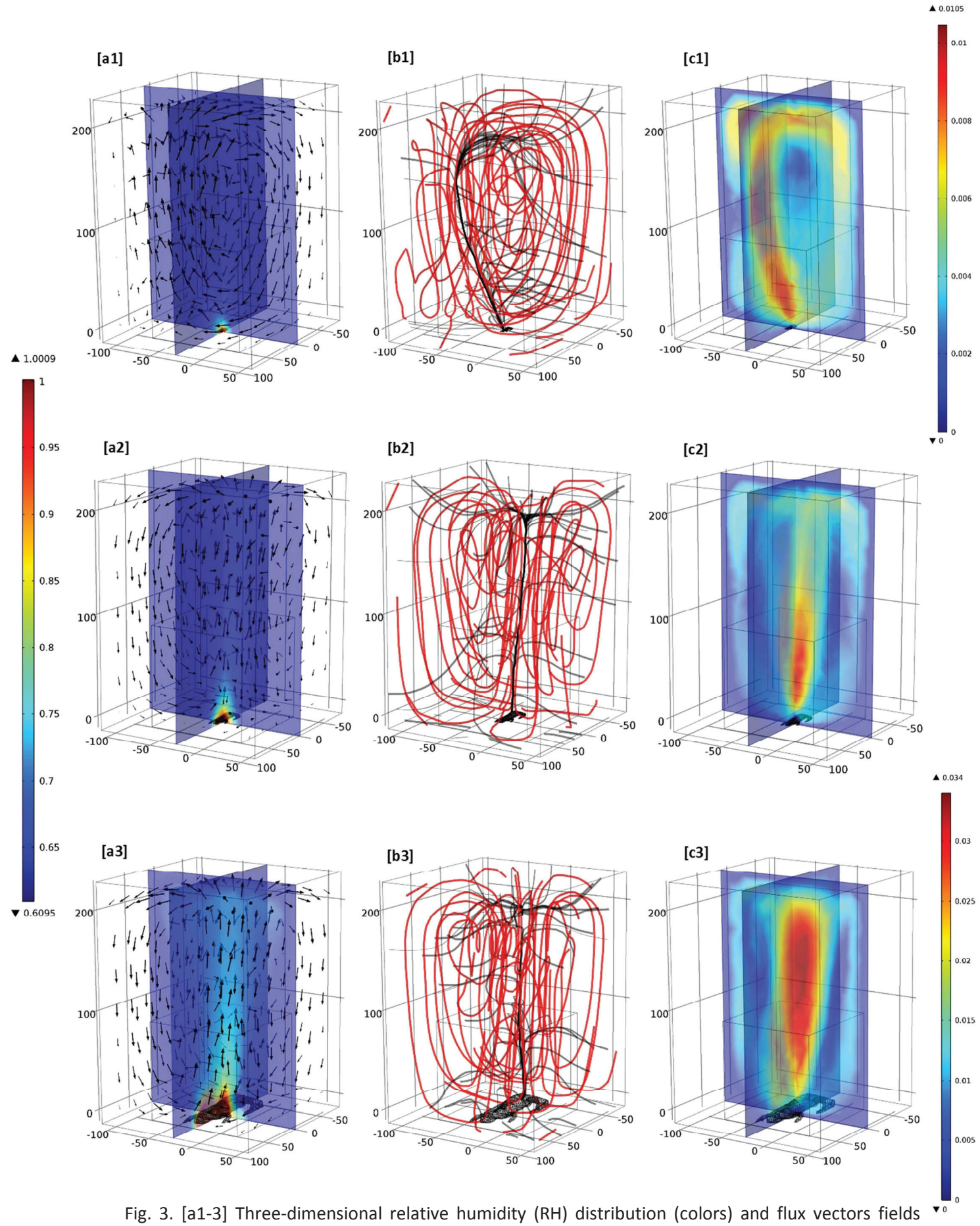

Fig. 3. [a1-3] Three-dimensional relative humidity (RH) distribution (colors) and flux vectors fields (arrows), [b1-3] 3D diffusive flux (black streamlines) and free advective flux (red streamlines), and [c1-3] 3D velocity magnitude [$m.s^{-1}$] (colors) of air flow at 60 min according to the numerical newt'

size: scale factor: 0.4, 1, and 2.5, respectively. Data from the CAD model, only presented at the climatic condition 2a1 (see Table 1 from article [2]). (Pictures from COMSOL Multiphysics v4.2).

CONCLUSION

In this paper we presented a free advection-diffusion model applied on 3D geometries of living amphibians in order to performed numerical analysis of TEWL in newts. As a first approach, and given our results from our DCE model (article [2]) we have not performed advanced numerical analysis. Nonetheless, our results from the CAD model strongly suggest that under our experimental conditions (the microbalance in quiescent atmosphere, Fig 1.) TEWL rates of the living newts, as well as their agar replicas, were purely diffusive. However, some recent studies on water droplets support that water evaporation in quiescent air is not purely diffusive (and thus that water evaporation rate should depends on both the RH and the humid air gradient across an evaporative free water surface) (Shahidzadeh-Bonn et al. 2006, Weon et al. 2011, Jodat and Moghiman 2012). It suggests that some environmental conditions should trigger free advection. In such environmental conditions, that remain to be determined, free advection would be likely to play a significant role in amphibian's TEWL. Both the driving forces for a water vapour transfers through free advection-diffusion (i.e. the RH and the humid air gradient between animal and ambient air) are controlled (in quiescent air) by the vapour concentration gradient that is set up between the animal and its environment. In this way, the habitat structure (geometric factor, volume, shape, it connection with atmosphere etc.), especially for shelters potentially used by amphibians (e.g. soil cavities, burrows, cracks) (e.g. Schwarzkopf and Alford 1996, Jehle et al. 2000, Seebacher and Alford 2002, Schabetsberger et al. 2004), in relation with the physical intrinsic characteristics (e.g. size, posture) of the wet-skinned organism could trigger such a free

advection phenomenon. However, this allows first information on the habitat structure used by these organisms, and then a modelling of their microenvironments as these organisms see them.

LITERATURE CITED

Debbissi C, Orfi J, Nasrallah SB (2003) Evaporation of water by free or mixed convection into humid air and superheated steam. *Int J Heat Mass transfer* 46:4703-4715

Dobkins DS, Gettinger RD, O'Connor MP (1989) Importance of retreat site for hydration state in *Bufo marinus* during dry rainy season. *Am Zool* 29:88A

Jehle R, Arntzen JW (2000) Post-breeding migration of newts (*Triturus cristatus* and *T. marmoratus*) with contrasting ecological requirements. *J Zool London* 251:297-306

Jodat A, Moghiman M (2012) An experimental assessment of the evaporation correlation for natural, forced and combined convection regimes. *Proc IME C J Mech Eng Sci* 226:145-153

Hillman SS, Withers PC, Drewes RC, Hillyard SD (2009) Ecological and environmental physiology of amphibians. Oxford University Press

Pough FH, Taigen TL, Stewart MM, Brussard PF (1983) Behavioural modification of evaporative water loss by a Puerto Rican frog. *Ecology* 64:244-252

Schabetsberger R, Jehle R, Maletzky A, Pesta J, Sztatecsny M (2004) Delineation of terrestrial reserves for amphibians: post-breeding migrations of Italian crested newts (*Triturus c. carnifex*) at high altitude. *Biol Cons* 117: 95-104

Schwarzkopf L, Alford RA (1996) Desiccation and shelter-site use in a tropical amphibian: comparing toads with physical models. *Funct Ecol*. 10:193-200

Seebacher F, Alford (2002) Shelter microhabitats determine body temperature and dehydration rates of a terrestrial amphibian (*Bufo marinus*). *J Herpetol* 36:69-75

Shahidzadeh-Bonn N, Rafai S, Azouni A, Bonn D (2006) Evaporating droplets. *J Fluid Mech* 549:307-313

Shoemaker VH, Hillman SS, Hillyard SD, Jackson DC, McClanahan LL, Withers PC, Wygoda ML (1992) Exchange of water, ions, and respiratory gases in terrestrial amphibians. In: Feder E, Burggren WW (ed) Environmental Physiology of the Amphibians. University of Chicago Press, Chicago

Spotila JR, O'Connor MP, Bakken GS (1992) Biophysics of heat and mass transfert. In: Feder E, Burggren WW (ed) Environmental Physiology of the Amphibians. University of Chicago Press, Chicago

Tracy CR (1976) A model of the dynamic exchange of water and energy between a terrestrial amphibian and its environment. *Ecol Monogr* 46:293-326

Weon BM, Je JH, Poulard C (2011) Convection-enhanced water evaporation. *AIP Advances* 012102

CHAPTER THREE

Diseases of Aquatic Organisms **104:215-224 (2013)**

Article 3: **Impact of both desiccation and exposure to an emergent skin pathogen on transepidermal water exchange in the palmate newt *Lissotriton helveticus***

Thomas Wardziak[1,*], Emilien Luquet[1, 2], Sandrine Plenet[1], Jean-Paul Léna[1], Laurent Oxarango[3] and Pierre Joly[1]

[1] Université de Lyon; UMR 5023 Ecologie des Hydrosystèmes Naturels et Anthropisés; Université Lyon 1 ; ENTPE; CNRS; 6 rue Raphaël Dubois, 69622 Villeurbanne, France

[2] Centre d'Ecologie Fonctionnelle et Evolutive, UMR 5175 CNRS, 1919 route de Mende, 34293 Montpellier Cedex 5, France

[3] LTHE, Université de Grenoble, BP 53, 38041 Grenoble Cedex, France.

* Corresponding author (thomas.wardziak@univ-lyon1.fr)

ABSTRACT: Amphibians are the vertebrate group most affected by global change. Their highly permeable skin is involved in maintaining homeostasis (e.g. water and electrolyte equilibrium), which makes them particularly vulnerable to climate warming and skin pathogens. This study focused on the impacts of both desiccation (as a potential consequence of climate warming) and exposure to *Batrachochytrium dendrobatidis*, an emergent skin pathogen of amphibians. *B. dendrobatidis* causes a lethal skin disease of amphibians called chytridiomycosis and is responsible for mass mortality events in several regions of the world. Because *B. dendrobatidis* colonizes the superficial layers of the epidermis, it is assumed to affect water transfers across the skin. We first investigated the behavioural postures of the palmate newt (*Lissotriton helveticus*) expressed in response to desiccation and their influence on transepidermal water loss (TEWL) rate. Simultaneously, we investigated the effects of repeated 24h exposure to *B. dendrobatidis* (i.e. every four days for 16 days) on the TEWL and ventral water absorption (VWA) rates of these newts. Our results suggest an efficient behavioural water-conserving mechanism, i.e. an "S"-shaped posture associated with a restricted activity rate, not affected by repeated exposure to *B. dendrobatidis*. Similarly, TEWL was not significantly affected in exposed newts. Interestingly, VWA was significantly reduced after just 24 hours exposure to *B. dendrobatidis* without modification until the end of the experiments. Our results suggest that *B. dendrobatidis* could rapidly inhibit rehydration of *L. helveticus* through fungal toxins and disrupt an essential function for survival.

KEY WORDS: *Batrachochytrium dendrobatidis*; Chytrid fungus; Emerging disease; Amphibian skin; Evaporative water loss; Water absorption; Water-conserving behaviour

INTRODUCTION

Climate warming and emerging infectious diseases (EIDs) are both major threats affecting biodiversity (Carey 2000, Harvell et al. 2002, Thomas et al. 2004). Climate warming is expected to lead to greater contrasts in rainfall distributions, with longer and more intense drought periods (IPCC 2007). Such environmental changes may lead to detrimental thermal and/or hydric conditions for organisms (e.g. shelter loss, intense drought periods with reduced water availability) that prevent them from maintaining homeostasis (e.g. water and electrolyte equilibrium) with direct physiological and functional consequences (Spotila & Berman 1976, Spotila et al. 1992, Shoemaker et al. 1992). EIDs can result from environmental changes in pathogen habitats although they can also emerge in new geographical areas (novel pathogen hypothesis; e.g. Laurance et al. 1996, Daszak et al. 1999, Rachowicz et al. 2005). The endemic pathogen hypothesis suggests that environmental changes (biotic and/or abiotic) can drive modifications in life history traits of native pathogens (virulence, survival, dispersal capacity) and/or host susceptibility (e.g. Kiesecker & Blaustein 1995, Schrag & Wiener 1995, Carey et al. 1999, Kiesecker et al. 2001, Rachowicz et al. 2005). EIDs can cause sub-lethal damage to hosts (e.g. developmental and physiological abnormalities) leading to the decline of host populations (Blaustein et al. 2012, Pounds et al. 2006, Garner et al. 2009). By disturbing the physiological functions of hosts, EIDs may also reduce the ability of individuals to maintain homeostasis and to respond to environmental change (Luquet et al. 2012). Consequently, climate warming can drive the emergence of infectious diseases and EIDs can increase the detrimental impacts of climate warming (Garner et al. 2011, Blaustein et al. 2012, Fisher et al. 2012). It is then crucial to study these two threats to biodiversity in concert in order to understand their detrimental

consequences. In this context, our study focuses on the impacts of both desiccation (as a potential consequence of climate warming) and exposure to an emergent pathogen in amphibians.

Amphibians are the vertebrate taxa most threatened by global change (Stuart et al. 2004). Their skin represents the key organ involved in maintaining homeostasis. As a consequence, these animals have a highly permeable and heavily vascularized epidermis allowing an efficient pathway for gas exchanges, and water and electrolyte absorption. However, these skin characteristics reduced the water retention ability and make amphibians highly vulnerable to transepidermal evaporative water loss (TEWL; Spotila et al. 1992, Shoemaker et al. 1992, Lillywhite 2006). A major challenge for amphibians in the terrestrial environment is therefore how to limit TEWL rate. TEWL is a passive diffusion process that depends primarily on physical conditions such as temperature and relative humidity of atmosphere (Spotila et al. 1992, Shoemaker et al. 1992, Lillywhite 2006). Amphibians develop adaptations to limit TEWL rate and to replenish body water loss by evaporation. They show behavioural adaptations like water-conserving postures to reduce the skin area exposed to atmosphere (e.g. Alvarado 1967, Gehlbach et al. 1969, Pough et al. 1983). A functional adaptation allows active water absorption in the ventral skin regions in contact with moistened substrates (called ventral water absorbtion, VWA). However, VWA efficiency depends on hydric environmental conditions (i.e. substrate water availability; Shoemaker et al. 1992, Spotila et al. 1992, Viborg & Rosenkilde 2004). Consequently, climate warming, with frequent and longer drought events, can expose amphibians to pronounced water imbalance leading to high desiccation risks.

The physiological importance of the skin also makes amphibians extremely sensitive to chytridiomycosis, an emergent skin disease caused by the pathogenic fungus

Batrachochytrium dendrobatidis. Cutaneous chytridiomycosis is a potentially lethal skin disease of amphibians known to contribute to population decline and mass-mortality events observed worldwide (Berger et al. 1998, Daszak et al. 1999, Bosch et al. 2001). As *B. dendrobatidis* is restricted to the superficial epidermis (Berger et al. 1998), this pathogen is suspected of affecting transepidermal water transfers. Two major, non-mutually exclusive, mechanisms have been proposed (Berger et al. 1998, Berger et al. 2005, Pessier et al. 1999): i) epidermal hyperplasia and hyperkeratosis can physically block transepidermal water transfers, and ii) a fungal toxin, or other active compounds released by the pathogen, can interfere with the osmoregulatory functions of the epidermis. Understanding the mechanisms of pathogenesis is an important step to providing explanations on how exposure to or infection with *B. dendrobatidis* can cause such global amphibian declines (Daszak et al. 2003). Few studies have so far focused on the physiological effects of *B. dendrobatidis* on amphibians. Recent laboratory studies suggested impairments in normal skin functions in *B. dendrobatidis*-infected frogs, such as electrolyte depletion, osmotic imbalance (Voyles et al. 2007, Voyles et al. 2009, Marcum et al. 2010, Voyles et al. 2012) and disruption in the ability to rehydrate (Carver et al. 2010). However, physiological responses to *B. dendrobatidis* exposure/infection still remain unclear.

The objective of the study is to quantify the impact of both desiccation events and exposure to *B. dendrobatidis* on transepidermal water exchange (i.e. TEWL and VWA rates) in an urodele species, the palmate newt *Lissotriton helveticus* during its terrestrial phase. We further investigate how newt behaviours (water-conserving postures) may influence the TEWL rate and how exposure to *B. dendrobatidis* affects these postures. Palmate newts are excellent models for such a study because this species is i) active during the warmest months (terrestrial phase), ii) highly sensitive to dehydration due to a high body surface to volume

ratio and iii) susceptible to *B. dendrobatidis* in the wild (Dejean et al. 2010). We performed laboratory experiments to test the following hypotheses: i) palmate newts exposed to desiccating conditions should exhibit restricted activity and specific water-conserving postures, ii) palmate newts exposed to *B. dendrobatidis* should exhibit disruption in TEWL and/or VWA rates.

MATERIALS AND METHODS

Animal collection

Adult male palmate newts *Lissotriton helveticus* (n = 64; mean body mass ± standard error (se): 0.627 ± 0.016 g; mean SVL (snout-vent length) ± se: 2.97 ± 0.02 cm) were sampled in May 2010 during their aquatic phase in forest ruts near Mépieu, France (05°26’28’’E, 45°43’56’’N). Both *Hyla arborea* (see Luquet et al. 2012) and *Bufo bufo* populations (Luquet E, Plénet S., Léna JP, unpublished data) have been widely sampled (c.a. 30 individuals per population) in the same sites than newts and in other sites throughout the Isère Département (France), and no *B. dendrobatidis* infection has been detected. As *B. dendrobatidis* is absent from the Isère Département, we can be pretty certain that sampled palmate newts were not infected with *B. dendrobatidis* before the experiment began. All individuals from this population were housed in aquaria providing both aquatic and terrestrial environments allowing them to leave the water. When the newts began their terrestrial stage, they were housed individually in plastic boxes (19 x 16.5 x 9.5 cm) lined with moistened cellulose paper, renewed weekly. The boxes were kept in climate-controlled rooms at 20 ± 1°C, 60 ± 10% relative humidity and with a 16:8 light:dark regime. Newts were fed with small crickets *ad libitum*.

Batrachochytrium dendrobatidis exposure

Individual newts at the terrestrial-stage were randomly assigned to control (n = 30) and *B. dendrobatidis* (n = 34) treatments. We used a *B. dendrobatidis* IA2004 043 isolate generated from a dead *Alytes obstetricans* metamorph collected from a mass mortality event in Spain, and known to be highly virulent (Farrer et al. 2011). For the control and *B. dendrobatidis* treatments, newts were transferred to individual plastic Petri dishes with lid (height = 1 cm, Ø = 9 cm) filled with 10 mL of tap water to ensure a fully hydrated body mass (i.e. the initial body mass, W_0) of the animals. To ensure adequate ventilation, the Petri dish lids were pierced with holes. Depending on the treatment, newts were repeatedly exposed to either 5 mL culture, containing a total dose of 15,000 – 75,000 zoospores at each inoculation (exposed newts), or 5 mL of sterile culture medium (control newts). The newts were exposed for 24 hours every four days for 16 days (4 exposures in total). Eight of the 30 control newts died during the second exposure because of an experimental error (i.e. these newts were transferred to unpierced petri dishes), and 7 of the 34 exposed newts died in the interval between the two periods of measurements. At the end of the experiment, we collected skin swab samples from 22 control newts (including the 8 dead individuals) and 22 exposed newts (including the 7 dead individuals). We were not able to perform infection detection on all individuals because of financial constraints. No further histological analyses were performed on the dead animals. We performed real-time PCR to assess the skin swab samples for *B. dendrobatidis* DNA (Boyle et al. 2004). Extractions were diluted by 1/10 before real-time PCR amplification, performed in duplicate, and with *B. dendrobatidis* genomic equivalent standards of 100, 10, 1, and 0.1 zoospore genome equivalents. All the PCRs were replicated twice, and we considered successful amplification in both reactions as

a positive signal of *B. dendrobatidis* presence. In the event that only one replicate from any sample did not amplify, this sample was run a third time. If this third amplification attempt did not result in an amplification profile, the sample was scored as negative for infection. No amplification in both replicates was taken as a true negative signal. All exposed newts were ethically euthanized with an overdose of MS222 in accordance with the recommendations of the AVMA Panel on Euthanasia.

Experimental design

Behavioural responses and transepidermal water exchange (TEWL and VWA rates) of all newts were investigated at two periods: after 24 hours (day1; n = 30 and 34 for control and exposed newts, respectively) and on day 16 (n = 22 and 27 for control and exposed newts, respectively) after the initial exposure. All the measurements were carried out in a climate chamber (50 x 60 x 80 cm), placed in a climate-controlled room at 20 ± 1°C, allowing the relative humidity to be controlled (i.e. 60 ± 3%) using silica gel. In order to perform measurements without any modification of ambient humidity, two holes were made in the front wall of the chamber, each equipped with a flexible duct ending in a latex glove. It was thus possible to manipulate the newts without opening the chamber by slipping hands and arms into these ducts.

Experiment 1. The purpose of this experiment was to study behavioural responses to desiccation (i.e. activity (moves per min) and postural adjustment (adoption of "S" or "I" posture per min)) and how exposure to *B. dendrobatidis* affected these behaviours. Each newt was placed in a dry plastic Petri dish (h = 2.5 cm, Ø = 9 cm) laid on a microbalance (Scaltec sbc 31; 0.001 g sensitivity). We continuously monitored their behaviour using JWatcher (1.0 version) software for both treatments during the desiccation period (see

Experiment 3 below). Newts with a posture characterized by a relatively straight body with no tail coil were considered to have the "I"-shaped posture. When the body was huddled up with the tail coiling along it, newts were considered to have the "S"-shaped posture (Fig. 1). We measured the time spent active relative to total dehydration time (moves per min) and the time spent inactive with the "I" or "S" posture relative to total inactivity time (adoption of "S" or "I" posture per min).

Fig. 1. Adult male palmate newt *Lissotriton helveticus* in the "S"-shaped posture and its agar model. Photographs taken by T. Wardziak and T. Colin.

Experiment 2. The purpose of this experiment was to evaluate the impact of postural adjustment ("I"-shaped *vs.* "S"-shaped postures) on the TEWL. For this purpose, we created agar models of palmate newts (n = 4 for each postural adjustment) using the method of Spotila & Berman (1976). To obtain replicas similar to our newts, agar models were cast from dead animals frozen in the desired posture and immersed in fluid alginate previously poured into a small plastic container. After hardening, the dead newts were removed and moulds filled with a solution of 3% agar, 97% water. Each agar model was placed in a dry plastic Petri

dish (h = 2.5 cm, Ø = 9 cm) laid on a microbalance (Scaltec sbc 31; 0.001 g sensitivity). We measured the body mass of agar models every 10 min until 10% loss of their W_0 was reached.

Experiment 3. The purpose of this experiment was, simultaneously with the behavioural experiment (see Experiment 1 above), to quantify the impact of exposure to *B. dendrobatidis* on transepidermal water exchange (i.e. TEWL and VWA rates). We estimated the TEWL rate by measuring the body mass loss of the newts every 10 min until they reached a 10% loss of W_0. To avoid biases due to the fact that newts could remain in close contact with the sides of the dish, and thus artificially reduce the TEWL rate, the Petri dish rim had been lined with wire mesh. We estimated the VWA rate by placing the newts in Petri dishes filled with 15 mL of tap water allowing them complete ventral absorption, immediately after the dehydration period. We measured body mass every 10 min, over a 60 min period, by moving newts to the microbalance after removing excess water with absorbent paper.

Statistical analysis

A first model (model 1) examine the effects of initial body mass (W_0), treatment (control or exposed newts), day of measurement (day 1 or day 16) and their interactions on behavioural responses, i.e. the activity (moves per min) and the postural adjustment (adoption of “S” or “I” posture per min). W_0, treatment and day were considered as fixed effects. A second model (model 2) investigate the effects of W_0, postural adjustment (i.e. either “I” or “S”), successive measurements made within the desiccation period (time) and their interactions on the TEWL rate of agar models. W_0, postural adjustment and time were considered as fixed effects. Both final models (model 3 for the TEWL rate and model 4 for VWA rate) examine the effects of W_0, treatment, day, time and their interactions on

transepidermal water exchange (i.e. TEWL and VWA rates). W_0, treatment, day and time were considered as fixed effects.

All these models took into account the correlated error between measurements made on a same individual as a random effect. For the model 3 and 4 another level of random effect was considered: the interaction individual × day. We selected the covariance structure for each model using the Akaike Information Criterion (AIC). For models 1 and 2, a compound symmetry covariance structure was used. For model 3, a first order autoregressive correlation between measurements was considered. For model 4, because the reabsorption experiment lasted 60 min it was possible to use an unconstrained covariance structure to model correlation error between measurements made over the same period.

The significance of variance heterogeneity was examined using a likelihood ratio test (LRT), and the related covariance parameter was removed from subsequent analyses if not significant. Restricted maximum likelihood (REML) estimates were used to test the significance of the fixed effects. The significance of explanatory terms was examined using non-sequential F-tests based on the Kenward-Roger correction for degrees of freedom (SAS Institute, 9.1.2 version software). Non-significant interactions were then successively removed to obtain the final model. All statistical analyses were carried out using SAS (SAS Institute, 9.1.2 version) software.

RESULTS

qPCR results and clinical chytridiomycosis

Real-time PCR revealed that the swabbed surviving control newts were negative for *B. dendrobatidis*. Furthermore, all the dead control newts were also negative for the pathogen

(Table 1). Repeated exposure to *B. dendrobatidis* infected 40% of the 15 surviving exposed newts, and all the dead exposed newts were positive for *B. dendrobatidis* (Table 1). We can assume that the dead exposed newts died of chytridiomycosis. Indeed, all these individuals were infected and genome equivalents showed that the number of *B. dendrobatidis* zoospores were around 20 times greater than for surviving exposed newts (Table 1). In addition, all exposed newts, i.e. surviving as well as dead newts, showed a sloughing of the whole body (i.e. from the ventral abdomen, flanks, dorsum, legs and tail) versus only two control newts (pers. obs.).

Table 1. Prevalence of chytrid infection and genome equivalents (GE) for all positive newts in this study. Prevalence was calculated as the proportion of individuals testing positive at 0.1 GE. GE are corrected for a 1/10 dilution factor.

		n	% positive (95% CI)	GE ± SE
Control Newt				
	living	14	0 (0-27)	/
	dead	8	0 (0-48)	/
Exposed Newt				
	living	15	40 (17-67)	1.13 (0.25)
	dead	7	100 (52-100)	20.35 (10.87)

Experiment 1

In model 1, we did not detect any significant variance heterogeneity between treatments either on activity (LRT_{2df} = 0.8, ns) or on postural adjustment (LRT_{2df} = 5.4, p = 0.067). Neither the W_0 of the newts, nor the treatment they underwent affected their activity (Table 2). However, animals tended to be less active during day 16 (day 1 *vs.* day 16 for control newts: 0.12 ± 0.02 *vs.* 0.09 ± 0.02; for exposed newts: 0.11 ± 0.02 *vs.* 0.08 ± 0.02 (estimates moves

per min ± se); Table 2). Neither the W_0 of animals, the treatment they underwent nor the day of measurement significantly affected the time spent in a given posture when inactive (Table 2). Newts did not modify their postural adjustment according to the treatment they experienced (control *vs.* exposed newts at day 1: 0.19 ± 0.03 *vs.* 0.20 ± 0.03; at day 16: 0.16 ± 0.03 *vs.* 0.17 ± 0.03 (estimates adoption of "I" posture per min ± se); Table 2).

Table 2. Model 1 analyses for newt activity (moves per min) and postural adjustment (adoption of "I" posture per min). The model included three fixed effects (initial body mass (W_0), treatment (control or exposed newts) and day of measurement (day 1 or day 16)) together with the interactions between these factors. Non-significant interactions were all excluded from the final model. The model took into account the correlated error between measurements made on a same individual as a random effect.

	moves per min			adoption of "I" posture per min		
	$d.f._n$, $d.f._d$	F	*P*	$d.f._n$, $d.f._d$	F	*P*
W_0	1, 63	0.03	0.8715	1, 68.1	1.22	0.2727
day	1, 58.1	3.32	0.0735	1, 62.1	1.00	0.3211
treatment	1, 54.2	0.12	0.7300	1, 59	0.06	0.8154

$d.f._n$, d.f. for the numerator; $d.f._d$, d.f. for the denominator.

Experiment 2

The model 2 indicated that the "S" posture had a significantly lower TEWL rate than the "I" posture (Table 3 and Fig. 2). The model also showed that the TEWL rate of agar models reduced throughout the dehydration experiment (Table 3 and Fig. 2) and lighter models had a lower TEWL rate than heavier ones (Table 3).

Table 3. Model 2 analyses for transepidermal water loss (TEWL) rate based on the posture of the agar models. The model included three fixed effects (initial body mass (W_0), posture ("I" or "S" posture) and successive measurements made within the desiccation period (time)) together with the interactions between these factors. Non-significant interactions were all excluded from the final model. The model took into account the correlated error between measurements made on a same individual as a random effect.

	TEWL rate		
	$d.f._n$, $d.f._d$	F	*P*
W_0	1, 13.5	20.75	0.0005
time	1, 24.1	15.35	0.0006
posture	1, 19.9	27.77	< 0.0001
time × posture	1, 24.1	5.24	0.0311

$d.f._n$, d.f. for the numerator; $d.f._d$, d.f. for the denominator.

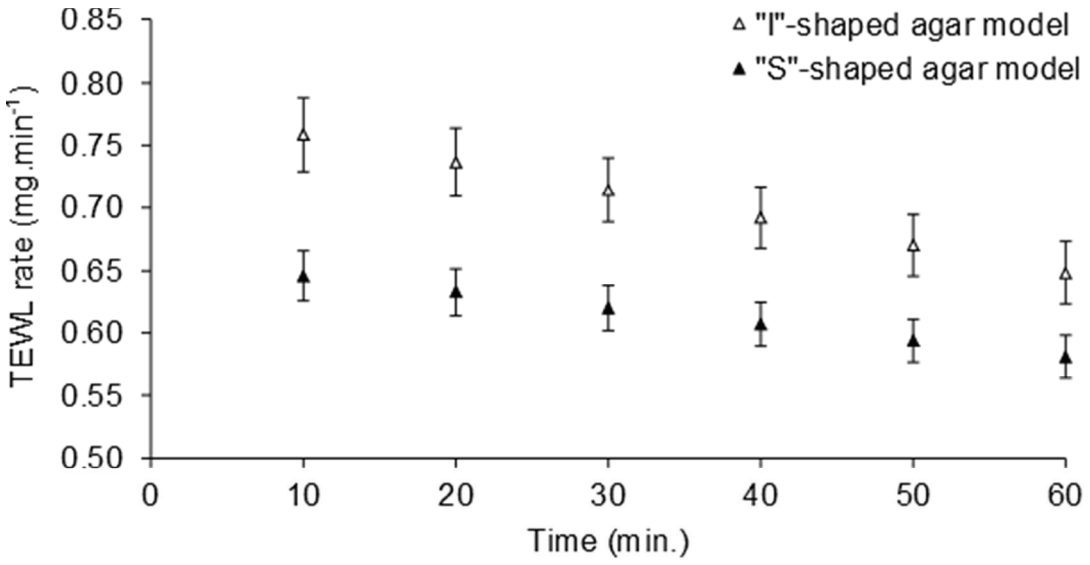

Fig. 2. Transepidermal evaporative water loss rate (TEWL, mixed-models, estimates ($mg.min^{-1}$) ± se) for a 60 min period for both the "I"- and the "S"-shaped agar models.

Experiment 3

In model 3, according to the AIC score, an autoregressive correlation was more supported than a constant one to analyse the TEWL rate during dehydration experiments (AIC score for autoregressive and constant correlations were -1232.9 and -1223.5, respectively). TEWL rates were significantly more variable among the exposed newts than among controls (LRT_{4df} = 68.2, $p < 0.001$) and this variance heterogeneity was more salient for the second batch of measurements than for the first (LRT_{4df} = 72.5, $p < 0.001$). No effect of treatment on the TEWL rate depending on the day of measurement was detected (Table 4 and Fig. 3a, 3b): contrast analyses showed that there was no significant difference between both treatments on day 1 ($F_{1,86.7}$ = 0.22; p = 0.64) and day 16 ($F_{1,115}$ = 3.62; p = 0.059). Nevertheless, while the TEWL rate did not significantly vary between the two measurement days in control newts ($F_{1,43.9}$ = 0.23; p = 0.63), we detected a significantly higher TEWL rate on day 16 in the case of the exposed newts ($F_{1,67.7}$ = 10.08; p = 0.002). However, the increase in TEWL rate in the exposed group, while statistically significant, was not biologically relevant, considering that the difference in water loss was about 0.9% of W_0 over a 60 min period (Fig. 3a). The TEWL rate was constant over the duration of the desiccation experiments, whatever the time period considered (Table 4 and Fig. 3a, b), but lighter animals had a lower TEWL rate than heavier ones (Table 4).

In model 4, the unconstrained correlation structure was used to analyse the VWA rate during rehydration experiments (AIC scores for the unconstrained structure, the autoregressive and constant forms were 827.3, 863.6 and 857.5, respectively). We did not detect significant variance heterogeneity between treatments (LRT_{21df} = 31.5, p = 0.0657), but the variance heterogeneity was significant between time periods (LRT_{21df} = 45.1, p = 0.0017). The results of this analysis showed that exposed newts exhibited a significantly

lower VWA rate than control newts, whatever the measurement day (Table 4 and Fig. 4a, b). The difference was about 1.6% of W_0 over a 60 min period for both measurement days (Fig. 4a). Moreover, the VWA rate declined as newts replenished their bodies with water (Table 4 and Fig. 4a, b), and the VWA rate was positively related to animal mass (Table 4).

Table 4. Model 3 and model 4 analyses for transepidermal water loss (TEWL) rate and ventral water absorption (VWA) rate, respectively. The models included four fixed effects (initial body mass (W_0), treatment (control or exposed newts), day of measurement (day 1 or day 16) and successive measurements made within the desiccation period (time)) together with the interactions between these factors. Non-significant interactions were all excluded from the final model. Two levels of random effect were considered. The models took into account the correlated error between measurements made on a same individual. Another level of random effect was considered: the interaction individual × day

	TEWL rate			VWA rate		
	$d.f._n$, $d.f._d$	F	*P*	$d.f._n$, $d.f._d$	F	*P*
time	1, 328	1.70	0.1931	1, 101	236.03	< 0.0001
W_0	1, 73.5	4.92	0.0296	1, 45.4	71.63	< 0.0001
day	1, 56.2	6.60	0.0129	1, 41.8	1.23	0.2745
treatment	1, 65.6	1.19	0.2800	1, 37.6	25.22	< 0.0001
treatment × day	1, 53.6	3.70	0.0599			

$d.f._n$, d.f. for the numerator; $d.f._d$, d.f. for the denominator.

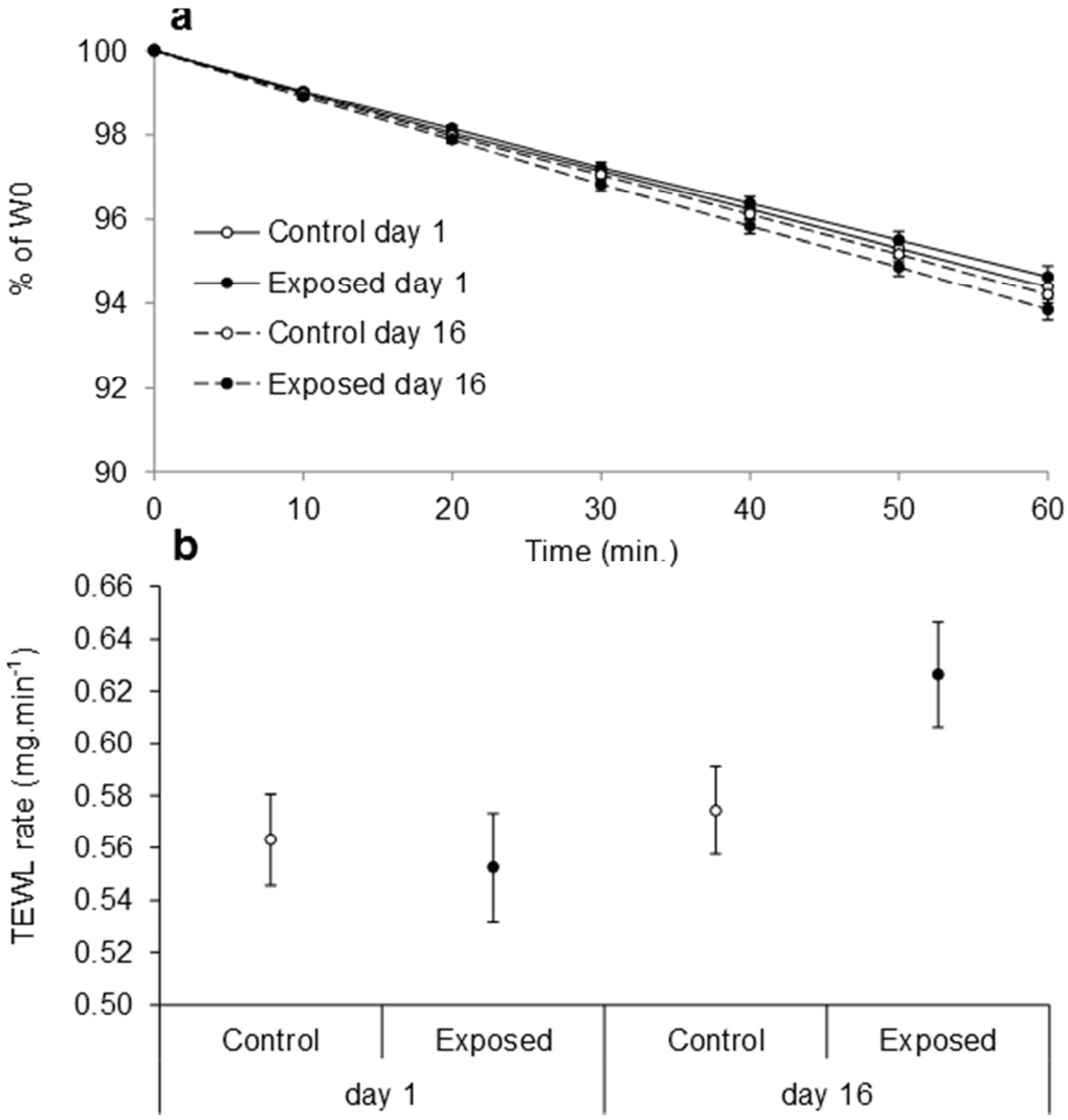

Fig. 3. (a) Transepidermal evaporative water loss (TEWL, mean % of the initial body mass W_0 ± se) for a 60 min period for both control and exposed *Lissotriton helveticus* 24 hours after initial exposure to *Batrachochytrium dendrobatidis* (day 1) and 16 days after repeated exposures. % of W_0 denotes the percentage of the initial body mass. (b) TEWL rate (mixed-models, estimates ($mg.min^{-1}$) ± se) for both treatments on day 1 and day 16.

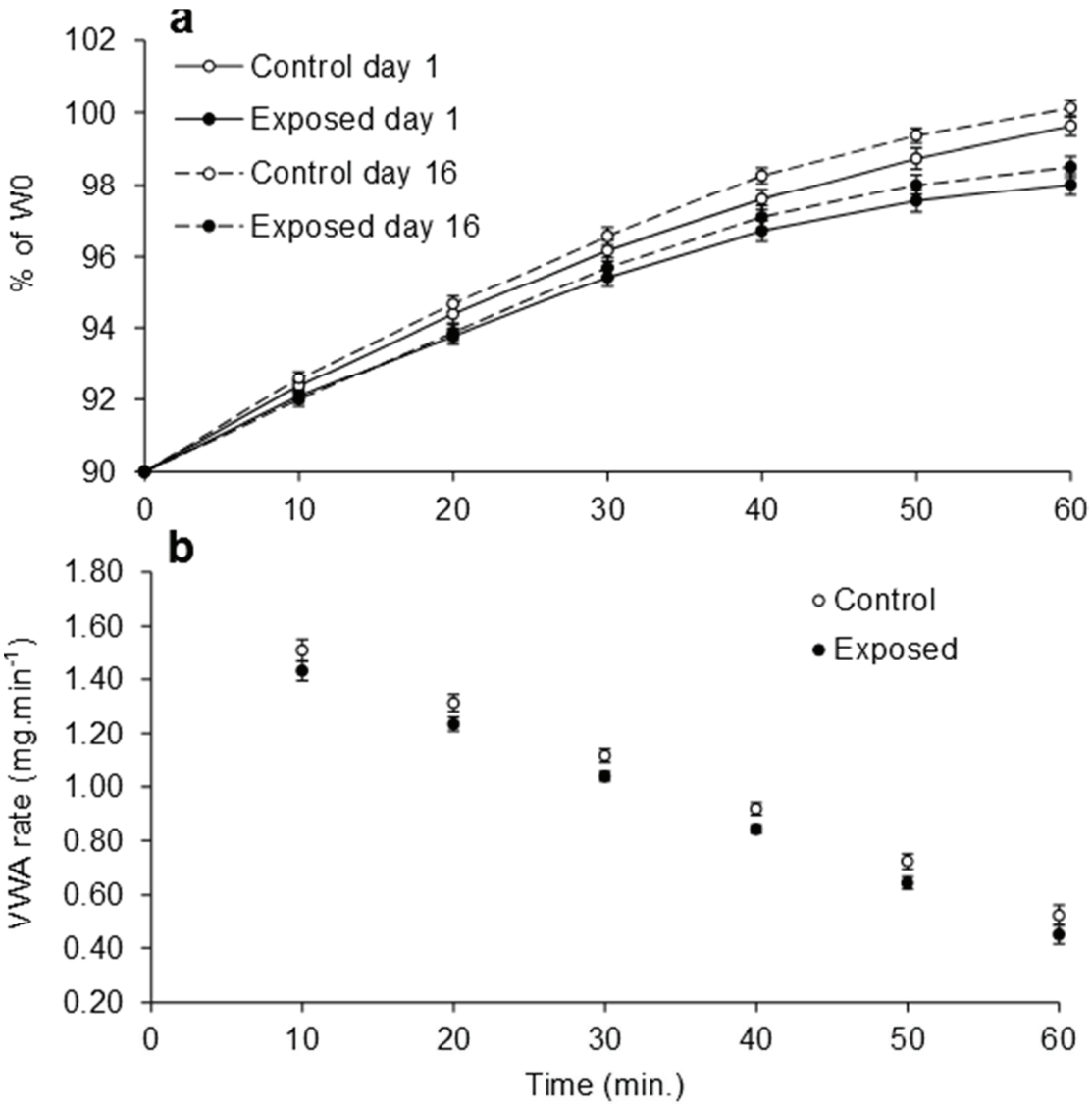

Fig. 4. (a) Rehydration (mean % of the initial body mass W_0 ± se) for both control and exposed *Lissotriton helveticus* 24 hours after initial exposure to *Batrachochytrium dendrobatidis* (day 1) and 16 days after repeated exposures. % of W_0 denotes the percentage of initial body mass. (b) Deceleration of ventral water absorption rate (VWA, mixed-models, estimates ($mg.min^{-1}$) ± se) for both control and exposed newts.

DISCUSSION

Adult male palmate newts expressed a restricted activity rate when exposed to desiccation stress. As shown in other salamander species exposed to desiccating conditions, inactivity is associated with a postural adjustment that consists of tightly coiling the body and the tail (Alvarado 1967, Gehlbach et al. 1969) to form an "S" shape. Alvarado (1967) reported that inactive terrestrial long-toed salamanders (*Ambystoma macrodactylum*) and tiger salamanders (*Ambystoma tigrinum*) with an "S"-shaped posture experienced a lower water loss rate than active animals. Our results on agar models also show that the "S" posture improves water economy relative to the "I" posture when inactive. The water economy of the "S" posture certainly reflects a reduction in the surface exposed to evaporation. Thus, our results suggest that restricted activity associated with water-conserving postures can be used as an emergency response by newts unable to escape from desiccating conditions to increase their chance of survival (Pough et al. 1983).

Numerous studies have shown that exposure to *B. dendrobatidis* can lead to behavioural modifications in amphibians such as the expression of lethargic behaviours associated with abnormal and depressed postures (e.g. Bosch et al. 2001, Nichols et al. 2001, Carver et al. 2010). Our results do not reveal that exposure to *B. dendrobatidis* has a significant effect on activity and posture in the laboratory. In our experiment, the duration of exposure may have been insufficient to observe such lethargic and/or depressive behaviour in palmate newts. Furthermore, we found that the TEWL rate between treatments had not changed, although the difference in TEWL rate was significant in the exposed newts between the two measurement days. It therefore seems unlikely that *B. dendrobatidis* impedes the TEWL in newts, as suggested by Carver et al. (2010) in infected hylid frog *Litoria raniformis*. In

contrast, our results suggest that *B. dendrobatidis* has an impact on the ventral rehydration capacity of newts. *B. dendrobatidis* exposure slowed down the VWA rate, although the decrease was quite low, given that the difference in water uptake between groups was about 1.6% of W_0 over a 60 min period. These results are consistent with the study of Carver et al. (2010) on infected hylid frogs, where a difference in water uptake of about 2-3% of W_0 over a 60 min period was found one week after inoculation with *B. dendrobatidis*. Surprisingly, in our study, VWA is impeded 24 hours after the first exposure to the pathogen without modifications until day 16. Such an impact of *B. dendrobatidis* seems to reflect a disruption in the water uptake function of the ventral epidermis and suggests the action of a fungal toxin or other active compounds, rather than *B. dendrobatidis* itself. Indeed, *B. dendrobatidis* takes a few days to establish itself in the amphibian epidermis, its whole life cycle taking 4-5 days (Berger et al. 2005), and may produce lethal toxins either before or after infection (Blaustein et al. 2005). Furthermore, the study by Rosenblum et al. (2008) supports the role of a fungal toxin in the pathogenesis of *B. dendrobatidis*, which may be driven by zoospores and zoosporangial secretions. More interestingly, the recent *in vitro* study by Brutyn et al. 2012 reports rapid (less than 4 hours) alterations in the structural integrity of the epidermis in *Xenopus laevis* after exposure to *B. dendrobatidis* zoospore secretions. As amphibian skin is physiologically active, disruption of epidermal structure through toxicity can compromise a number of critical skin functions including the ability to rehydrate or osmoregulate (Voyles et al. 2009, Carver et al. 2010, Marcum et al. 2010, Rosenblum et al. 2012, Voyles et al. 2012). However, the exact mechanisms of VWA disruption in the palmate newt are still unknown. In White's tree frogs (*Litoria caerulea*) infected with *B. dendrobatidis,* a disruption in electrolyte ion transport has been found (Voyles et al. 2009). Such a disruption suggests an epidermal electrolyte channel disruption

(Voyles et al. 2009) and a decrease in ion channel gene expression (Rosenblum et al. 2012). In amphibians, rapid VWA is dependent on water channels inserted into the epidermal layers (i.e. aquaporins; see Connolly et al. 1998, Hasegawa et al. 2003, Suzuki et al. 2007). We can suppose that VWA is impeded by *B. dendrobatidis* through an epidermal aquaporin disruption. However, the distribution of aquaporins in the epidermis remains to be established in urodeles. Further experiments are needed to investigate whether a reduction in rehydration ability in amphibians is due to an inhibition of epidermal aquaporins.

Our results, together with those of Voyles et al. (2007, 2009, 2012), Carver et al. (2010), Marcum et al. (2010) and Rosenblum et al. (2012), support the epidermal dysfunction hypothesis, which suggests that *B. dendrobatidis* compromises the ability of amphibians to osmoregulate or rehydrate. Such disruption of a crucial physiological process, even when small, can at least alter the adaptability of amphibians during their terrestrial phase in the wild and even their survival, especially in the context of a warming climate and prolonged or intensified drought events. This refers to the climate-linked epidemic hypothesis (e.g. Pounds and Crump 1994, Lampo et al. 2006, Pounds et al. 2006) and the drought-linked chytridiomycosis hypothesis (e.g. Burrowes et al. 2004, Lampo et al. 2006, Kriger 2009), which propose that abnormal climatic conditions can exacerbate chytridiomycosis outbreaks. However, these hypotheses remain highly controversial (Alford et al. 2007, Lips et al. 2008, Rohr et al. 2008, Kriger 2009). As stated by Kriger (2009), these hypotheses are inconsistent with our current knowledge of *B. dendrobatidis* physiology and ecology, and that dry conditions should reduce the severity of the pathogen. Nevertheless we have evidence that droughts actually increase outbreaks (Burrowes et al. 2004, Lampo et al. 2006). We can ask whether such impacts on transepidermal water exchanges by *B. dendrobatidis* in the palmate newt are sufficient to cause mortality in a climate change

context. However, we are not in a position yet to answer this question and further experiments are needed to conclude a link between climate change and the physiological effects of *B. dendrobatidis* on this species.

Acknowledgements. We warmly thank Estefanía Pérez Broto and Clément Brustel for their valuable help and support in the field and laboratory. We are grateful to M.C. Fisher and T.W.J. Garner for providing the *Batrachochytrium dendrobatidis* strain. We also thank Théotime Colin for providing the *L. helveticus* agar model picture. We finally thank Patricia Hulmes, a native English speaker, and three anonymous referees who helped to improve this manuscript. This study was supported by a grant from the Ministère de l'Enseignement Supérieur et de la Recherche and was conducted with the approval of the Préfecture de l'Isère (decision 2010-04110) and the Ethical Committee of University Lyon 1 in accordance with the current French laws and with the approval of the Director of Veterinary Services (DSV permit n°692661232).

LITERATURE CITED

Alford RA, Bradfield KS, Richards SJ (2007) Global warming and amphibian losses. *Nature* 447:E3-E4

Alvarado RH (1967) The significance of grouping on water conservation in *Ambystoma*. *Copeia* 3:667-668

Berger L, Hyatt AD, Speare R, Longcore JE (2005) Life cycle stages of the amphibian chytrid *Batrachochytrium dendrobatidis*. *Dis Aquat Org* 68:51-63

Berger L, Speare R, Daszak P, Green DE and 10 others (1998) Chytridiomycosis causes amphibian mortality associated with population declines in the rain forests of Australia and Central America. *Proc Natl Acad Sci USA* 95:9031-9036

Blaustein AR, Gervasi1 SS, Johnson PTJ, Hoverman JT, Belden LK, Bradley PW, Xie GY (2012) Ecophysiology meets conservation: understanding the role of disease in amphibian population declines. *Phil Trans R Soc* B 367:1688-1707

Blaustein AR, Romansic JM, Scheessele EA, Han BA, Pessier, AP, Longcore JE (2005) Interspecific variation in susceptibility of frog tadpoles to the pathogenic fungus *Batrachochytrium dendrobatidis*. *Conserv Biol* 19:1460-1468

Bosch J, Martinez-Solano I, Garcia-Paris M (2001) Evidence of a chytrid fungus infection involved in the decline of the common midwife toad (*Alytes obstetricans*) in protected areas of central Spain. *Biol Conserv* 97:331-337

Boyle DG, Boyle DB, Olsen V, Morgan JAT, Hyatt AD (2004) Rapid quantitative detection of chytridiomycosis (*Batrachochytrium dendrobatidis*) in amphibian samples using real-time Taqman PCR assay. *Dis Aquat Org* 60:141-148

Brutyn M, D'Herde K, Dhaenens M, Van Rooij P and 8 others (2012) *Batrachochytrium dendrobatidis* zoospore secretions rapidly disturb intercellular junctions in frog skin. *Fungal Genet Biol* 49:830–837

Burrowes PA, Joglar RL, Green DE (2004) Potential causes for amphibian declines in Puerto Rico. *Herpetologica* 60:141-154

Carey C (2000) Infectious disease and worldwide declines of amphibian populations, with comments on emerging diseases in coral reef organisms and in humans. *Environ health perspect* 108:143-150

Carey C, Cohen N, Rollins-Smith L (1999) Amphibian declines: an immunological perspective. *Develop Comp Immunol* 23:459-472

Carver S, Bell BD, Waldman B (2010) Does chytridiomycosis disrupt amphibian skin function? *Copeia* 2010:487-495

Connolly DL, Shanahan CM, Weissberg PL (1998) The aquaporins. A family of water channel proteins. *Int J Biochem Cell B* 30:169-172

Daszak P, Berger L, Cunningham, AA, Hyatt AD, Green DE, Speare R (1999) Emerging infectious diseases and amphibian population declines. *Emerging Infect Dis* 5:735-748

Daszak P, Cunningham AA, Hyatt AD (2003) Infectious disease and amphibian population declines. *Divers Distrib* 9:141-150

Dejean T, Miaud C, Ouellet M (2010) La chytridiomycose : une maladie émergente des amphibiens. *Bull Soc Herp Fr* 134:27-46

Farrer RA, Weinert LA, Bielby J, Garner TWJ and 11 others (2011) Multiple emergences of genetically diverse amphibian-infecting chytrids include a globalized hypervirulent recombinant lineage. *Proc Nat Acad Sci USA* 108:18732-18736

Fisher MC, Henk DA, Briggs CJ, Brownstein JS, Madoff LC, McCraw SL, Gurr SJ (2012) Emerging fungal threats to animal, plant and ecosystem health. *Nature* 484:186-194

Garner TWJ, Rowcliffe JM, Fisher MC (2011) Climate change, chytridiomycosis or condition: an experimental test of amphibian survival. *Glob Change Biol* 17:667-675

Garner TWJ, Walker S, Bosch J, Leech S, Rowcliffe JM, Cunningham AA, Fisher MC (2009) Life history tradeoffs influence mortality associated with the amphibian pathogen *Batrachochytrium dendrobatidis*. *Oikos* 118:783-791

Gehlbach FR, Kimmel JR, Weems WA (1969) Aggregations and body water relations in tiger salamanders (*Ambystoma tigrinum*) from the Grand Canyon rims, Arizona. *Physiol Zool* 42:173-182

Harvell CD, Mitchell CE, Ward JR, Altizer S, Dobson AP, Ostfeld RS, Samuel MD (2002) Climate warming and disease risks for terrestrial and marine biota. *Science* 296:2158-2162

Hasegawa T, Tanii H, Suzuki M, Tanaka S (2003) Regulation of water absorption in the frog skins by two vasotocin-dependent water-channel aquaporins, AQP-h2 and AQP-h3. *Endocrinology* 144:4087-4096

IPCC (2007) Working group I report, climate change 2007: “the physical science basis”. The fourth assessment report of the intergovernmental panel on climate change, Paris

Kiesecker JM, Blaustein AR (1995) Synergism between UV-B radiation and a pathogen magnifies amphibian embryo mortality in nature. *Proc Nat Acad Sci USA* 92:11049-11052

Kiesecker JM, Blaustein AR, Belden LK (2001) Complex causes of amphibian population declines. *Nature* 410:681-684

Kriger KM (2009) Lack of evidence for the drought-linked chytridiomycosis hypothesis. *J Wildlife Dis* 45:537-541

Lampo M, Rodriguez-Contreras A, La Marca E, Daszak P (2006) A chytridiomycosis epidemic and a severe dry season precede the disappearance of *Atelopus* species from the Venezuelan Andes. *Herpetol J* 16:395-402

Laurance WF, McDonald KR, Speare R (1996) Epidemic disease and the catastrophic decline of Australian rain forest frogs. *Conserv Biol* 10:406-413

Lillywhite HB (2006) Water relations of tetrapod integument. *J Exp Biol* 209:202-226

Lips KR, Diffendorfer J, Mendelson JR III, Sears MW (2008) Riding the wave: reconciling the roles of disease and climate change in amphibian declines. *PLoS Biol* 6:441-454

Luquet E, Garner TWJ, Léna JP, Bruel C, Joly P, Lengagne T, Grolet O, Plénet S (2012) Genetic erosion in wild populations makes resistance to a pathogen more costly. *Evolution* 66:1942–1952

Marcum RD, St-Hilaire S, Murphy PJ, Rodnick KJ (2010) Effects of *Batrachochytrium dendrobatidis* infection on ion concentrations in the boreal toad *Anaxyrus* (Bufo) *boreas boreas*. *Dis Aquat Org* 91:17-21

Nichols DK, Lamirande EW, Pessier AP, Longcore JE (2001) Experimental transmission of cutaneous chytridiomycosis in dendrobatid frogs. *J Wildlife Dis* 37:1-11

Pessier AP, Nichols DK, Longcore JE, Fuller MS (1999) Cutaneous chytridiomycosis in poison dart frogs (*Dendrobates* spp.) and white's tree frogs (*Litoria caerulea*). *J Vet Diagn Invest* 11:194-199

Pough FH, Taigen TL, Stewart MM, Brussard PF (1983) Behavioural modification of evaporative water loss by a Puerto Rican frog. *Ecology* 64:244-252

Pounds JA, Bustamante MR, Coloma LA, Consuegra JA and 10 others (2006) Widespread amphibian extinctions from epidemic disease driven by global warming. *Nature* 439:161-167

Pounds JA, Crump ML (1994) Amphibian declines and climate disturbance: the case of the golden toad and the harlequin frog. *Conserv Biol* 8:72-85

Rachowicz LJ, Hero JM, Alford RA, Taylor JW, Morgan JAT, Vredenburg VT, Collins JP, Briggs CJ (2005) The novel and endemic pathogen hypotheses: competing explanations for the origin of emerging infectious diseases of wildlife. *Conserv Biol* 19:1441-144

Rohr JR, Raffel TR, Romansic JM, McCallum H, Hudson PJ (2008) Evaluating the links between climate, disease spread, and amphibian declines. *Proc Nat Acad Sci USA* 105:17436-17441

Rosenblum EB, Poorten TJ, Settles M, Murdoch GK (2012) Only skin deep: shared genetic response to the deadly chytrid fungus in susceptible frog species. *Mol Ecol* 21:3110–3120

Rosenblum EB, Stajich JE, Maddox N, Eisen MB (2008) Global gene expression profiles for life stages of the deadly amphibian pathogen *Batrachochytrium dendrobatidis*. *Proc Nat Acad Sci USA* 105:17034-17039

Shoemaker VH, Hillman SS, Hillyard SD, Jackson DC, McClanahan LL, Withers PC, Wygoda ML (1992) Exchange of water, ions, and respiratory gases in terrestrial amphibians. In: Feder E, Burggren WW (ed) Environmental Physiology of the Amphibians. University of Chicago Press, Chicago, pp. 125-150

Shoemaker VH, Nagy KA (1977) Osmoregulation in amphibians and reptiles. *Ann Rev Physiol* 39:449-471

Schrag SJ, Wiener P (1995) Emerging infectious diseases: what are the relative roles of ecology and evolution? *Trends Ecol Evol* 10:319-324

Spotila JR, Berman EN (1976) Determination of skin resistance and the role of skin in controlling water loss in amphibians and reptiles. *Comp Biochem Physiol* 55A:407-411

Spotila JR, O'Connor MP, Bakken GS (1992) Biophysics of heat and mass transfert. In: Feder E, Burggren WW (ed) Environmental Physiology of the Amphibians. University of Chicago Press, Chicago, pp. 59-80

Stuart SN, Chanson JS, Cox NA, Young BE, Rodrigues ASL, Fishman DL, Waller RW (2004) Status and trends of amphibian declines and extinctions worldwide. *Science* 306:1783-1786

Suzuki M, Hasegawa T, Ogushi Y, Tanaka S (2007) Amphibian aquaporins and adaptation to terrestrial environments: a review. *Comp Biochem Physiol* 148A:72-81

Thomas CD, Cameron A, Green RE, Bakkenes M and 15 others (2004) Extinction risk from climate change. *Nature* 427:145-148

Viborg AL, Rosenkilde P (2004) Water potential receptors in the skin regulate blood prefusion in the ventral pelvic patch of toads. *Physiol Biochem Zool* 77:39-49

Voyles J, Berger L, Young S, Speare R, Webb R, Warner J, Rudd D, Campbell R, Skerratt LF (2007) Electrolyte depletion and osmotic imbalance in amphibians with chytridiomycosis. *Dis Aquat Org* 77:113-118

Voyles J, Vredenburg VT, Tunstall TS, Parker JM, Briggs CJ, Rosenblum EB (2012) Pathophysiology in Mountain Yellow-Legged Frogs (*Rana muscosa*) during a Chytridiomycosis Outbreak. *PLoS One* 7(4):e35374

Voyles J, Young S, Berger L, Campbell C and 7 others (2009) Pathogenesis of chytridiomycosis, a cause of catastrophic amphibian declines. *Science* 326:582-585

GENERAL CONCLUSION

In a context of climate change, it is critical to predict how organisms might be affected in their physical relations with environment. This topic is an urgent interdisciplinary challenge for developing effective conservation strategies. Amphibians are the vertebrate group most affected by ecological changes because of permanent exchanges of respiratory gasses, heat and water through their permeable skin. Biophysical ecology is specifically concerned in predicting how ecological changes might affect organisms and their physical relations. It represent an interdisciplinary field which combines fundamental physical laws that govern general fluid motion (i.e. heat transfer, mass transfer, and momentum transfer principles) with ecophysiology, behavioural ecology, and the study of animal properties (size, shape, skin characteristics, etc.) to derive mechanistic models of energy and mass balance at different scales.

In the context of the biophysical ecology, appropriate methods were developed to evaluate and to model the specific physical and physiological characteristics of water transfers in the amphibians (skin resistance to mass transfer of water vapour, skin surface areas that contribute to these transfers, complex outer morphology of the organism) (article [1]). These characteristics represent key traits in order to develop accurate mechanistic model of mass transfers, allowing one to generalize from measurements of transepidermal evaporative water loss (TEWL) rates under particular microclimatic combinations (temperature, vapour gradient, wind speed) to any other combination (Tracy 1976, Kearney and Porter 2009).

Agar replicas of *L. helveticus* were created in order to compare the TEWL rates of living newts to those of a free water surface (which has no capacity to limit evaporation) (articles [1, 3]). Agar replicas were essentially identical to living newts (except for their lack of animation). Nonetheless, this method has been proved to be useful and efficient to understand the key mechanism of water transfer with the atmosphere. As many wet-skinned organisms, *L. helveticus* did not show any physiological adaptation to restrain evaporation. As a consequence, the way to reduce TEWL rate consists essentially in behavioural adaptations, such as adoption of a particular posture in order to reduce the surface area that contribute to water evaporation (article [1, 3]). Along this work, we showed that in the laboratory the palmate newt expressed two types of postures: a posture characterized by a relative straight body with no tail coil (the "I"-shaped posture), and an efficient stereotyped water-conserving posture when the body is huddled up with the tail coiled along it (the "S"-shaped posture) (articles [1, 2, 3]). These results suggest that the "S"-shaped posture could reduce TEWL rates up to 20% and thus may have significant consequences on survival in the terrestrial environment. These results also highlight the importance to capture the skin surface areas that contribute to water transfers depending on the expressed postures.

For the first time in the field of the biophysical ecology, we presented a scanner-based non-invasive virtual sectioning technique to model the three-dimension (3D) complex outer morphology of an amphibian. We generated 3D geometries of *L. helveticus* using a Magnetic resonance imaging (MRI)-based 3D reconstruction method performed via volume-rendering by a "segmentation" process (see Laforsh et al. 2012 for details) carried out using a graph-cuts algorithm (Jacinto et al. 2012) (article [1]). The geometries allow us to derive accurate

quantitative data on functional skin surface areas involved in water transfers. The 3D information (volume and surface) of the scanned animal are obtained in standard format that makes them suitable for simulation application of mass transfers. This digital imaging and computerized 3D-modelling appears as a promising technique which, in the case of my thesis, has opened an original way to study and model TEWL between an amphibian and its physical environment.

Models of dynamic exchange of water (but also of energy) have been established for the amphibians (Tracy 1976, Spotila et al. 1992). As discussed in the article [2] the model of water transfer developed by Tracy (1976,) which is currently used in integrative biophysical studies in amphibians (e.g. Porter and Mitchell 2006, Kearney and Porter 2009, Bartlet et al. 2010) describes TEWL only under forced advection. Since amphibians tend to select their habitat to limit their TEWL, developing a model for quiescent air conditions could benefit to further studies. Using COMSOL Multiphysics software, we successfully developed a 3D diffusion-controlled evaporation (DCE) model in calm air based on the Fick's first law to simulate TEWL in *L. helveticus* at various conditions of temperature (15 – 30°C) and relative humidity (RH) (40 – 80%) (article [2]). The finite element method was used to solve the differential equations of diffusion over the 3D geometries of *L. helveticus* obtained by MRI (article [1]). The model describes the TEWL with skin (i.e. the external boundary of the newts' geometries) physically acting as a free water surface, and at thermal equilibrium. In this way, the model incorporates both physical (body size, posture) and physiological (skin characteristics) key traits of a TEWL model for *L. helveticus*. Our DCE model has been shown to be adequate to predict TEWL rates of the living experimental newts, as well as their agar replicas in a large range of climatic conditions under a lack of forced advection. In other

words, our results suggest that in our experimental condition, TEWL rate of the newts was purely diffusive.

However, some recent studies on water droplets support that water evaporation in quiescent air is not purely diffusive (Shahidzadeh-Bonn et al. 2006, Weon et al. 2011, Jodat and Moghiman 2012). This suggests that some environmental conditions may trigger an autonomous water vapour transport termed the free advection. Indeed, for free water surface in calm air, water vapour molecules can be theoretically transported away from an evaporative surface through air motion generated by buoyancy because, all things being equal, humid air is lighter than dry air. As a first approach, we developed a combined free advection-diffusion (CAD) model applied on 3D geometries of living amphibians. However, the increase of TEWL predicted by the CAD model (between 8% and 66% compared to the DCE model) failed to improve the agreement with experiments obtained using the purely diffusive DCE model. Nonetheless, the habitat structure (geometric factor, volume, shape, its connection with atmosphere etc.), especially for shelters potentially used by amphibians (e.g. soil cavities, burrows, cracks) (e.g. Schwarzkopf and Alford 1996, Jehle et al. 2000, Seebacher and Alford 2002, Schabetsberger et al. 2004), in relation with the physical intrinsic characteristics (e.g. size, posture) of the wet-skinned organism may trigger such a free advection phenomenon. It is hoped that the proposed models will be used and improved to give a new quantitative basic overview, and a new firm theoretical framework, of the interrelatedness of amphibian's physical interaction with their terrestrial environment. Moreover, it is hoped that the original approach used in this work could open new ways in the field of the biophysical ecology for amphibians and other wet-skinned taxa.

Finally, we focused on a biotic factor, the skin pathogen *Batrachochytrium dendrobatidis* (*Bd*), as a potential disruptive factor of water transfers (TEWL and transepidermal water absorption (TWA)) in amphibians (article [3]). Indeed, the actual physiological states experienced by an amphibian might be influenced by biotic factors such as pathogens through their interactions with the physical and/or physiological intrinsic characteristics of the animal. Our results suggest that *Bd* seems unable to affect TEWL in *L. helveticus*, but support the epidermal dysfunction hypothesis, which suggests that this pathogen compromises the ability of amphibians to rehydrate. Our results also suggest that *Bd* could rapidly inhibit rehydration of *L. helveticus* through disruption of the active processes of TWA via fungal toxins or other active compounds released by the pathogen. Such disruption of a crucial physiological process, even when small, can at least alter the adaptability of amphibians during their terrestrial phase in the wild and even their survival. This detrimental effect could be even more noticeable taking into account evidences that droughts actually increase pathogen outbreaks (Burrowes et al. 2004, Lampo et al. 2006). One can ask whether such impacts on transepidermal water exchanges by *Bd* in the palmate newt are sufficient to cause mortality in a climate change context. However, we are not in a position yet to answer this question and further experiments are needed to conclude a link between climate change and the physiological effects of *Bd* on this species.

FUTURE DIRECTIONS

Currently, our DCE model represents a first approach of a species-specific biophysical model that describes the 3D TEWL of *L. helveticus* inside a simplified geometry under well controlled conditions. This work opens several perspectives mainly concerning the actual environmental conditions encountered by the animal in the wild.

Modelling the water relations between amphibians and their microhabitats

Transepidermal evaporative water loss. Amphibians do not passively experience their environment but actively construct or select them. The habitat structure in relation with intrinsic characteristics of these organisms should have crucial influences of the intensity of mass transfers. Water vapour transfers in ambient air that drive TEWL are controlled by the vapour concentration gradients imposed between the animal and its environment. Thus, the shape and nature of the microhabitat most probably have a crucial influence on the intensity of TEWL rate. As far as shelters, and specially soil cavities, are considered, several factors should limit the TEWL rate: geometric factors such as the volume of the shelter and the shape of its connection with the atmosphere, thermal factors such as the temperature decrease with depth in soils, hygrometric factors such as the moisture transfer from the soil to the air inside a cavity or the vegetation. Given that the predictive accuracy of our DCE model was verified in simplified conditions, it should be used to simulate TEWL in more complex geometries corresponding to realistic micro-habitat. However, detailed informations on microhabitats used by these organisms are required to tackle this work. Currently few studies have focused on the amphibian microhabitat characterisations (Seebacher and Alford 2002, Browne and Paszkowski 2010) and are limited to large animals.

Concerning small amphibian species (as *L. helveticus*), no currently available tracking apparatus could be used. This field of research remains widely opened and should bring extremely precious data to study the interaction between newts and their environment.

Transepidermal water absorption. Water intake from the soil is the major and critical way for amphibians to balance water loss by evaporation (Tracy 1976, Shoemaker and Nagy 1977, Spotila et al. 1992, Shoemaker et al. 1992, Hillman et al. 2009). These water transfers were not explored during my thesis but remain crucial to understand the water relations between wet-skinned organisms and their microhabitats. As discussed in the introduction part of this thesis, a generalized transient-state model describing water exchange between the frog *Rana pipiens* and an unsaturated soil was developed by Tracy (1976). However, this model has never been validated against realistic soil conditions which water transfer properties could vary in wide range depending on the complex nature of soils. Such a model should also be revisited in the light of the critical physiological processes involved in TWA (electrolyte and aquaporin epithelial channels, vascular perfusion). The amphibian skin is a critical active pathway of TWA and future models should consider the major active phenomena of the amphibian skin implying changes in biological variables such as the skin hydraulic conductivity and/or the osmotic potential of the animal. In addition, as demonstrated in this thesis, biotic factors such, as pathogens, are able to disrupt the TWA probably through disruption of an active physiological process of water transport. However, this still remain unclear. Future TWA models, through considering the major active phenomena involved in water uptake, should improve our understandings on how pathogens such as *Bd* compromise the ability of amphibians to osmoregulate or rehydrate through their skin.

Towards a more integrative approach of the amphibian-environment physical relations

Microclimatic conditions of a given habitat (temperature, RH, wind velocity, substrate conditions) are strongly influenced by the interaction between climate, local structure, vegetation and soil (Tracy 1976, Spotila et al. 1992, Porter and Mitchell 2006, Kearney and Porter 2009, Bartlet et al. 2010). Deriving realistic microclimatic variables from available macroclimatic data is then a very challenging problem. In addition, amphibian characteristics such as its size, shape, or its posture alters through different ways the temporal and spatial changes of the water vapour gradients (driving force for TEWL) initially imposed by its habitat. In the same way, when an amphibian experiences a transepidermal water absorption (TWA) from a soil, this leads to complex temporal and spatial changes in the soil hydraulic properties (water potential, hydraulic conductivity) immediately around the animal (Tracy 1976, Spotila et al. 1992). In other words, environmental changes determine the environmental variables of the habitat structure which interact with the intrinsic characteristics of the animal to create a mosaic of microenvironment conditions (Kearney and Porter 2009, Bartlet et al. 2010). Any mechanistic model of organism-environment physical relations should therefore capture this two-way interaction in realistic way.

LITERATURE CITED

Alford RA, Bradfield KS, Richards SJ (2007) Global warming and amphibian losses. *Nature* 447:E3-E4

Alvarado RH (1967) The significance of grouping on water conservation in *Ambystoma*. *Copeia* 3:667-668

Alvarado RH (1972) The effects of dehydration on water and electrolytes in *Ambystoma tigrinum*. *Physiol Zool* 45:43-53

Amey AP, Grigg GC (1995) Lipid-reduced evaporative water loss in two arboreal hylid frogs. *Comp Biochem Physiol* 111:283-291

Audette M, Rivière D, Ewend M, Enquobahrie A, Valette S (2011) Approach-guided controlled resolution brain meshing for FE-based interactive neurosurgery simulation. Workshop on Mesh Processing in Medical Image Analysis, in conjunction with MICCAI 2011, Toronto, Canada, 176-186

Barari A, Omidvar M, Ghotbi AR, Ganji DD (2009) Assessment of water penetration problem in unsaturated soils. *Hydrol Earth Sci Discuss* 6:3811-3833

Bellard C, Bertelsmeier C, Leadley P, Thuiller W, Courchamp F (2012) Impacts of climate change on the future of biodiversity. *Ecol let* 15:365-377

Berger L, Hyatt AD, Speare R, Longcore JE (2005) Life cycle stages of the amphibian chytrid *Batrachochytrium dendrobatidis*. *Dis Aquat Org* 68:51-63

Berger L, Speare R, Daszak P, Green DE and 10 others (1998) Chytridiomycosis causes amphibian mortality associated with population declines in the rain forests of Australia and Central America. *Proc Natl Acad Sci USA* 95:9031-9036

Blaustein AR, Gervasi SS, Johnson PTJ, Hoverman JT, Belden LK, Bradley PW, Xie GY (2012) Ecophysiology meets conservation: understanding the role of disease in amphibian population declines. *Phil Trans R Soc B* 367:1688-1707

Blaustein AR, Romansic JM, Scheessele EA, Han BA, Pessier, AP, Longcore JE (2005) Interspecific variation in susceptibility of frog tadpoles to the pathogenic fungus *Batrachochytrium dendrobatidis*. *Conserv Biol* 19:1460-1468

Bosch J, Martinez-Solano I, Garcia-Paris M (2001) Evidence of a chytrid fungus infection involved in the decline of the common midwife toad (*Alytes obstetricans*) in protected areas of central Spain. *Biol Conserv* 97:331-337

Bolker BM, Brooks ME, Clark CJ, Geange SW, Poulsen JR, Stevens MHH, White JSS (2009) Generalized linear mixed models: a practical guide for ecology and evolution. *Trends Ecol Evol* 24:127-135

Bottomley PA, Roger HH, Foster TH (1986) NMR imaging shows water distribution and transport in plant root systems in situ. *Proc Natl Acad Sci USA* 83:87–89

Bozinovic F, Calosi P, Spicer JI (2011) Physiological correlates of geographic range in animals. *Anu Rev Ecol Evol Syst* 42:155-179

Boykov Y, Jolly MP (2001) Interactive graph cuts for optimal boundary and region segmentation of objects in N-D images. International Conference on Computer Vision (ICCV) 1:105-112

Boyle DG, Boyle DB, Olsen V, Morgan JAT, Hyatt AD (2004) Rapid quantitative detection of chytridiomycosis (*Batrachochytrium dendrobatidis*) in amphibian samples using real-time Taqman PCR assay. *Dis Aquat Org* 60:141-148

Browne CL, Paszkowski CA (2010) Hibernation sites of western toads (*Anaxyrus boreas*): characterization and management implications. *Herpetol Cons Biol* 5:49-63

Brutyn M, D'Herde K, Dhaenens M, Van Rooij P and 8 others (2012) *Batrachochytrium dendrobatidis* zoospore secretions rapidly disturb intercellular junctions in frog skin. *Fungal Genet Biol* 49:830–837

Burrowes PA, Joglar RL, Green DE (2004) Potential causes for amphibian declines in Puerto Rico. *Herpetologica* 60:141-154

Buttemer A (1990) Effect of temperature on evaporative water loss of the Australian tree frogs *Litoria caerulea* and *Litoria chloris*. *Physiol Zool* 63:1043-1057

Campbell CR, Voyles J, Cook DI, Dinudom A (2012) Frog skin epithelium: electrolyte transport and chytridiomycosis. *Inter J Biochem Cell Biol* 44:431-434

Carey C (2000) Infectious disease and worldwide declines of amphibian populations, with comments on emerging diseases in coral reef organisms and in humans. *Environ health perspect* 108:143-150

Carey C, Cohen N, Rollins-Smith L (1999) Amphibian declines: an immunological perspective. *Develop Comp Immunol* 23:459-472

Carver S, Bell BD, Waldman B (2010) Does chytridiomycosis disrupt amphibian skin function? *Copeia* 2010:487-495

Connolly DL, Shanahan CM, Weissberg PL (1998) The aquaporins. A family of water channel proteins. *Int J Biochem Cell B* 30:169-172

Daszak P, Berger L, Cunningham, AA, Hyatt AD, Green DE, Speare R (1999) Emerging infectious diseases and amphibian population declines. *Emerging Infect Dis* 5:735-748

Daszak P, Cunningham AA, Hyatt AD (2003) Infectious disease and amphibian population declines. *Divers Distrib* 9:141-150

Datta AK (2002) Diffusion mass transfer: unsteady-state. In: Biological and bioenvironmental heat and mass transfer. Cornell University, New York pp. 285-305

Debbissi C, Orfi J, Nasrallah SB (2003) Evaporation of water by free or mixed convection into humid air and superheated steam. *Int J Heat Mass transfer* 46:4703-4715

Deegan RD, Bakajin O, Dupont TF, Huber G, Nagel SR, Witten TA (1997) Capillary flow as the cause of ring stains from dried liquid drops. *Nature* 389:827-829

Dejean T, Miaud C, Ouellet M (2010) La chytridiomycose : une maladie émergente des amphibiens. *Bull Soc Herp Fr* 134:27-46

Dobkins DS, Gettinger RD, O'Connor MP (1989) Importance of retreat site for hydration state in Bufo marinus during dry rainy season. *Am Zool* 29:88A

Farquhar M, Palade GE (1965) Cell junctions in amphibian skin. *J Cell Biol* 26:263-291

Farrer RA, Weinert LA, Bielby J, Garner TWJ and 11 others (2011) Multiple emergences of genetically diverse amphibian-infecting chytrids include a globalized hypervirulent recombinant lineage. *Proc Nat Acad Sci USA* 108:18732-18736

Feder ME, Burggren WW (1985) Cutaneous gas exchange in vertebrates: design, patterns, control and implications. *Biol Rev* 60:1-45

Fisher MC, Garner TWJ, Walker SF (2009) Global emergence of *Batrachochytrium dendrobatidis* and amphibian chytridiomycosis in space, time, and host. *Annu Rev Microbiol* 63:291-310

Fisher MC, Henk DA, Briggs CJ, Brownstein JS, Madoff LC, McCraw SL, Gurr SJ (2012) Emerging fungal threats to animal, plant and ecosystem health. *Nature* 484:186-194

Garner TWJ, Rowcliffe JM, Fisher MC (2011) Climate change, chytridiomycosis or condition: an experimental test of amphibian survival. *Glob Change Biol* 17:667-675

Garner TWJ, Walker S, Bosch J, Leech S, Rowcliffe JM, Cunningham AA, Fisher MC (2009) Life history tradeoffs influence mortality associated with the amphibian pathogen *Batrachochytrium dendrobatidis*. *Oikos* 118:783-791

Gehlbach FR, Kimmel JR, Weems WA (1969) Aggregations and body water relations in tiger salamanders (*Ambystoma tigrinum*) from the Grand Canyon rims, Arizona. *Physiol Zool* 42:173-182

Guo P, Hillyard SD, Fu BM (2003) A two-barrier compartment model for volume flow across amphibian skin. *Am J Physiol Integr Comp Physiol* 285:R1384-R1394

Harvell CD, Mitchell CE, Ward JR, Altizer S, Dobson AP, Ostfeld RS, Samuel MD (2002) Climate warming and disease risks for terrestrial and marine biota. *Science* 296:2158-2162

Hasegawa T, Tanii H, Suzuki M, Tanaka S (2003) Regulation of water absorption in the frog skins by two vasotocin-dependent water-channel aquaporins, AQP-h2 and AQP-h3. *Endocrinology* 144:4087-4096

Hillel D (1998) Flow of water in unsaturated soil. In: Hillel D (ed.) Environmental soil physics pp. 203-242

Hillman SS, Withers PC, Drewes RC, Hillyard SD (2009) Ecological and environmental physiology of amphibians. Oxford University Press

Hillyard SD, Willumsen NJ (2011) Chemosensory function of amphibian skin: integrating epithelial transport, capillary blood flow and behaviour. *Acta Physiol* 202:533-548

IPCC (2007) Working group I report, climate change 2007: "the physical science basis". The fourth assessment report of the intergovernmental panel on climate change, Paris

Jacinto H, Kéchichan R, Desvignes M, Prost R, Valette S (2012) A Web Interface for 3D Visualization and Interactive Segmentation of Medical Images, Web3D 2012, Los-Angeles, USA, 2012. RTF Tagged XML BibTex Google Scholar

Jaynes DB, Rogowski AS (1983) Applicability of Fick's law to gas diffusion. *Soil Sci Soc Am J* 47:425-430

Jodat A, Moghiman M (2012) An experimental assessment of the evaporation correlation for natural, forced and combined convection regimes. *Proc IME C J Mech Eng Sci* 226:145-153

Kearney M, Porter W (2009) Mechanistic niche modelling: combining physiological and spatial data to predict species'ranges. *Ecol Let* 12:334-350

Kéchichan R, Valette S, Desvignes M, Prost R (2011) Efficient Multi-Object Segmentation of 3D Medical Images Using Clustering and Graph Cuts. IEEE International Conference on Image Processing, Brussels, Belgium, 2196-2200

Kiesecker JM, Blaustein AR (1995) Synergism between UV-B radiation and a pathogen magnifies amphibian embryo mortality in nature. *Proc Nat Acad Sci USA* 92:11049-11052

Kiesecker JM, Blaustein AR, Belden LK (2001) Complex causes of amphibian population declines. *Nature* 410:681-684

Kilpatrick AM, Briggs CJ, Daszak P (2010) The ecology and impact of chytridiomycosis: an emerging disease of amphibians. *Trends Ecol Evol* 25:109-118

Kosugi K, Hopmans JW, Dane JH (2002) Parametric models. In: Dane JH, Topp GC (eds.) Methods of soil analysis, part I, Physical methods, 3rd edn. Madison: SSSA, pp. 739-757

Kriger KM (2009) Lack of evidence for the drought-linked chytridiomycosis hypothesis. *J Wildlife Dis* 45:537-541

Laforsh C, Imhof H, Sigl R, Settles M, Heß M, Wanninger A (2012) Application of computational 3D-modeling in organismal biology. In: Alexandru C (ed), Modeling and simulation in engineering. InTech, Rijeka, pp. 117–142

Lampo M, Rodriguez-Contreras A, La Marca E, Daszak P (2006) A chytridiomycosis epidemic and a severe dry season precede the disappearance of *Atelopus* species from the Venezuelan Andes. *Herpetol J* 16:395-402

Laurance WF, McDonald KR, Speare R (1996) Epidemic disease and the catastrophic decline of Australian rain forest frogs. *Conserv Biol* 10:406-413

Leij FJ, Russel WB, Lesh SM (1997) Closed-form expression for water retention and conductivity data. *Ground Water* 35:848-858

Lillywhite HB (2006) Water relations of tetrapod integument. *J Exp Biol* 209:202-226

Lips KR, Diffendorfer J, Mendelson JR III, Sears MW (2008) Riding the wave: reconciling the roles of disease and climate change in amphibian declines. *PLoS Biol* 6:441-454

Luquet E, Garner TWJ, Léna JP, Bruel C, Joly P, Lengagne T, Grolet O, Plénet S (2012) Genetic erosion in wild populations makes resistance to a pathogen more costly. *Evolution* 66:1942–1952

Maclean IMD, Wilson RJ (2011) Recent ecological responses to climate change support predictions of high extinction risk. *PNAS* 108:12337-12342

Maina JN (1989) The morphology of the lung of the East African tree frog *Chiromantis petersi* with observations on the skin and the buccal cavity as secondary gas exchange organs. A TEM and SEM study. *J Anat* 165:29-43

Marangio MS, Anderson JD (1977) Soil moisture preference and water relations of the marbled salamander, *Abystoma opacum* (Amphibia, Urodela, Ambystomatidae). *J Herpetol* 11:169-176

Marcum RD, St-Hilaire S, Murphy PJ, Rodnick KJ (2010) Effects of *Batrachochytrium dendrobatidis* infection on ion concentrations in the boreal toad *Anaxyrus (Bufo) boreas boreas*. *Dis Aquat Org* 91:17-21

Markowski P, Richardson Y (2011) Mesoscale meteorology in midlatitudes. Penn State University, University Park, PA, USA.

McClanahan L, Baldwin R (1969) Rate of water uptake through the integument of the desert toad, *Bufo punctatus*. *Comp Biochem Physiol* 28:381-389

Navas CA, Araujo C (2000) The use of agar models to study amphibian thermal ecology. *J Herpetol* 32:330-334

Nichols DK, Lamirande EW, Pessier AP, Longcore JE (2001) Experimental transmission of cutaneous chytridiomycosis in dendrobatid frogs. *J Wildlife Dis* 37:1-11

Nguyen TA, Dresselaers T, Verboven P, D'hallewin G, Culeddu N, Van Hecke P, Nicolaï (2006) Finite element modelling and MRI validation of 3D transient water profiles in pears during postharvest storage. *J Sci Food Agric* 86:745-756

Parmesan C (2006) Ecological and Evolutionary responses to climate change. *Annu Rev Ecol Evol Syst* 37:637-669

Pessier AP, Nichols DK, Longcore JE, Fuller MS (1999) Cutaneous chytridiomycosis in poison dart frogs (*Dendrobates spp.*) and white's tree frogs (*Litoria caerulea*). *J Vet Diagn Invest* 11:194-199

Pinheiro JC, Bates DM, DebRoy S, Sarkar D, The R Core Team (2009) nlme: linear and nonlinear mixed effects models. *R package version* 3: 1-96

Porter WP, Mitchell JW, Beckman WA, DeWitt CB (1973) Behavioral implications of mechanistic ecology, Thermal and behavioural modelling of desert ectotherms and their microenvironment. *Oecologia* 13:1-54

Pough FH, Taigen TL, Stewart MM, Brussard PF (1983) Behavioural modification of evaporative water loss by a Puerto Rican frog. *Ecology* 64:244-252

Pounds JA, Bustamante MR, Coloma LA, Consuegra JA and 10 others (2006) Widespread amphibian extinctions from epidemic disease driven by global warming. *Nature* 439:161-167

Pounds JA, Crump ML (1994) Amphibian declines and climate disturbance: the case of the golden toad and the harlequin frog. *Conserv Biol* 8:72-85

R Development Core Team (2013) R: a language and environment for statistical computing. R Foundation for Statistical Computing, Vienna

Rachowicz LJ, Hero JM, Alford RA, Taylor JW, Morgan JAT, Vredenburg VT, Collins JP, Briggs CJ (2005) The novel and endemic pathogen hypotheses: competing explanations for the origin of emerging infectious diseases of wildlife. *Conserv Biol* 19:1441-144

Ray C (1958) Vital limits and rates of desiccation in salamanders. *Ecology* 39:75-83

Richard BG, Peth S (2009) Modelling soil physical behavior with particular reference to soil science. *Soil and Tillage Research* 102:216-224

Rohr JR, Raffel TR, Romansic JM, McCallum H, Hudson PJ (2008) Evaluating the links between climate, disease spread, and amphibian declines. *Proc Nat Acad Sci USA* 105:17436-17441

Rollins-Smith L, Woodhams D (2011) Amphibian immunity: Staying in tune with the environment. In: Demas GE, Demas G, Nelson RJ (eds.) Ecoimmunology. Oxford, United Kingdom: Oxford University Press; pp. 92143.

Rosenblum EB, Poorten TJ, Settles M, Murdoch GK (2012) Only skin deep: shared genetic response to the deadly chytrid fungus in susceptible frog species. *Mol Ecol* 21:3110–3120

Rosenblum EB, Stajich JE, Maddox N, Eisen MB (2008) Global gene expression profiles for life stages of the deadly amphibian pathogen *Batrachochytrium dendrobatidis*. *Proc Nat Acad Sci USA* 105:17034-17039

Schabetsberger R, Jehle R, Maletzky A, Pesta J, Sztatecsny M (2004) Delineation of terrestrial reserves for amphibians: post-breeding migrations of Italian crested newts (*Triturus c. carnifex*) at high altitude. *Biol Cons* 117:95-104

Schrag SJ, Wiener P (1995) Emerging infectious diseases: what are the relative roles of ecology and evolution? *Trends Ecol Evol* 10:319-324

Schwarzkopf L, Alford RA (1996) Desiccation and shelter-site use in a tropical amphibian: comparing toads with physical models. *Funct Ecol* 10:193-200

Seebacher F, Alford (2002) Shelter microhabitats determine body temperature and dehydration rates of a terrestrial amphibian (*Bufo marinus*). *J Herpetol* 36:69-75

Shahidzadeh-Bonn N, Rafai S, Azouni A, Bonn D (2006) Evaporating droplets. *J Fluid Mech* 549:307-313

Shoemaker VH, Hillman SS, Hillyard SD, Jackson DC, McClanahan LL, Withers PC, Wygoda ML (1992) Exchange of water, ions, and respiratory gases in terrestrial amphibians. In: Feder E, Burggren WW (ed) Environmental Physiology of the Amphibians. University of Chicago Press, Chicago

Shoemaker VH, Nagy KA (1977) Osmoregulation in amphibians and reptiles. *Ann Rev Physiol* 39:449-471

Skerrat LF, Berger L, Speare R, Cashins S, McDonald KR, Phillott AD, Hines HB, Kenyon N (2007) Spread of chytridiomycosis has caused the rapid global decline and extinction of frogs. *EcoHealth* 4:125-134

Spight TM (1967) The water economy of salamanders: exchange of water with the soil. *Biol Bull* 132:126-132

Spight TM (1968) The water economy of salamanders: evaporative water loss. *Physiol Zool* 41:195-203

Spotila JR, Berman EN (1976) Determination of skin resistance and the role of skin in controlling water loss in amphibians and reptiles. *Comp Biochem Physiol* 55A**:**407-411

Spotila JR, O'Connor MP, Bakken GS (1992) Biophysics of heat and mass transfert. In: Feder E, Burggren WW (ed) Environmental Physiology of the Amphibians. University of Chicago Press, Chicago

Stuart SN, Chanson JS, Cox NA, Young BE, Rodrigues ASL, Fishman DL, Waller RW (2004) Status and trends of amphibian declines and extinctions worldwide. *Science* 306:1783-1786

Suzuki M, Hasegawa T, Ogushi Y, Tanaka S (2007) Amphibian aquaporins and adaptation to terrestrial environments: a review. *Comp Biochem Physiol* 148A:72-81

Suzuki M, Tanaka S (2009) Molecular and cellular regulation of water homeostasis in anuran amphibians by aquaporins. *Comp Biochem Physiol A* 153:231-241

Thomas CD, Cameron A, Green RE, Bakkenes M and 15 others (2004) Extinction risk from climate change. *Nature* 427:145-148

Tracy CR (1976) A model of the dynamic exchange of water and energy between a terrestrial amphibian and its environment. *Ecol Monogr* 46:293-326

Tracy CR, Betts G, Tracy CR, Christian KA (2007) Plaster models to measure operative temperature and evaporative water loss of amphibians. *J Herpetol* 41:597-603

Tracy CR, Welch WR, Porter WP (1980) Properties of air: a manual for use in biophysical ecology. Third Edition, University of Wisconsin Technical Report

van Genuchten MT (1980) A closed-form equation for predicting the hydraulic conductivity of unsaturated soils. *Soil Sci Soc Am J* 44:892-898

van Genuchten MT, Pachepsky YA (2011) Hydraulic properties of unsaturated soils. In: Glinski J, Horabik J, Lipiec J (eds.) Encyclopedia of agrophysics pp. 368-376

van Rooij P, Martel A, D'Herde K, Brutyn M, Croubels S, et al. (2012) Germ Tube Mediated Invasion of *Batrachochytrium dendrobatidis* in Amphibian Skin Is Host Dependent. *PLoS ONE* 7(7): e41481. doi:10.1371/journal.pone.0041481

Viborg AL, Rosenkilde P (2004) Water potential receptors in the skin regulate blood prefusion in the ventral pelvic patch of toads. *Physiol Biochem Zool* 77:39-49

Voyles J, Berger L, Young S, Speare R, Webb R, Warner J, Rudd D, Campbell R, Skerratt LF (2007) Electrolyte depletion and osmotic imbalance in amphibians with chytridiomycosis. *Dis Aquat Org* 77:113-118

Voyles J, Vredenburg VT, Tunstall TS, Parker JM, Briggs CJ, Rosenblum EB (2012) Pathophysiology in Mountain Yellow-Legged Frogs (*Rana muscosa*) during a Chytridiomycosis Outbreak. *PLoS One* 7(4):e35374

Voyles J, Young S, Berger L, Campbell C and 7 others (2009) Pathogenesis of chytridiomycosis, a cause of catastrophic amphibian declines. *Science* 326:582-585

Wardziak T, Luquet E, Plenet S, Léna JP, Oxarango L, Joly P (2013) Impact of both desiccation and exposure to an emergent skin pathogen on transepidermal water exchange in the palmate newt (*Lissotriton helveticus*). *Dis Aquat Org* 104:215-224

Weon BM, Je JH, Poulard C (2011) Convection-enhanced water evaporation. *AIP Advances* 012102

Withers PC, Hillman SS (2001) Allometric and ecological relationships of ventricle and liver mass in anuran amphibians. *Funct Ecol* 15:60-69

Xia Y, Sarafis V, Campbell EO, Callaghan PT (1993) Non-invasive imaging of water flow in plants by NMR microscopy. *Protoplasma* 173:170–176

Young JE, Christian KA, Donnellan S, Parry D (2005) Comparative analysis of cutaneous evaporation water loss in frogs demonstrates correlation with ecological habits. *Physiol Biochem Zool* 78:847-856

Dans un contexte de changement climatique, il est essentiel de prévoir comment les organismes peuvent être affectés dans leurs relations physiques avec l'environnement. Les amphibiens représentent le groupe des vertébrés le plus sensible aux changements environnementaux, en raison d'une perte en eau par évaporation transépidermique (PEET) permanente. Ma thèse vise à mettre en place des approches pour mesurer et modéliser avec précision les surfaces de la peau contribuant à la PEET; établir les lois de transfert d'eau amphibien-environnement; et fournir une meilleure compréhension des réponses physiologiques face au pathogène *Batrachochytrium dendrobatidis*. Ces expériences ont été réalisées sur des tritons palmés (*Lissotriton helveticus*) mâles adultes en phase terrestre. Nos résultats suggèrent que *L. helveticus* ne présente aucune adaptation physiologique pour limiter la PEET, les moyens étant limités à l'expression d'une posture en forme de "S". Une méthode de reconstruction 3D basée sur l'Imagerie par Résonance Magnétique a été utilisée pour générer des géométries 3D des tritons utilisables pour mesurer leur surface, et à des fins de simulation. Nous avons ainsi réalisé une analyse numérique en 3D des PEET, et avons proposé une relation pour estimer cette perte dans une large gamme de conditions climatiques. Enfin, nos résultats supportent l'hypothèse de dysfonctionnement épidermique, suggérant que *B. dendrobatidis* compromet la capacité des amphibiens à se réhydrater. Ma thèse devrait contribuer à développer de nouvelles approches en sciences des relations eau-amphibiens, et à améliorer nos connaissances sur les effets des changements environnementaux sur les organismes.

Climate and biodiversity: application of recent methodological developments in the study and the modelling of transepidermal evaporative water loss in an amphibian

In a context of climate change, it is critical to predict how organisms might be affected in their physical relations with environment. Amphibians are among the vertebrate groups the most affected by ecological changes, because of permanent transepidermal evaporative water loss (TEWL) through their skin. My thesis aims at setting up approaches to measure and model accurately the functional skin surface areas that contribute to TEWL, establishing laws of water transfer between an amphibian and its physical environment, and providing understanding on physiological responses to the skin pathogen *Batrachochytrium dendrobatidis*. We conducted experiments on adult males of the palmate newt (*Lissotriton helveticus*) during their terrestrial phase. Our results suggest that *L. helveticus* did not show any physiological adaptations to restrain TEWL. The ways to reduce TEWL result essentially in the expression of a stereotyped "S"-shaped water-conserving posture. We used a Magnetic Resonance Imaging-based 3D reconstruction method to generate 3D geometries of newt that is suitable for measuring skin surface areas, and for simulation purposes. We successfully performed 3D numerical analysis of TEWL, and proposed an original relationship to estimate TEWL rates in a large range of temperature and humidity. Finally, our results support the epidermal dysfunction hypothesis, which suggests that *B. dendrobatidis* compromises the ability of amphibians to rehydrate. My thesis would contribute to open new approaches to the science of amphibian water relations, and improve our knowledge of the effects of ecological changes on organisms.

Ecophysiologie – Ecologie biophysique

Mots-clés: Amphibien ; Changement climatique ; Evapotranspiration ; Comportement ; Modélisation ; Imagerie ; Pathogène

Key-words: Amphibian ; Climate change ; Water loss ; Water-conserving behaviour ; Modelling ; Imaging ; Pathogen

UMR CNRS 5023 Laboratoire d'Ecologie des Hydrosystèmes Naturels et Anthropisés (LEHNA)
Université Lyon1, 43 Bd. Du 11 novembre 1918, 69622 Villeurbanne cedex.